AD

TECHNICAL REPORT ECOM-01960-F

HF SPACED LOOP ANTENNA

FINAL REPORT

BY

J.D.MOORE · M.P.CASTLES

JULY 1967

DISTRIBUTION STATEMENT

Each transmittal of this document outside the Department of Defense must have prior approval of CG,U.S. Army Electronics Command, Fort Monmouth,N.J. Attn: AMSEL-WL-C

ECOM

UNITED STATES ARMY ELECTRONICS COMMAND · FORT MONMOUTH, N.J.

CONTRACT DA28-043-AMC-01960(E)

SOUTHWEST RESEARCH INSTITUTE (16-1855)

San Antonio,Texas

Approved For Release 2001/09/03 : CIA-RDP76-00451R000200010013-1

NOTICES

Disclaimers

The findings in this report are not to be construed as an official Department of the Army position unless so designated by other authorized documents.

The citation of trade names and names of manufacturers in this report is not to be construed as official Government indorsement or approval of commercial products or services referenced herein.

Disposition

Destroy this report when it is no longer needed. Do not return it to the originator.

Approved For Release 2001/09/03 : CIA-RDP76-00451R000200010013-1

TECHNICAL REPORT ECOM-01960-F JULY 1967

HF SPACED LOOP ANTENNA

FINAL REPORT

1 FEBRUARY 1966 TO 31 JANUARY 1967

Report No. 4

CONTRACT NO. DA 28-043AMC-01960(E)

DA TASK NO. 5B6 79191 D908 07 12

SwRI PROJECT 16-1855

DISTRIBUTION STATEMENT

Each transmittal of this document outside the Department or Defense must have prior approval of CG, U.S. ARMY ELECTRONICS COMMAND, Fort Monmouth, N.J. Attn. AMSEL-WL-C

Prepared By

J.D. MOORE AND M.P. CASTLES

SOUTHWEST RESEARCH INSTITUTE

SAN ANTONIO, TEXAS

For

U. S. ARMY ELECTRONICS COMMAND, FORT MONMOUTH, N. J.

Approved By

John D. Moore

for DOUGLAS N. TRAVERS, Director

Applied Electromagnetics

Approved For Release 2001/09/03 : CIA-RDP76-00451R000200010013-1

1. ABSTRACT

Coaxial spaced loop antenna theory is reviewed with emphasis on patterns as a function of signal polarization and angle of elevation. Experimental work with three broadband antennas has verified that the desired theoretical performance can be obtained in a practical design.

The major effort of this project was an advanced development/feasibility model of an HF spaced loop delivered as a component of a 4 to 8-MHz direction finder system. The rotation pedestal and visual indicator of existing DF systems were used with minor modifications. The evaluation of the HF spaced loop DF set verified that the CW sensitivity design goal of 10 μv/m was met over the operating range. The desired DF accuracy requirement for skywave signals was achieved for elevation angles of arrival up to 85°, and 561 azimuth bearings on stations at distances greater than 300 miles between 4 and 8 MHz produced a standard deviation of 2.67°.

Possible design improvements are listed based upon the design, construction, and evaluation experience of the first model. A major engineering improvement in the aural null control method would be valuable, in which case the spaced loop can be used more effectively in a manual left-right or automatic left-right DF mode. High speed sampling using this capability is suggested as a method of reducing response time on keyed signals. An alternative solution would be faster antenna rotation.

2. TABLE OF CONTENTS

2. TABLE OF CONTENTS (Cont'd)

3. LISTS

3.1 List of Illustrations

3.1 List of Illustrations (Cont'd)

3.1 List of Illustrations (Cont'd)

3.1 List of Illustrations (Cont'd)

3.1 List of Illustrations (Cont'd)

3.2 List of Tables

4. FACTUAL DATA

4.1 Phase I - Study and Experimental Investigation

4.1.1 Introduction

The spaced loop antenna has been the subject of frequent but unsustained development. Several workers have stated that the antenna offered distinct advantages for both general and specific applications in the HF frequency range. The work of Caplin and Bagley[1]* in World War II produced a mobile spaced loop direction finder with reasonable sensitivity and reported excellent skywave performance. The system was used strictly in an aural null mode. At that time, the system development was apparently dropped because Adcock systems with high speed goniometer and cathode ray tube indicators were much easier to use than the aural null spaced loop system developed by Caplin and Bagley.

More recently, Bailey[2] refers to the spaced loop antenna as a rotating interferometer. He states that the rotating spaced loop antenna can be an effective high angle direction finder provided a major technological breakthrough can be achieved with the spaced loop. Primary problems were, as he saw them, sensitivity and response time.

The work of this program under the guidance of Technical Guidelines for DD&F No. 810000 titled "HF Spaced Loop Antenna," dated 25 October 1965, has concentrated on the development of a spaced loop antenna for portable use in the frequency range of 4 to 8 MHz. The final advanced development/feasibility model delivered is used with a modified portable antenna pedestal of the AN/PRD-7 and 8 type.

It is felt that the advanced development/feasibility HF coaxial spaced loop antenna developed under this program presents a significant advance in the state-of-the-art in spaced loop engineering. It is, however, recognized that significant improvements may be made in the present development. A later section of this report outlines these possible improvements.

The experimental work of this program along with details of the design phase were discussed at length in the three quarterly reports.[3, 4, 5] The emphasis of this report will be placed on the construction and evaluation of the final development/feasibility model. However, a review of the

*Superscript numbers refer to List of References at end of this report.

theoretical data given in Quarterly Report No. 1[3] indicates that the theoretical portion should be repeated here with revisions for clarification of certain points.

4.1.2 Review of Spaced Loop Theory

There are three common spaced loop types. They are: the coaxial, the vertical coplanar, and the horizontal coplanar spaced loop antennas. The three types are illustrated in Figure 1 where the antennas are shown with a parallel opposition connection. The loops of the spaced loops of Figure 1 could be connected in a series opposition connection to obtain the spaced loop mode; however, the parallel opposition connection shown will generally yield the highest first parallel resonant frequency. The loops could also be connected in a parallel aiding or series aiding connection to obtain a simple loop mode.[7]

Far field radiation terms for the three common spaced loop antennas are available from the published field equations for the general spaced loop antenna.[8, 9] The near field terms will not be considered because, with the exception of local site effects and reradiation, this development has only considered far field signals. These equations are:

Spaced Loop	Polarization: Vertical		Polarization: Horizontal	
Coaxial	$E_\theta = \frac{-I\beta^3 V\omega\mu}{2\pi}\left[\frac{1}{j\beta r}\right]\sin\theta\sin 2\phi$	(1)	$E_\phi = \frac{I\beta^3 V\omega\mu}{2\pi}\left[\frac{1}{j\beta r}\right]\sin 2\theta\sin^2\phi$	(2)
Vertical Coplanar	$E_\theta = \frac{I\beta^3 V\omega\mu}{\pi}\left[\frac{1}{j\beta r}\right]\sin\theta\sin^2\phi$	(3)	$E_\phi = \frac{I\beta^3 V\omega\mu}{4\pi}\left[\frac{1}{j\beta r}\right]\sin 2\theta\sin 2\phi$	(4)
Horizontal Coplanar	$E_\theta = 0$	(5)	$E_\phi = \frac{-I\beta^3 V\omega\mu}{2\pi}\left[\frac{1}{j\beta r}\right]\sin^2\theta\sin\phi$	(6)

where

V = volume of spaced loop antenna (loop area multiplied by number of turns in each loop times loop spacing)

ϕ = azimuth

θ = angle of incidence

I = average loop current

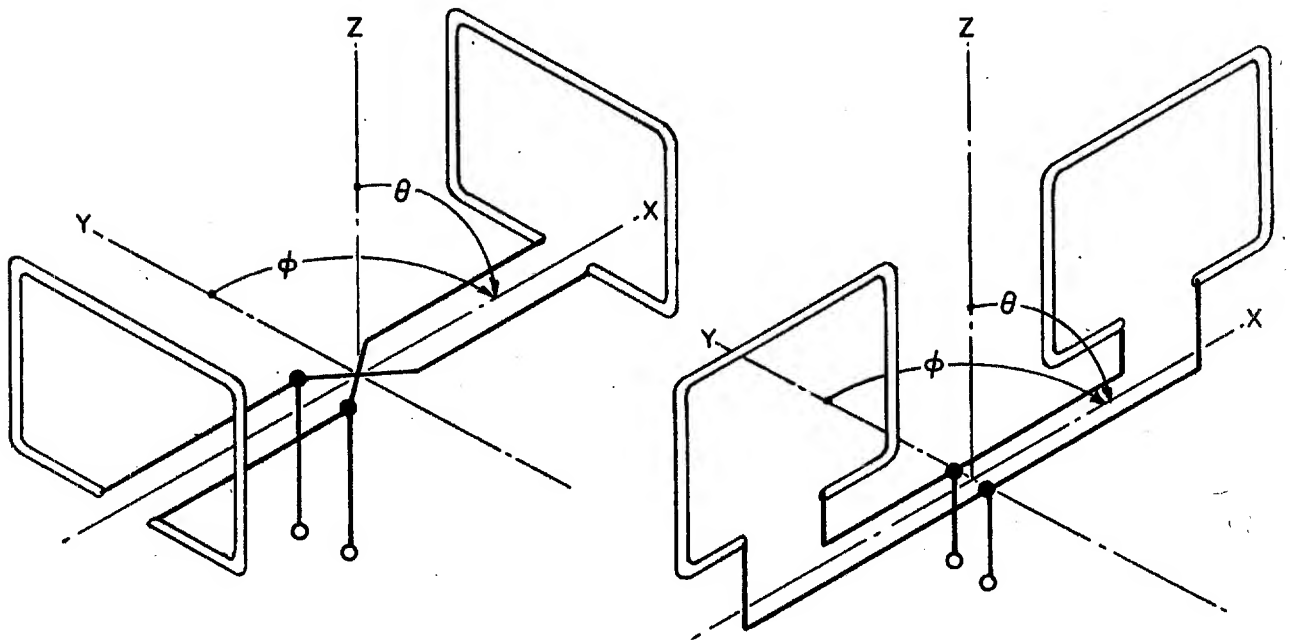

a. COAXIAL SPACED LOOP PARALLEL OPPOSITION

b. VERTICAL COPLANAR SPACED LOOP PARALLEL OPPOSITION

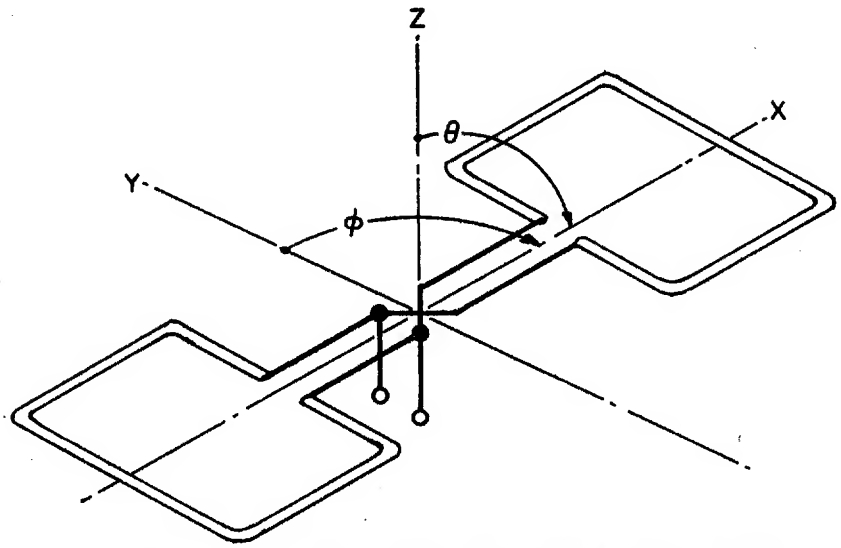

c. HORIZONTAL COPLANAR SPACED LOOP PARALLEL OPPOSITION CONNECTION

FIGURE 1 COMMON SPACED LOOP ANTENNAS

β = $2\pi/\lambda$ where λ is the wavelength

ω = 2π times frequency

μ = permeability of medium

r = radial distance from the center of the antenna

From the far field radiation term equations for the horizontal coplanar spaced loops [Equations (5) and (6)], it was obvious that this antenna could be eliminated for further consideration because it has no response for vertical polarization.

The equivalent equations for a simple loop antenna orientated so the plane of the loop is parallel to the loops of the coaxial spaced loop of Figure 1 are:

Polarization

Vertical $$E_\theta = \frac{jI\beta^2 A\omega\mu}{2\pi}\left[\frac{1}{j\beta r}\right]\cos\phi \qquad (7)$$

Horizontal $$E_\phi = \frac{jI\beta^2 A\omega\mu}{2\pi}\left[\frac{1}{j\beta r}\right]\cos\theta\sin\phi \qquad (8)$$

where A = effective area of the loop (number of turns times loop area).

The equations for the coaxial spaced loop, the vertical coplanar spaced loop, and the simple loop indicate that both the elevation response and azimuth response of the antenna are independent of frequency. The terms in front of the trigonometric functions determine the amplitude and phase of the antenna output voltage. The equations for the coaxial spaced loop, vertical coplanar spaced loop, and simple loop may be simplified if each equation is divided by a normalizing term but retaining phase. If the following normalizing terms are used:

Coaxial Spaced Loop and Vertical Coplanar Spaced Loop

$$N = \frac{I\beta^3 V\omega\mu}{4\pi}\left|\frac{1}{j\beta r}\right| \qquad (9)$$

Simple Loop

$$N = \frac{I\beta^2 A\omega\mu}{2\pi}\left[\frac{1}{j\beta r}\right] \qquad (10)$$

The resulting normalized far field radiation terms with phase retained for vertical and horizontal polarization for the three antennas are:

Antenna	Polarization	
	Vertical	Horizontal
Coaxial Spaced Loop	$V_\theta = -2 \sin\theta \sin 2\phi$ (11)	$V_\phi = 2 \sin 2\theta \sin^2\phi$ (12)
Vertical Coplanar Spaced Loop	$V_\theta = 4 \sin\theta \sin^2\phi$ (13)	$V_\phi = \sin 2\theta \sin 2\phi$ (14)
Simple Loop	$V_\theta = j \cos\phi$ (15)	$V_\phi = j \cos\theta \sin\phi$ (16)

From the normalized equations, it can be seen that the elevation patterns for the coaxial and vertical coplanar spaced loops are identical. The normalized elevation patterns for these two spaced loops and the simple loop antenna are given in Figure 2. (These elevation patterns exist in free space at all azimuth angles except at the nulls, as indicated in Figure 2.) The spaced loops have a maximum along the horizontal and a minimum overhead for vertical polarization, while they have the maximum at 45° above the horizontal for horizontal polarization. On the basis of the elevation patterns alone, there was no significant difference (for the requirements of this program) between the coaxial spaced loop and the vertical coplanar spaced loop.

For the 4 to 8-MHz frequency range, only groundwave signals will be continuously vertically polarized. The skywave polarization will vary from pure vertical polarization and to pure horizontal polarization with these two conditions probably occurring only a small percentage of the time. It is felt by workers at Southwest Research Institute that the four null $\sin 2\phi$ pattern is easier to interpret than the two null $\sin^2\phi$ pattern. Therefore, it appeared that the coaxial spaced loop would be the more desirable for this requirement where both groundwave and skywave signals are anticipated. It also had the advantage of being a better known design, and, perhaps, less critical to build for vertical polarization.

Analytical work performed for the Bureau of Ships[8] and summarized in the literature[9] indicated another factor. The patterns for the vertical coplanar spaced loop antenna change significantly as the antenna moves into the near field of a signal, whereas the coaxial spaced loop pattern is the same for both near field and far field signals. The vertical coplanar

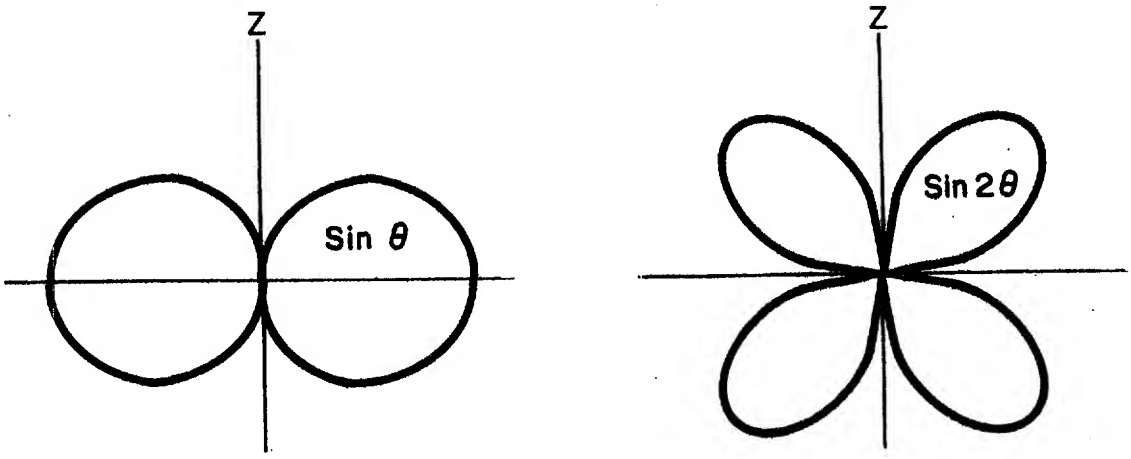

VERTICAL POLARIZATION
($\phi \neq 0°, 90°, 180°$, OR 270°)

HORIZONTAL POLARIZATION
($\phi \neq 0°$ OR 180°)

COAXIAL SPACED LOOP
VERTICAL COPLANAR SPACED LOOP

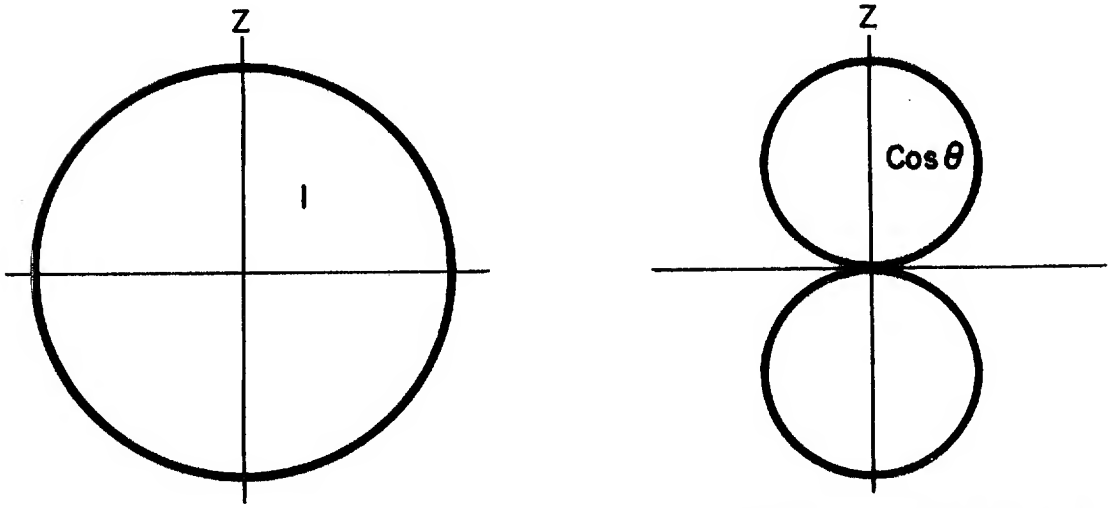

VERTICAL POLARIZATION
($\phi \neq 90°$ OR 270°)

HORIZONTAL POLARIZATION
($\phi \neq 0°$ OR 180°)

SIMPLE LOOP

FIGURE 2.

NORMALIZED ELEVATION PATTERNS FOR THE COAXIAL SPACED LOOP, THE VERTICAL COPLANAR SPACED LOOP, AND THE SIMPLE LOOP ANTENNAS.

would be more affected by local site conditions and the presence of a support mast. For these reasons, it is felt that the coaxial spaced loops should be used for the current requirement.

The same analysis has produced an excellent method of predetermining spaced loop signal plus noise to noise sensitivity in terms of antenna parameters. The specific application of this technique to this development is discussed in Quarterly Report No. 1. [3]

4.1.3 Sense for the Coaxial Spaced Loop Antenna

The choice of the coaxial spaced loop for the portable and mobile land-based requirement of this program led to a need to extend the previous work performed in the 20 to 150-MHz frequency range in order to meet an increase in angle of elevation requirement from 45° to 85°. [7, 10-18] The sense method used for the 20 to 150-MHz antenna was also reviewed in terms of the increased angle of elevation requirement.

When both the coaxial spaced loop and simple loop are used individually, there remains a two-way ambiguity for all signal polarizations. This two-way ambiguity can be resolved by summing the coaxial spaced loop with a simple loop of the proper amplitude and phase (the loop must be parallel to the loops of the coaxial spaced loop). If the simple loop output is shifted by 90° and an amplitude control factor A is applied from the normalized far field radiation terms [Equations (11), (12), (15), and (16)], the sense function can be described by the following expression:

$$E_{sense} = \underbrace{\underbrace{\text{Vertical}}_{-2 \sin\theta \sin 2\phi} + \underbrace{\text{Horizontal}}_{2 \sin 2\theta \sin^2\phi}}_{\text{Coaxial Spaced Loop}} + \underbrace{\underbrace{\text{Vertical}}_{A(\cos\phi} + \underbrace{\text{Horizontal}}_{\cos\theta \sin\phi)}}_{\text{Simple Loop}} \qquad (17)$$

The resulting sense pattern shifts the correct spaced loop null in a clockwise direction. (The reciprocal null, which is 180° from the correct bearing, is shifted counterclockwise.) If the simple loop signal is shifted in phase by 270°, then the correct spaced loop null is shifted counterclockwise.

4.1.4 Theoretical Coaxial Spaced Loop DF and Sense Patterns

A computer program has evolved from work on a VHF spaced loop antenna under Contract DA 28-043 AMC-01633(E) which permitted the rapid computation of the theoretical antenna patterns as a function of signal polarization and angle of elevation. The computer program for the calculation of coaxial spaced loop patterns, simple loop patterns, and sense patterns as used to calculate the theoretical patterns given in Quarterly Report No. 1[3] was correct. However, the equation describing the program contained errors. The program based on the normalized far field terms of Equations (11), (12), (15), and (16) with the appropriate corrections is

$$V_T = E_v e^{jP_v} \left[-2 \sin\theta \sin 2\phi \, E_{cx} e^{j\Phi_{cx}} + \cos\phi \, E_{LX} e^{j\Phi_{LX}}\right] + E_h e^{jP_h} \left[2 \sin 2\theta \sin^2\phi \, E_{cx} e^{j\Phi_{cx}} + \cos\theta \sin\phi \, E_{LX} e^{j\Phi_{LX}}\right] \quad (18)$$

where

θ - angle of incidence measured from the perpendicular

ϕ - azimuth angle

E_v - amplitude of the incident vertically polarized wave

P_v - phase of the incident vertically polarized wave

E_h - amplitude of the incident horizontally polarized wave

P_h - phase of the incident horizontally polarized wave

E_{cx} - arbitrary amplitude constant for coaxial spaced loop

Φ_{cx} - arbitrary phase constant for coaxial spaced loop

E_{LX} - arbitrary amplitude constant for simple loop perpendicular to spaced loop axis

Φ_{LX} - arbitrary phase constant for simple loop perpendicular to spaced loop axis

Using this revised program, the free space patterns (reflected wave neglected) were calculated for the coaxial spaced loop, the simple

loop, clockwise sense (simple loop phase advanced 90°) and counterclockwise sense (simple loop phase advanced 270°). Patterns were calculated at $\theta = 5°$ (85° above the horizontal); $\theta = 15°$ (75° above the horizontal); $\theta = 25°$ (65° above the horizontal); $\theta = 45°$ (45° above the horizontal); $\theta = 60°$ (30° above the horizontal); $\theta = 78°$ (12° above the horizontal); and $\theta = 90°$ (0° above the horizontal). The amplitude A for the simple loop sense function of Equation (17) was one for angles of incidence of $\theta = 78°$, $\theta = 30°$, and $\theta = 45°$. The value of A was set at 0.5 for $\theta = 25°$, $\theta = 15°$, and $\theta = 5°$ to obtain a more readable sense pattern at these higher angles of signal elevation. *

The polarization conditions considered were:

Polarization	Polarization Description
$E_v = 1$, $P_v = 0°$ $E_h = 0$, $P_h = 0°$	Vertical
$E_v = 0.9$, $P_v = 0°$ $E_h = 0.4$, $P_h = 0°$	Mixed Linear
$E_v = 1$, $P_v = 0°$ $E_h = 1$, $P_h = 0°$	Mixed 45° Linear
$E_v = 1$, $P_v = 45°$ $E_h = 1$, $P_h = 0°$	Mixed Elliptical
$E_v = 0.4$, $P_v = 0°$ $E_h = 0.9$, $P_h = 0°$	Mixed Linear
$E_v = 0$, $P_v = 0°$ $E_h = 1$, $P_h = 0°$	Horizontal
$E_v = 1$, $P_v = 0°$ $E_h = 0.707$, $P_h = 90°$	Eliptical (almost circular)

The patterns obtained at horizontal incidence ($\theta = 90°$); 12° above the horizontal ($\theta = 78°$); 30° above the horizontal ($\theta = 60°$); and 45° above the horizontal ($\theta = 45°$) for the coaxial spaced loop and simple loop are given in Figure 3. The inverted coaxial spaced loop patterns and the inverted simple loop patterns are plotted on the same polar diagram with

*The experimental work of Section 4.2 indicated, however, that one value of sense injection produced useful sense patterns for all signal angles of elevation up to and including 85°.

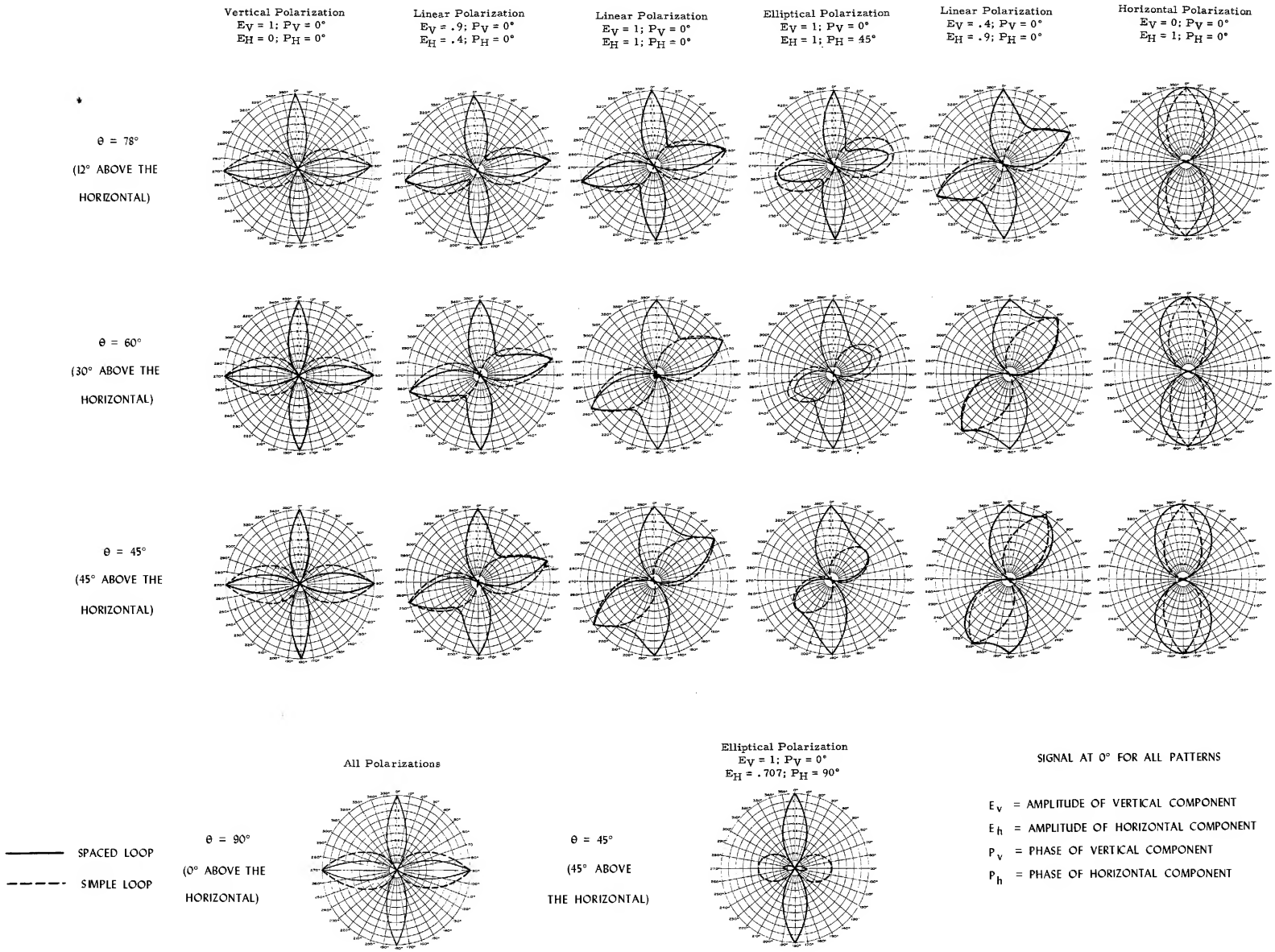

FIGURE 3

COAXIAL SPACED LOOP AND SIMPLE LOOP PATTERNS AS A FUNCTION OF SIGNAL POLARIZATION AND ANGLE OF INCIDENCE

go over

the spaced loop as a solid line and the simple loop as a dashed line. All of the patterns at $\theta = 90°$ are not given because only the vertical component will exist at this angle of incidence. The signal is at 0° azimuth for all patterns.

The DF and sense patterns obtained are given in Figures 4, 5, 6, 7, 8, and 9 with each illustration giving the patterns for one angle of incidence. The patterns of these six figures are inverted plots with the pattern minimum on the outside of the polar diagram as in Figure 3. The coaxial spaced loop pattern (the solid line) and the simple loop pattern (the dashed line) are plotted together. The clockwise sense pattern, the counterclockwise sense pattern, and the sense pattern with 90° deflection plate switching are given. The patterns at $\theta = 90°$ (0° above the horizontal) are not given because they are similar to the vertical polarization patterns ($E_v = 1$, $P_v = 0$, $E_h = 0$, and $P_h = 0°$) at $\theta = 78°$ (12° above the horizontal).

It will be noted that all of the coaxial spaced loop antenna patterns in Figures 3 through 9 have one pair of nulls which remain in the same position for all signal polarizations and angles of incidence. (This pair of nulls is called the spaced loop nulls.) The simple loop (with the plane of the loop chosen parallel to the loops of the coaxial spaced loop) has nulls which shift in position from 90° and 270° for vertical polarization to 0° and 180° for horizontal polarization. The simple loop nulls agree in position with the unwanted nulls (loop nulls) of the coaxial spaced loop pattern. If elliptical or circular polarization is present, both the loop nulls of the coaxial spaced loop pattern and the simple loop nulls are blurred (the null depth is decreased). In practice, with skywave signals, the shifting in position and blurring of the loop nulls of the coaxial spaced loop pattern serves to identify them while the spaced loop nulls are identified by the fact that their position does not change significantly.

The significance of the patterns of Figures 3 through 9 was, first, the coaxial spaced loop yields bearing information for all signal polarizations for angles of incidence of 5° to 90° (angles of arrival of 85° to 0°). Second, the sense system works for all conditions. Third, deflection plate switching of the sense pattern will simplify operator pattern interpretation.

4.1.5 Experimental Investigation

The experimental investigation involved the design, construction, and evaluation of three breadboard HF coaxial spaced loop antennas as discussed in the three quarterly reports.[3, 4, 5] All of the breadboard antennas were constructed using brass and copper materials with soldered joints. The investigation of coaxial spaced loop antennas with multiturn

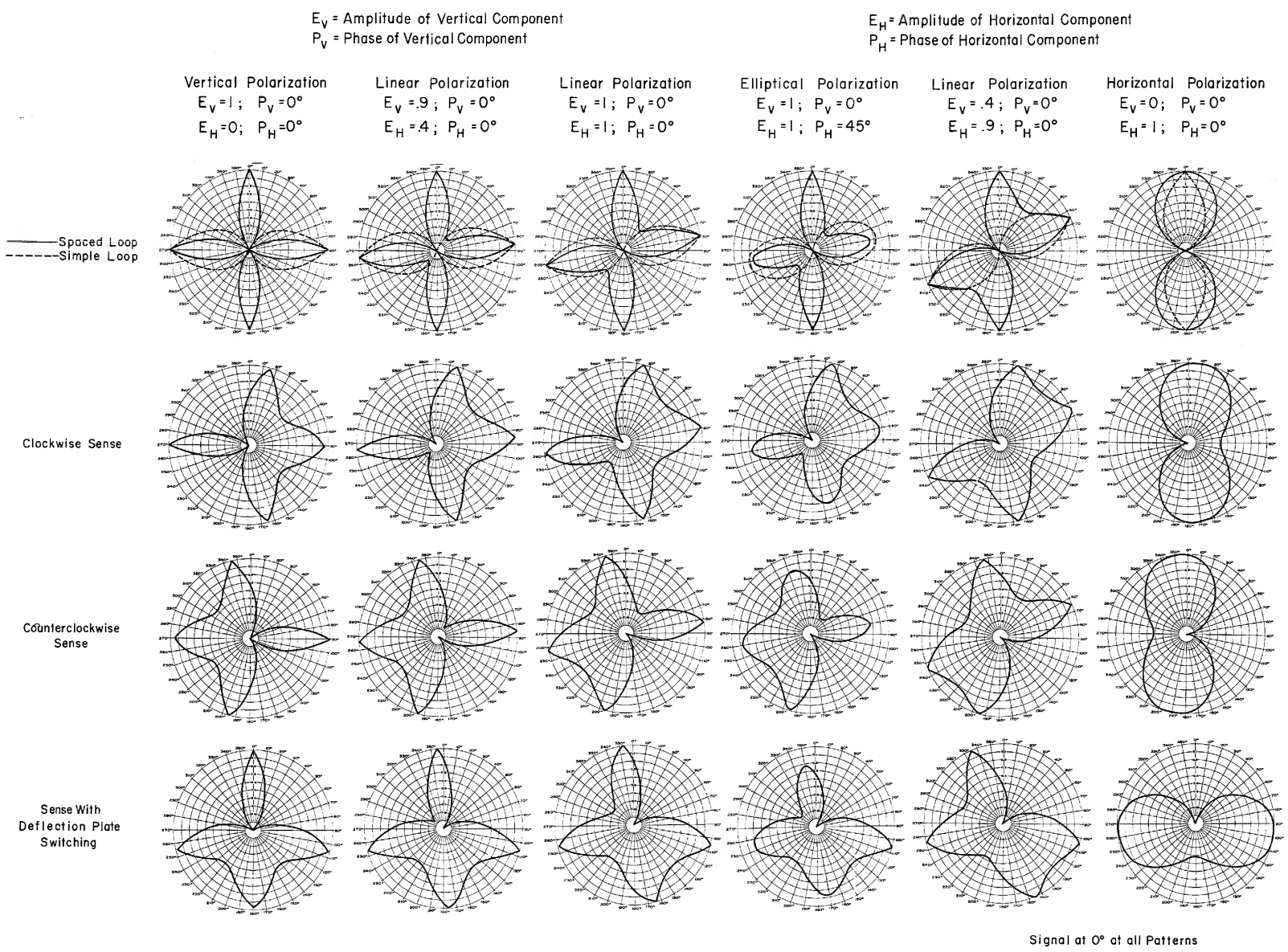

FIGURE 4.

COAXIAL SPACED LOOP AND SENSE PATTERNS AS A FUNCTION OF SIGNAL POLARIZATION AT θ = 78° (12° ABOVE THE HORIZONTAL)

Approved For Release 2001/09/03 : CIA-RDP76-00451R000200010013-1

Approved For Release 2001/09/03 : CIA-RDP76-00451R000200010013-1

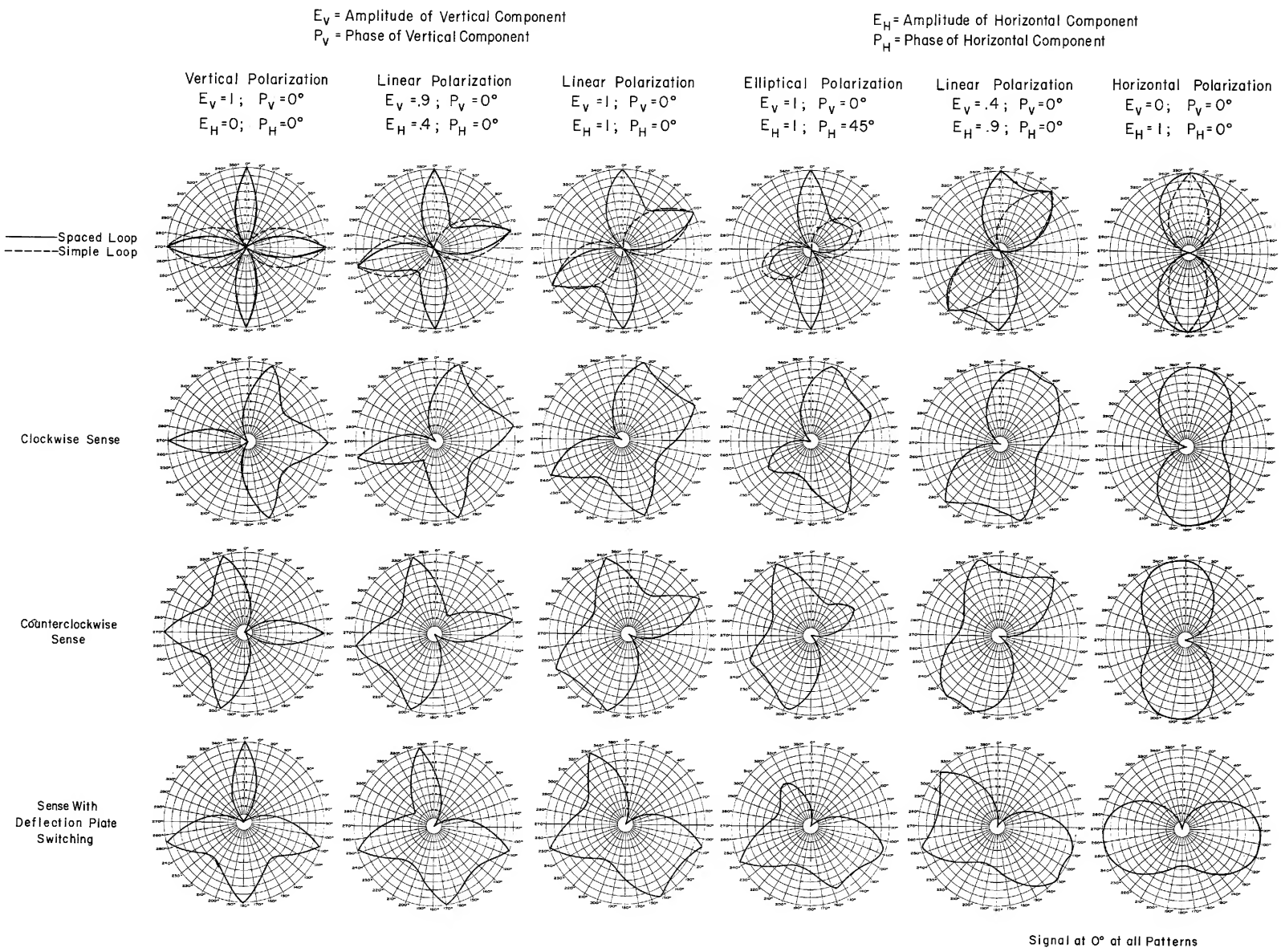

FIGURE 5 .

COAXIAL SPACED LOOP AND SENSE PATTERNS AS A FUNCTION OF SIGNAL POLARIZATION AT θ = 60° (30° ABOVE THE HORIZONTAL)

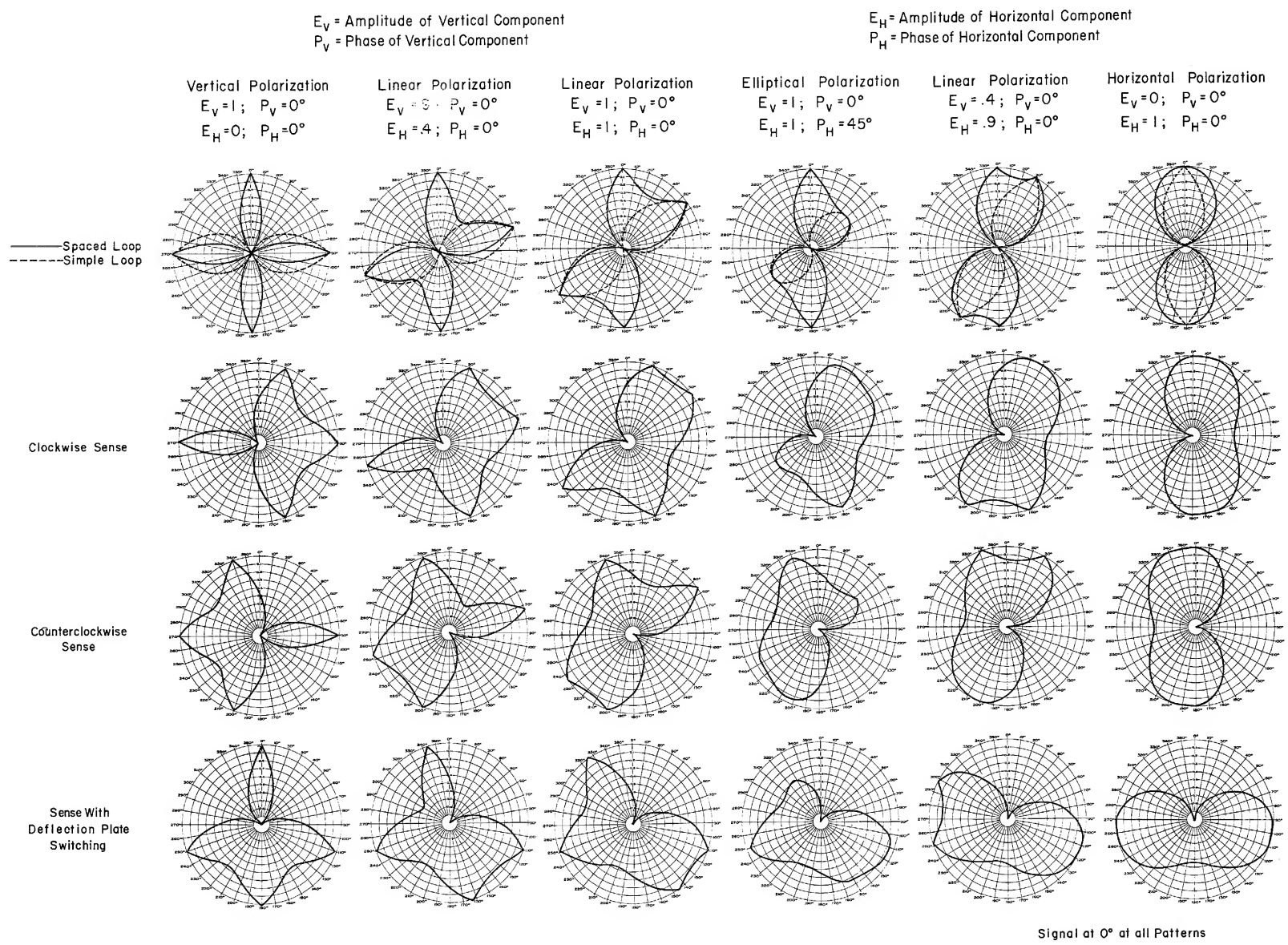

FIGURE 6 .

COAXIAL SPACED LOOP AND SENSE PATTERNS AS A FUNCTION OF SIGNAL POLARIZATION AT θ =45° (45° ABOVE THE HORIZONTAL)

Approved For Release 2001/09/03 : CIA-RDP76-00451R000200010013-1

Approved For Release 2001/09/03 : CIA-RDP76-00451R000200010013-1

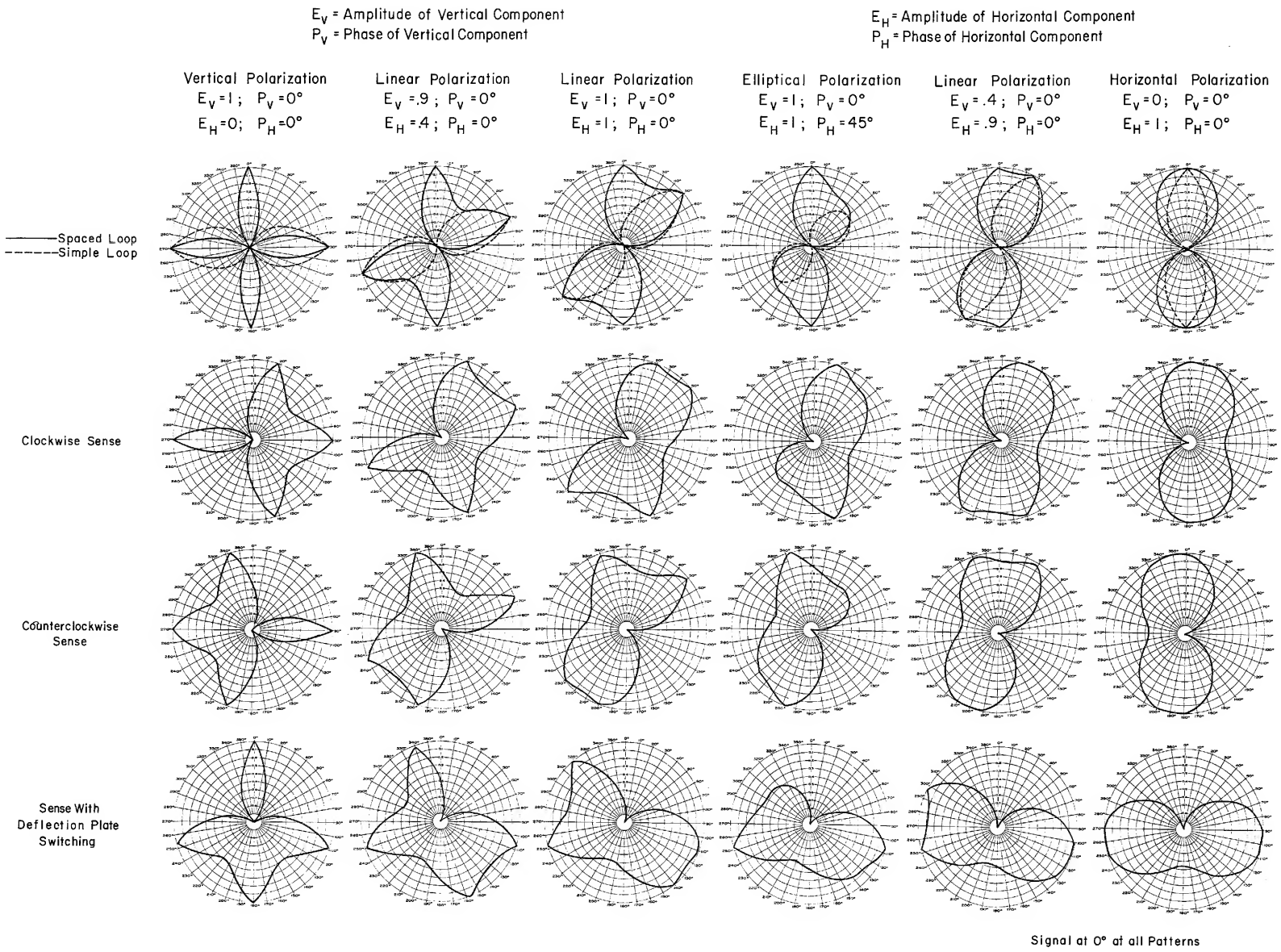

FIGURE 7.

COAXIAL SPACED LOOP AND SENSE PATTERNS AS A FUNCTION OF SIGNAL POLARIZATION AT θ = 25° (65° ABOVE THE HORIZONTAL)

Approved For Release 2001/09/03 : CIA-RDP76-00451R000200010013-1

E_V = Amplitude of Vertical Component
P_V = Phase of Vertical Component

E_H = Amplitude of Horizontal Component
P_H = Phase of Horizontal Component

Vertical Polarization	Linear Polarization	Linear Polarization	Elliptical Polarization	Linear Polarization	Horizontal Polarization
$E_V = 1$; $P_V = 0°$	$E_V = .9$; $P_V = 0°$	$E_V = 1$; $P_V = 0°$	$E_V = 1$; $P_V = 0°$	$E_V = .4$; $P_V = 0°$	$E_V = 0$; $P_V = 0°$
$E_H = 0$; $P_H = 0°$	$E_H = .4$; $P_H = 0°$	$E_H = 1$; $P_H = 0°$	$E_H = 1$; $P_H = 45°$	$E_H = .9$; $P_H = 0°$	$E_H = 1$; $P_H = 0°$

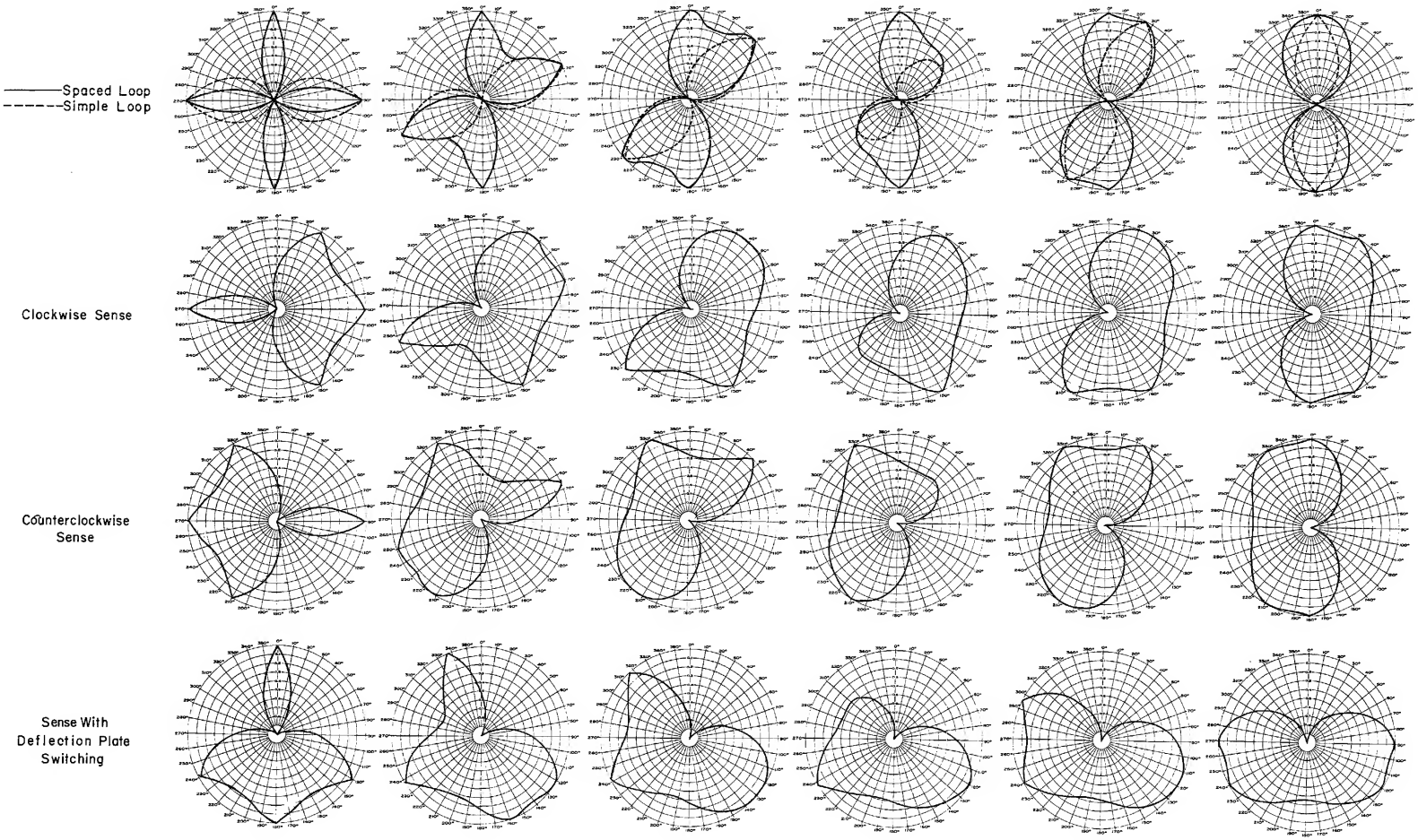

FIGURE 8.

COAXIAL SPACED LOOP AND SENSE PATTERNS AS A FUNCTION OF SIGNAL POLARIZATION AT $\theta = 15°$ (75° ABOVE THE HORIZONTAL)

Approved For Release 2001/09/03 : CIA-RDP76-00451R000200010013-1

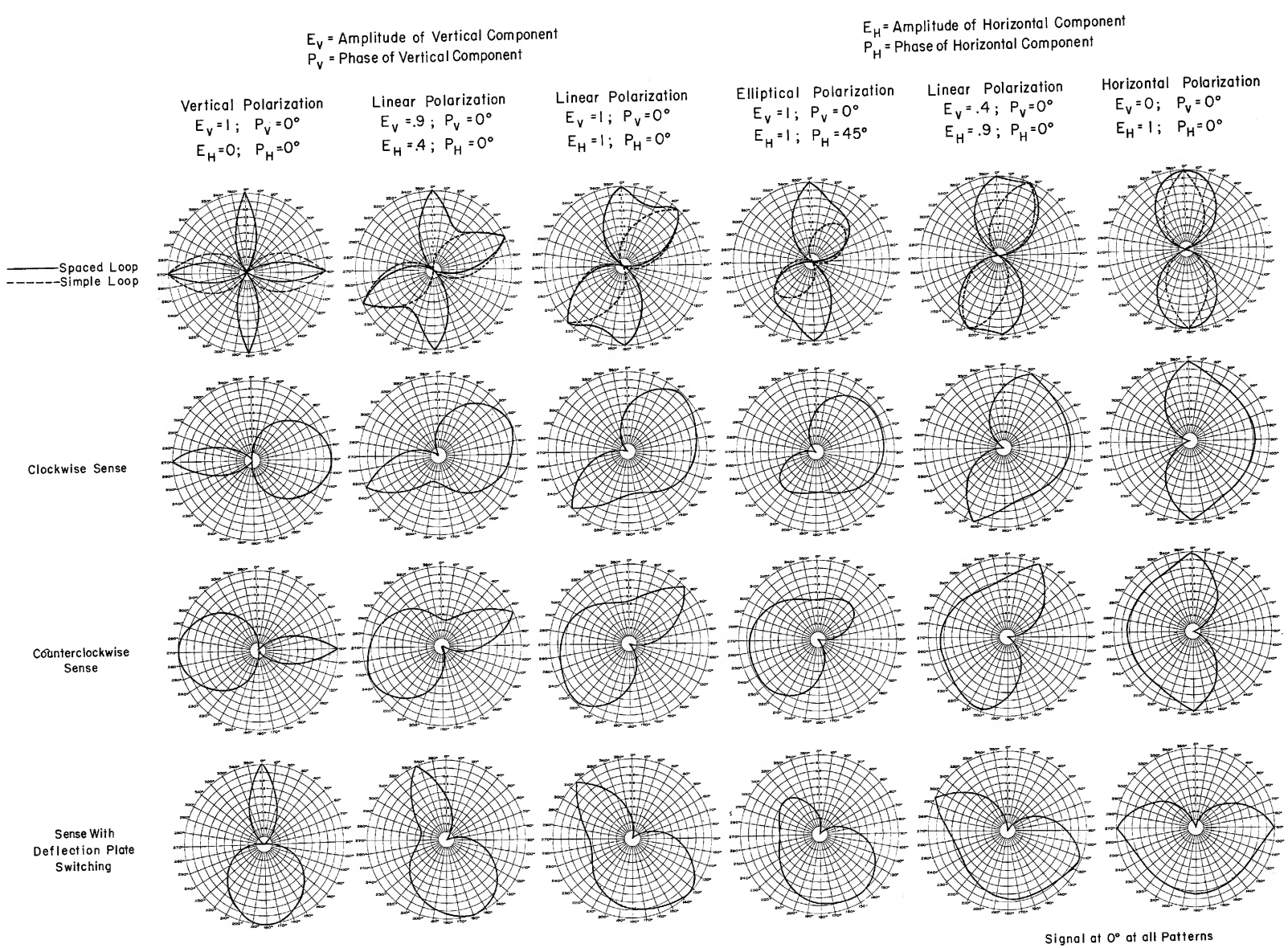

FIGURE 9.

COAXIAL SPACED LOOP, AND SENSE PATTERNS AS A FUNCTION OF SIGNAL POLARIZATION AT θ = 5° (85° ABOVE THE HORIZONTAL)

loops was pursued in the first two breadboard models to the extent necessary to determine the feasibility of this approach. The use of multiple turn loops significantly reduces the dimensions of a coaxial spaced loop for a given sensitivity. The third model was then designed and constructed based upon the anticipated design for the final advanced development/ feasibility model. Evaluation and modification of this third model was continued until as many design parameters for the final model could be finalized as possible.

The first model of the breadboard HF coaxial spaced loop antenna is illustrated in Figure 10. This model has 14-in. square loops spaced approximately 40 in. apart. Each loop was wound with five closely spaced turns. As discussed in Quarterly Report No. 1, [3] the pattern quality of the spaced loop mode of the antenna was only fair. The effective volume of the antenna was approximately 1/3 of the anticipated required volume for a 10 microvolt per meter sensitivity. (Effective volume is defined as loop area times number of turns times spacing.) The measured sensitivity was approximately 30 microvolts per meter using the CW method.

The second model breadboard HF coaxial spaced loop antenna is shown mounted on a modified AN/PRD-7 and 8 pedestal in Figure 11. This model had 24-in. square loops spaced approximately 54 in. apart. Each loop was wound with three turns spaced 1/8 in. apart. The model was based upon the third model which was being designed at the time. The construction technique was believed adequate only for impedance measurements; however, limited field tests were performed. Sensitivity approached the design goal while the pattern quality was again fair with some dipole distortion evident. [3]

The third model of a breadboard HF coaxial spaced loop antenna as shown in Figure 12 was constructed with increased precision as thought necessary to meet the DF and sensitivity requirements. The loops, as in the second breadboard model, are 24 in. square spaced approximately 54 inches. The individual loops are wound with three turns spaced approximately 1/8 in. apart. The antenna is shown mounted on a modified AN/PRD-7 and 8 pedestal in Figure 13. The third model contained all the remote control functions anticipated for the final model.

It will be noted that all of the breadboard antennas discussed use twin gaps or balanced gap shielded loops. Because of the success with the balanced gap arrangement as compared to the single gap antenna in work under Contract DA 28-043 AMC-01633(E), [7, 14, 15] single gap arrangements were not considered in this development. The work in the referenced reports with VHF spaced loop antennas had indicated in comparison tests that the twin or balanced gap configuration was superior to the conventional

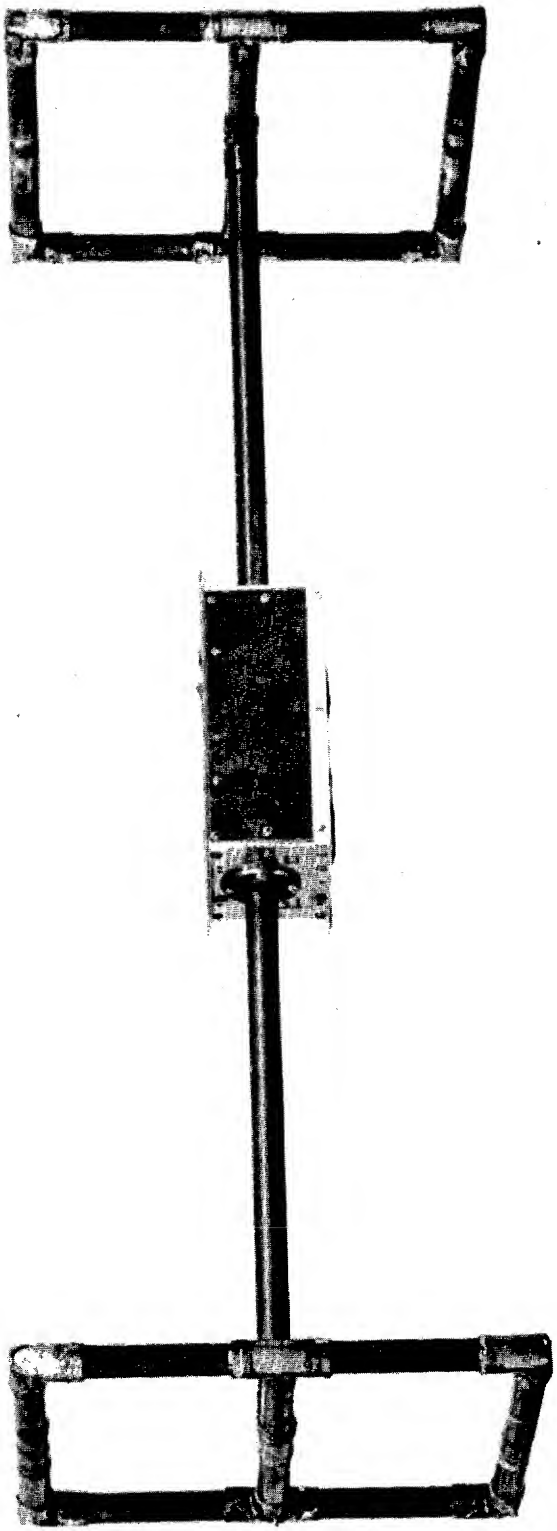

C-25924

FIGURE 10

BREADBOARD HF COAXIAL SPACED LOOP ANTENNA (MODEL 1)

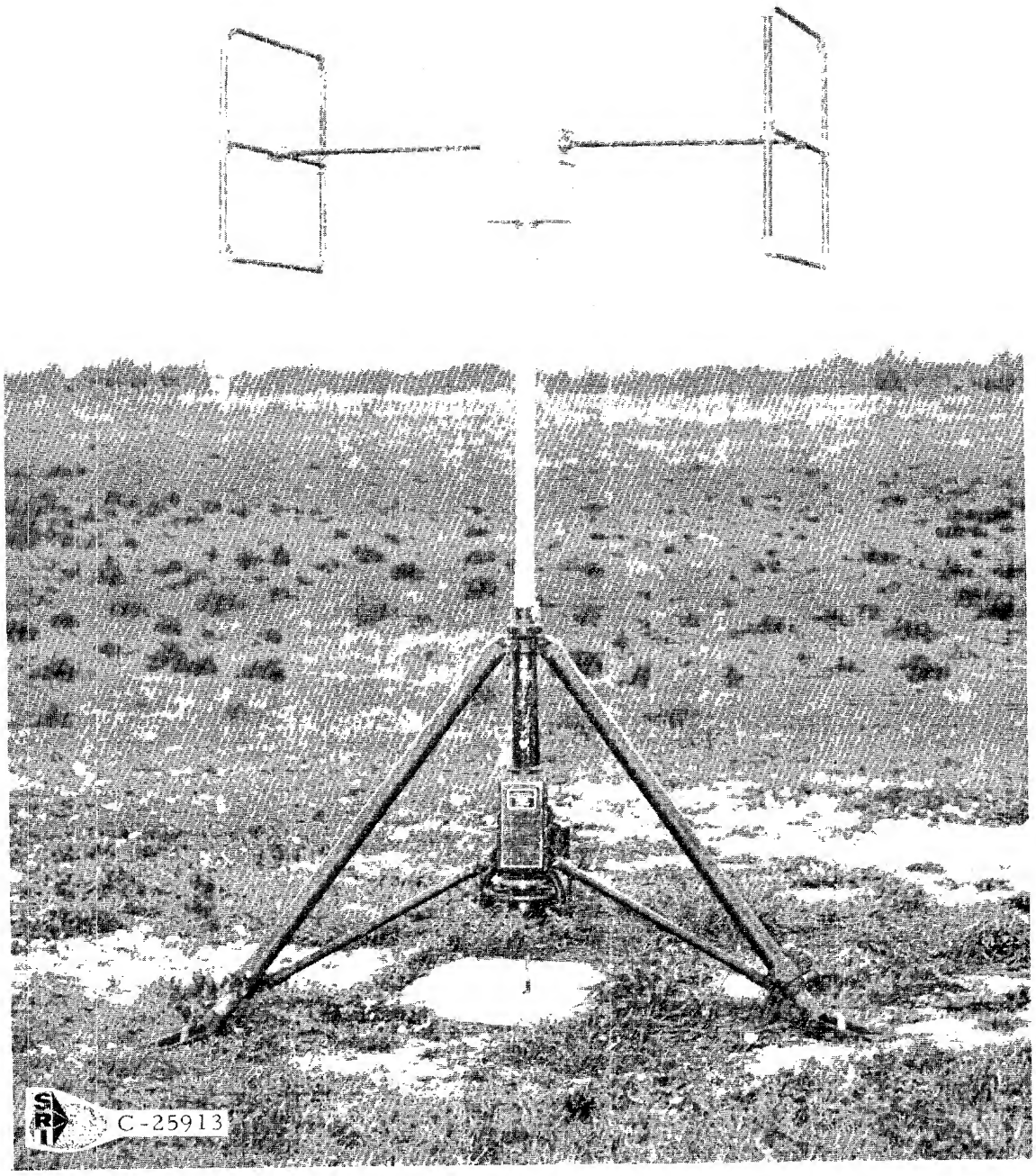

FIGURE 11

BREADBOARD HF COAXIAL SPACED LOOP ANTENNA (MODEL 2)
MOUNTED ON THE AN/PRD-7 AND 8 PEDESTAL

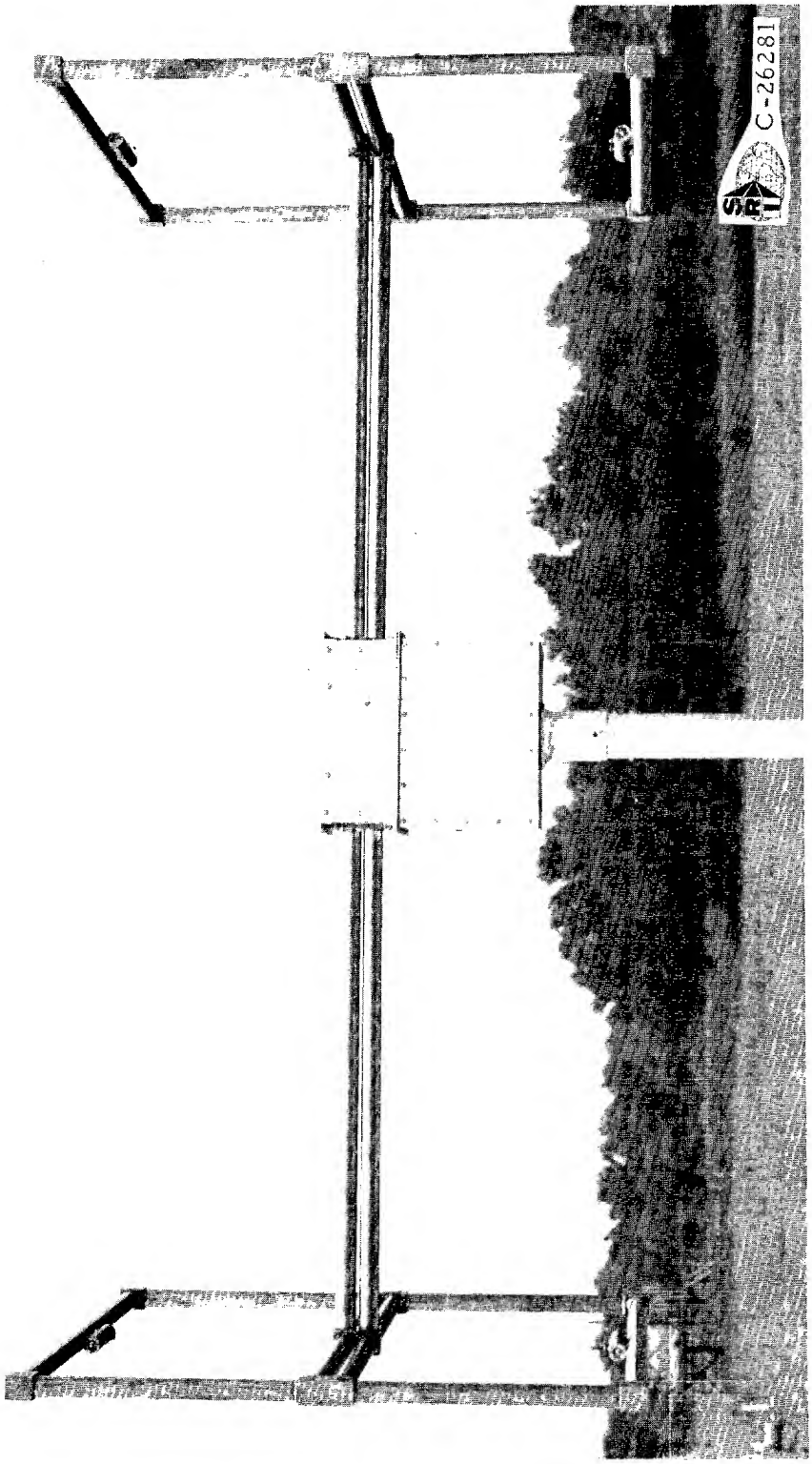

FIGURE 12

BREADBOARD HF COAXIAL SPACED LOOP ANTENNA (MODEL 3)

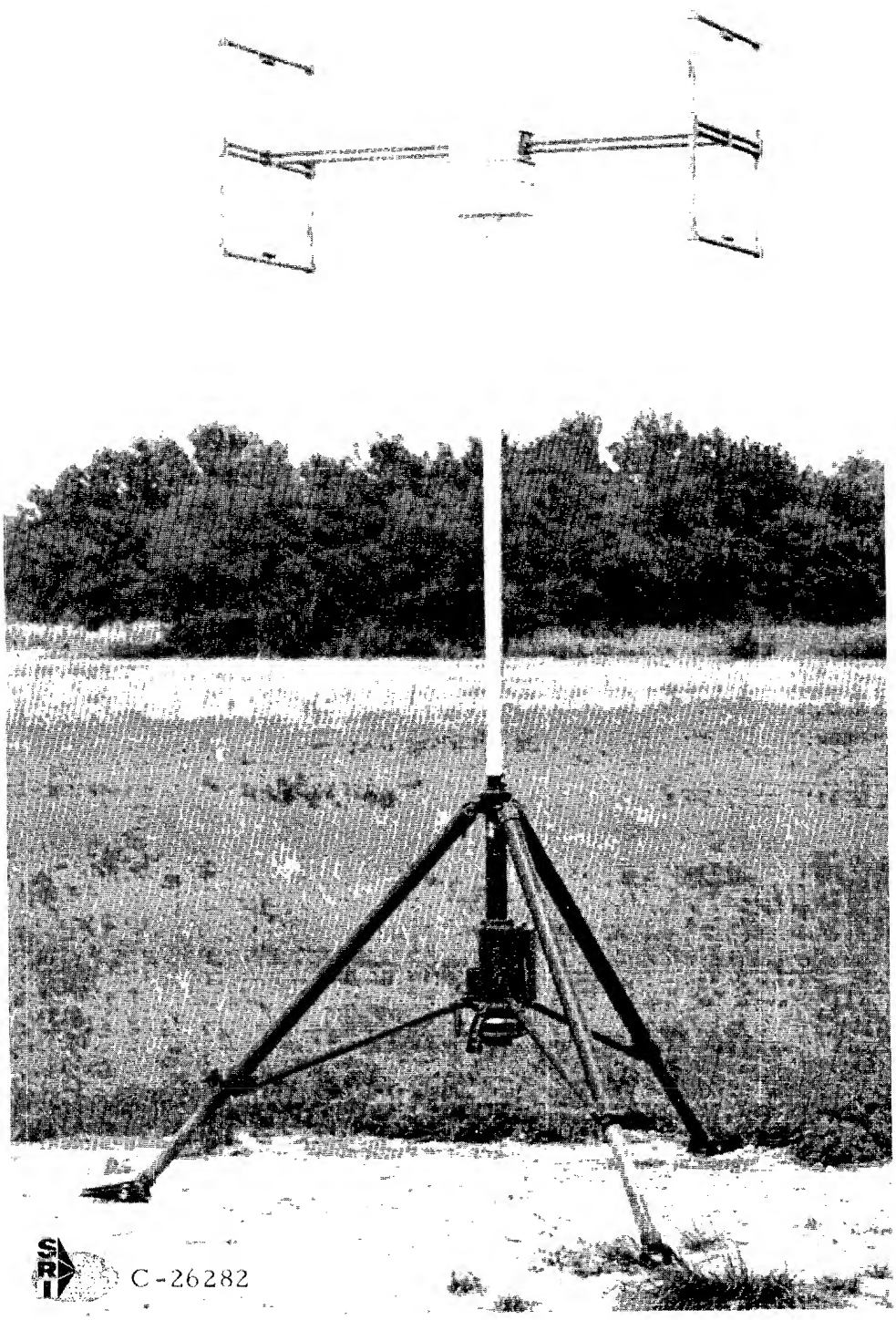

FIGURE 13

BREADBOARD HF COAXIAL SPACED LOOP ANTENNA (MODEL 3)
MOUNTED ON THE AN/PRD-7 AND 8 PEDESTAL

single gap arrangement. The relative position of the two gaps with respect to the support mast was important in the VHF antennas. However, there was no significant difference in the HF spaced loop work to date between placing the gaps on the top and bottom or on the sides.

The third breadboard model with various modifications has served as the basis for design of the final advanced development/feasibility model discussed in subsequent sections. A description of the antenna, discussions of modifications, and a description of the evaluation of the antenna may be found in the three quarterly reports.[3, 4, 5] The evaluation has included skywave bearing accuracy tests which were partially reported in Quarterly Report No. 2.[4] All skywave bearing data obtained with the third breadboard model are presented in Section 4.3.3.5 of this report so that it may be compared with the data obtained with the final advanced development/feasibility model.

4.2 Phase II - Design Phase

The design phase has been covered in the previous reports for this program.[3, 4, 5] The design was based upon the successful third breadboard model with a change to welded aluminum construction and a change in design to allow disassembly of the final model to produce a portable HF spaced loop antenna. The weight of the materials used in this first model is conservative, resulting in a total weight which is more than necessary. Other improvements have become obvious as this first unit was constructed and evaluated. A number of possible design improvements are given in Section 4.3.5.

The design of the advanced development/feasibility model of an HF spaced loop antenna has included the antenna structure, the rotation pedestal, and the interconnecting cables associated with the system. The equipment has been designed to be compatible with the DF indicator for the AN/TRD-20, or equivalent, and the radio receiver R-901/PRD. Neither of these equipments was furnished during the program, and the design was based on available information on the equipments.

The third model of the breadboard antenna was continuously updated throughout the design phase to incorporate the changes necessitated by a practical design. At the end of the design phase, the breadboard antenna was essentially the same as the anticipated final advanced development/feasibility model with the exception of materials and the provision for disassembly.

It should be pointed out that several parameters of the HF spaced loop are difficult to specify. Probably the most critical aspect of the

spaced loop is obtaining a balance between the two sides of the antenna. This may be equated to having equal impedance between the two loop elements of the antenna. It is estimated that the impedance of the two sides of the antenna as measured at the center crossover point must be equal within 0. 1 percent. This exceeds the measurement accuracies of most impedance bridges in the HF frequency range. The parameters given in the improved design section include the mechanical and electrical tolerances believed necessary to meet this requirement.

4. 3 Phase III - Equipment Construction and Evaluation

4. 3. 1 Introduction

The advanced development/feasibility model of the HF spaced loop antenna was designed and constructed as part of a portable HF spaced loop direction finder set (or system). The system will be discussed initially, followed by discussions of the individual components with emphasis on the antenna. The receiver and DF indicator specified by the U. S. Army were not furnished. Substitute equipments discussed in subsequent sections were used to complete the system.

4. 3. 2 Description of the HF Spaced Loop Direction Finder Set

4. 3. 2. 1 System Description

The components of the HF spaced loop direction finder set are detailed in Table 1. The modifications of components to be furnished by the U. S. Army are given. These modifications are detailed in the section covering the individual component. The pedestal modification is complete on the unit shipped, but the details of the minor modifications are given in Section 4. 3. 2. 3 so that other units may be modified if desired.

The equipment listed in Table 1 furnished by this laboratory is shown in the transit bags in Figure 14. The largest rectangular canvas covered case in Figure 14 contains the disassembled antenna and mast extension sections. The small rectangular canvas transit case contains the control unit for the pedestal and the antenna and the control unit to indicator cable. The pedestal, 100-ft control cable, and compass are enclosed in a transit carrying bag similar to the type normally used with the AN/PRD-7 and 8 system.

The components of the portable HF spaced loop DF set furnished by this laboratory have a total weight of 144. 5 lb. Table 2 gives the transit bag number, transit bag nomenclature, and details the components contained within each transit bag.

TABLE 1

List of Components for Portable HF Spaced Loop Direction Finder Set

Equipment	Quantity	Source	Modifications
Advanced development/ feasibility model of an HF spaced loop antenna	1	SwRI	None
Mast extensions	2	SwRI	None
Pedestal (modified AN/PRD-7&8 type)	1	SwRI - purchased from AEL	As detailed in section 4.3.2.3
Pedestal control cable	1	SwRI	None
Pedestal and antenna control unit	1	SwRI	None
Control unit to indicator cable	1	SwRI	None
AN/ TRD-20, AN/ TRQ-23, or AN/ PRD-5 DF indicator	1	U.S. Army	a) Verify wiring of the unit for the recommended interconnect schematic, Figure 15. b) Improve overall performance for spaced loop as detailed in section 4.3.2.5.1
R-901/ PRD receiver	1	U.S. Army	Improve video detector linearity and set video DC level for DF indicator as necessary as detailed in section 4.3.2.5.2
AN/ PRD-7&8 battery pack or equivalent	1	U.S. Army	None
Power cable to indicator	1	U.S. Army	As required with type indicator used
Video cable - receiver to indicator	1	U.S. Army	Per Figure 15 and actual receiver used.

Approved For Release 2001/09/03 : CIA-RDP76-00451R000200010013-1

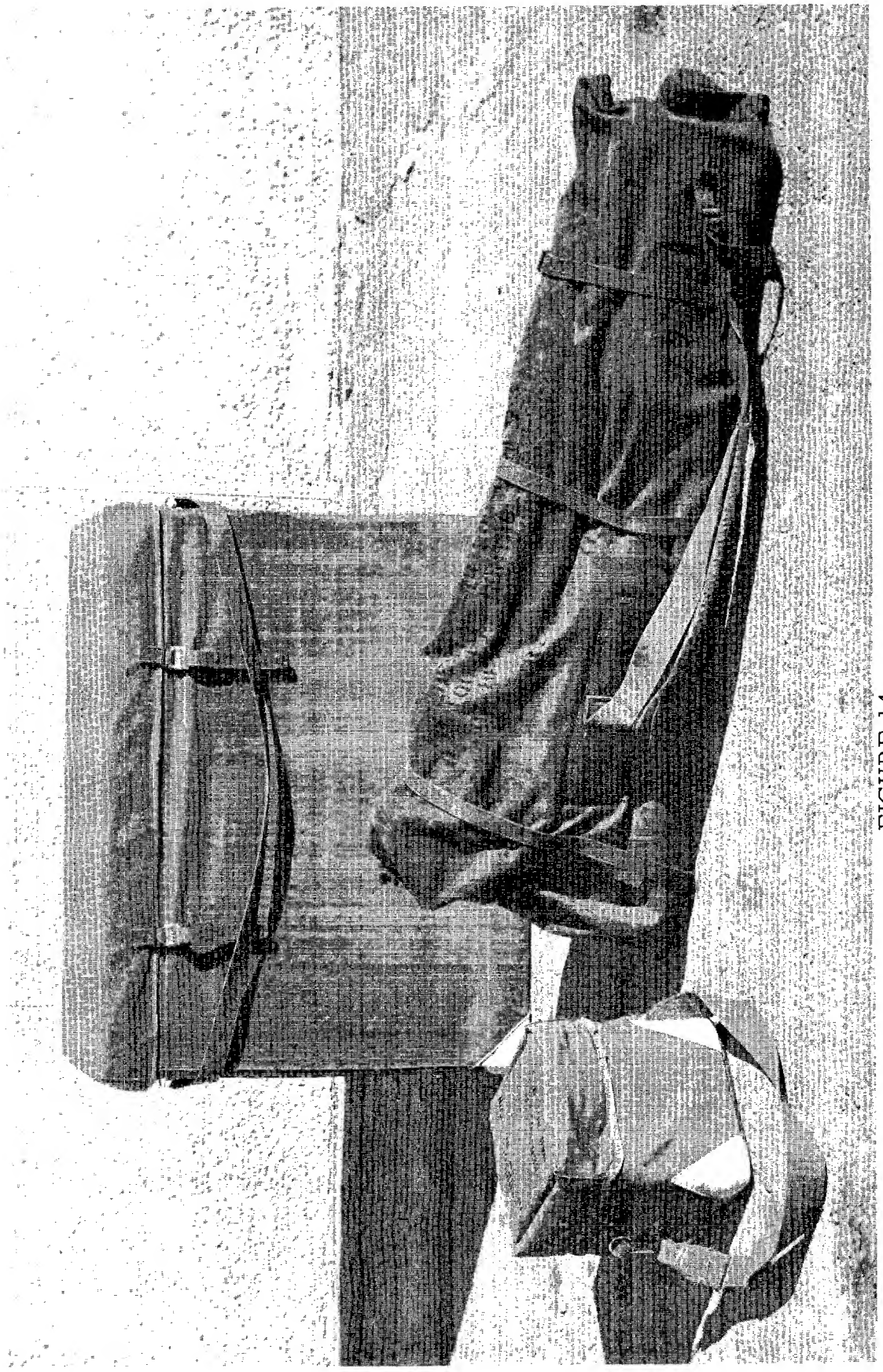

FIGURE 14
COMPONENTS OF PORTABLE HF SPACED LOOP DIRECTION FINDER SET
CONSTRUCTED BY SOUTHWEST RESEARCH INSTITUTE
SHOWN IN TRANSIT BAGS

TABLE 2
Transit Bag Nomenclature, Contents, and Weights
For the HF Spaced Loop DF Set

Transit Bag Number and Nomenclature	Part Name	Qty.	Unit Wt.	Total Wt.
Bag 1 - Antenna, HF spaced loop DF set	Loop assembly	2	3.75	7.5
	Boom element assembly	2	2.25	4.5
	Electronics assembly	1	9.0	9.0
	Loop braces	8	.5	4.0
	Mast extensions	2	2.5	5.0
	Transit bag	1	27.0	27.0
	TOTAL WEIGHT			57.0 lbs.
Bag 2 - Pedestal, tripod, compass, 100-ft. control cable for DF set	Modified AN/PRD-7&8 pedestal	1	49.0	49.0
	100-ft. pedestal control cable	1	18.0	18.0
	Compass	1	.5	.5
	Transit bag	1	7.5	7.5
	TOTAL WEIGHT			75.0 lbs.
Bag 3 - Control unit for the HF spaced loop DF set	Control unit for the HF spaced loop DF set	1	9.5	9.5
	Control unit to indicator cable	1	.5	.5
	Transit bag	1	2.5	2.5
	TOTAL WEIGHT			12.5 lbs.

Bag 4 — Indicator
Bag 5 — Power
Bag 6 — Receiver

If all components of the system listed in Table 1 were available, then the recommended interconnection schematic of Figure 15 is applicable. Figure 15 also gives the schematic of the mast extensions used between the pedestal and antenna. The shielding and ground circuits are necessary to avoid stray pickup on the control leads. The mast extensions used with the VHF spaced loop developed under Contract DA 28-043 AMC-01633(E) are similar; therefore, the masts are keyed so that both mate with the pedestal but so that the VHF and HF antennas cannot be placed on the wrong mast.

The interconnection cables associated with the DF indicator and the R-901/PRD receiver are based on available information. However, available schematics of DF indicators of the AN/TRD-20, AN/TRQ-23, or AN/PRD-5 types vary slightly in circuitry. For this reason, it is suggested that Figure 15 be compared to the particular unit which will be used by the U. S. Army. Control cables distinctly associated with equipments not furnished the contractor are not included for this reason.

In the evaluation of the HF spaced loop antenna, an R-390A/U receiver with a separate outboarded IF amplifier and DF video detector was used in place of R-901/PRD receiver. Information on the IF amplifier and DF video detector is given in Section 4. 3. 2. 5. 2.

4. 3. 2. 2 Advanced Development/Feasibility HF Spaced Loop Antenna

The advanced development/feasibility model of an HF spaced loop antenna represents the primary emphasis of this program. This section will emphasize a description of the antenna in the form delivered to the U. S. Army. Critical specifications will be given in the section on an improved design (Paragraph 4. 3. 5).

The advanced development/feasibility model of the HF spaced loop antenna, Serial No. 1, is shown in the transit case in Figure 16. Included in this transit case with the disassembled antenna components are the two mast sections. The canvas transit case is filled with foamed polyurethane with slots to retain the antenna components.

The components of the HF spaced loop antenna are shown in front of the transit bag in Figure 17. The antenna is shown assembled in Figure 18. The break-apart connectors between the loops, boom elements, and center electronics housing are identical to those used on the VHF spaced loop antennas developed under Contract DA 28-043 AMC-01633(E) as discussed in References 14 and 18. Quick disconnect clamps are used to hold the five major parts of the antenna together when assembled. Braces are

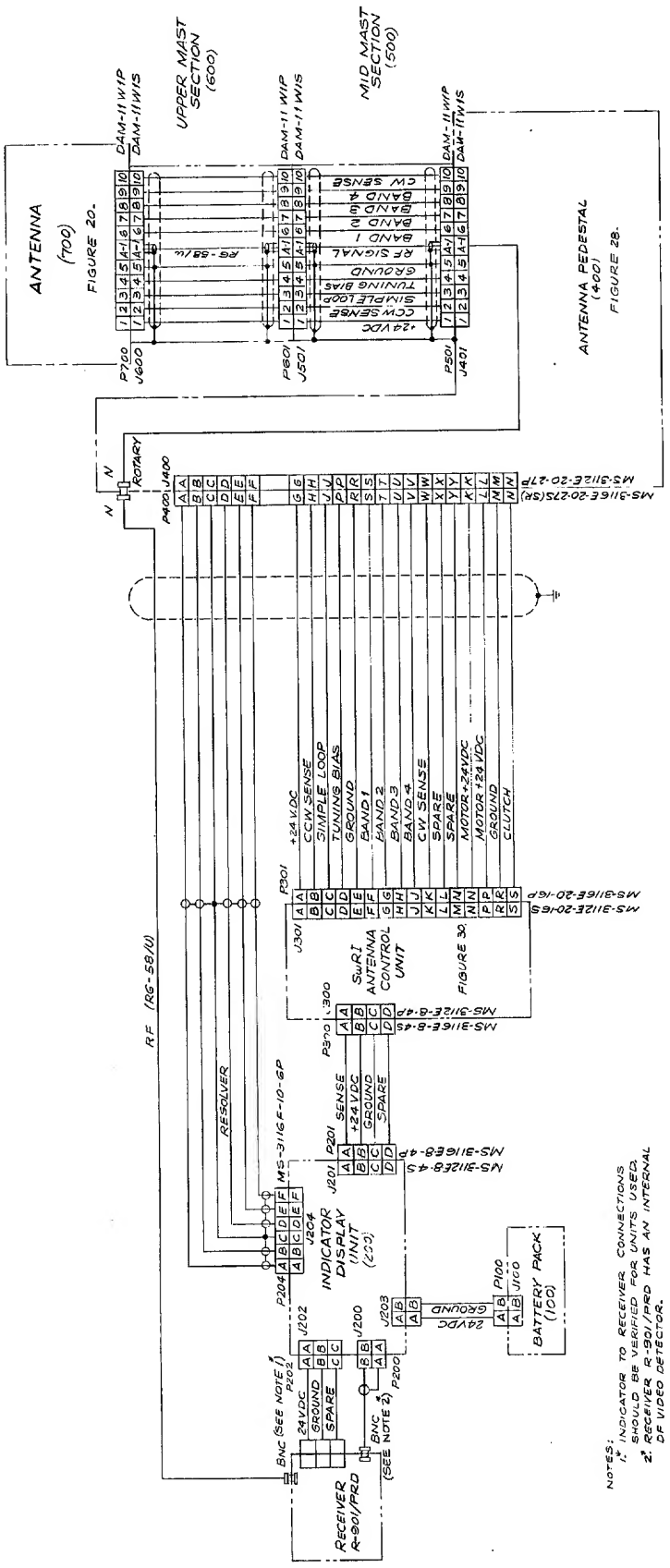

FIGURE 15. INTERCONNECTION AND MAST EXTENSION SCHEMATIC

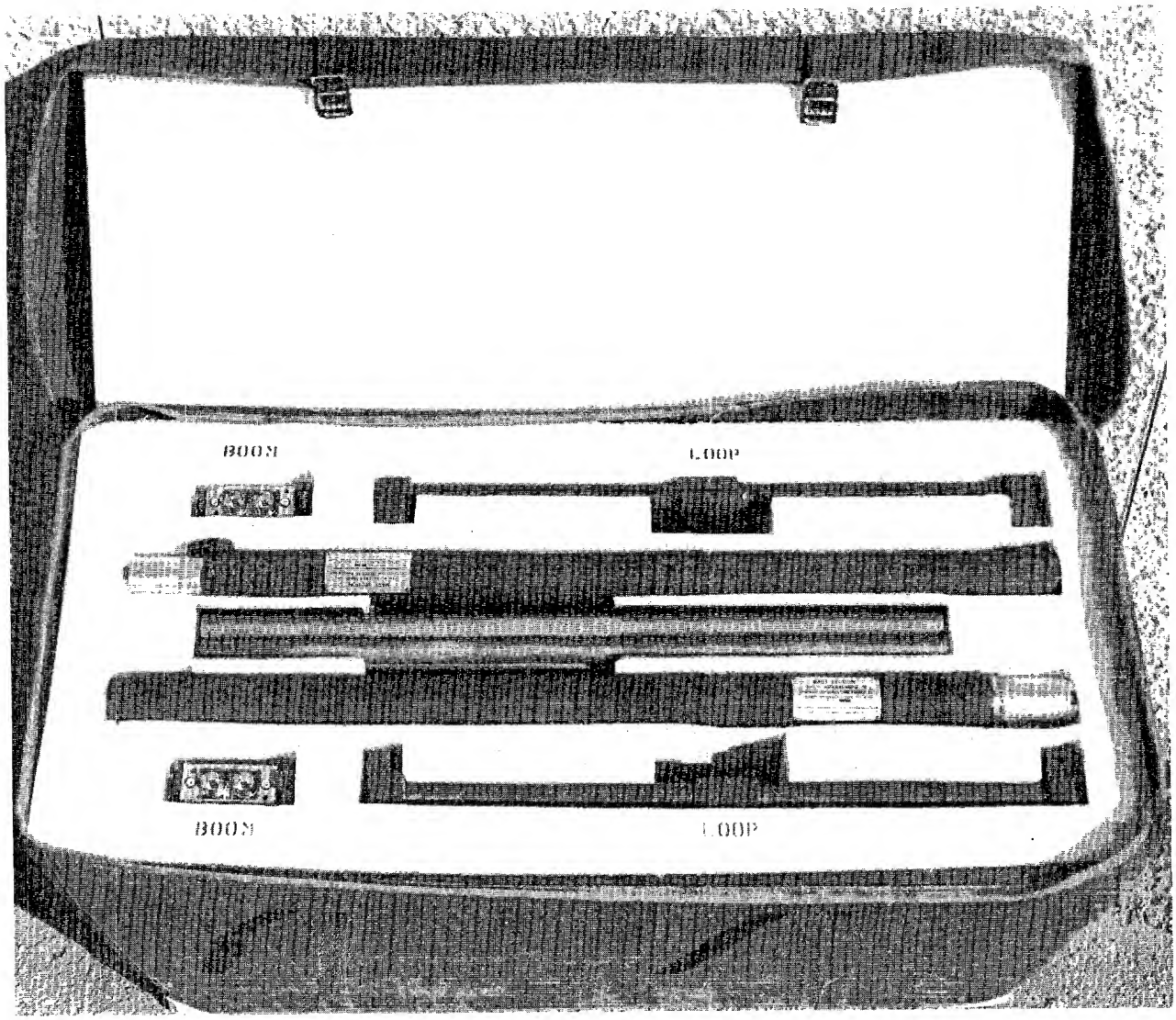

FIGURE 16
THE DISASSEMBLED PORTABLE HF SPACED LOOP ANTENNA
IN THE TRANSIT CASE

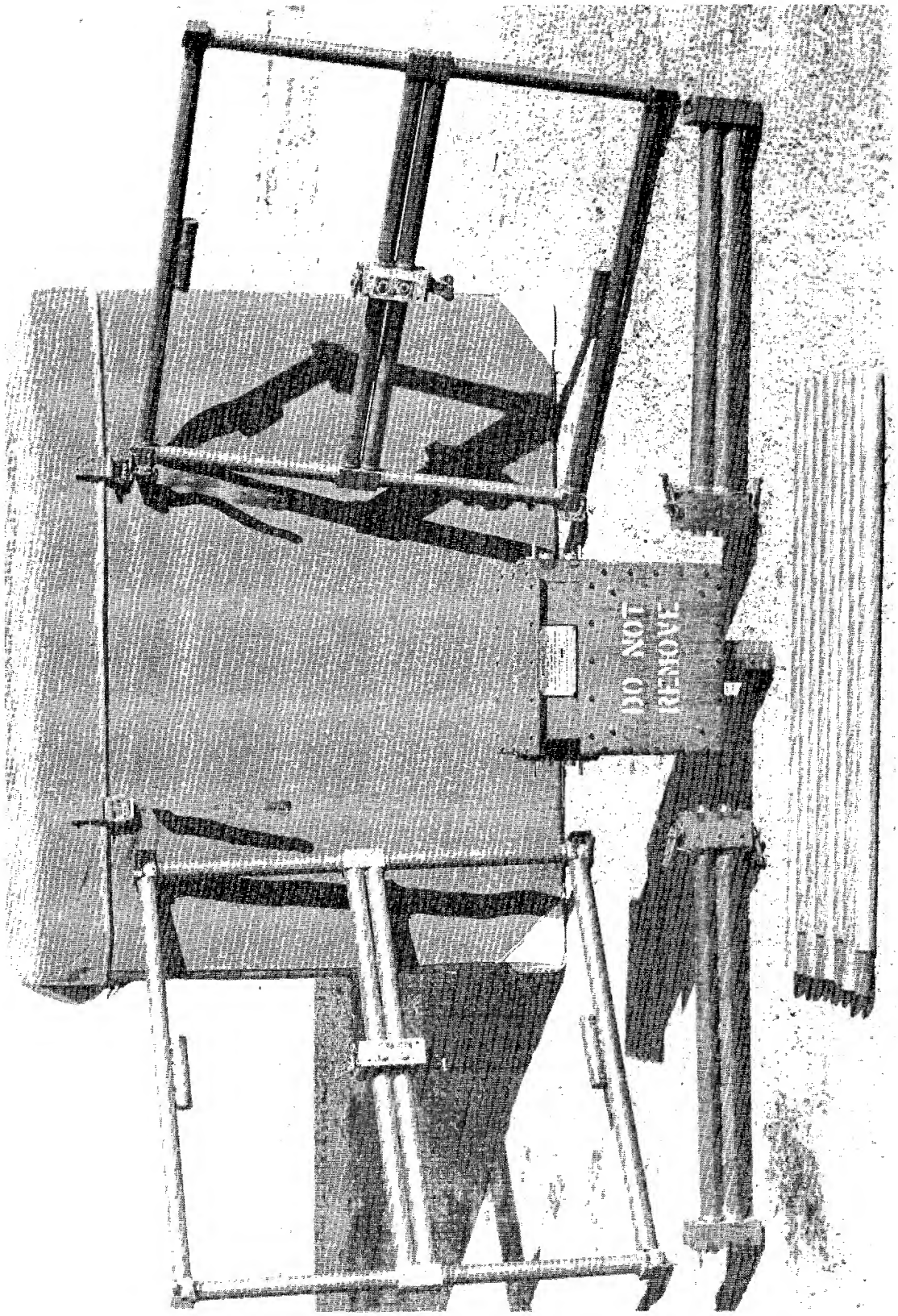

FIGURE 17
THE DISASSEMBLED PORTABLE HF SPACED LOOP ANTENNA

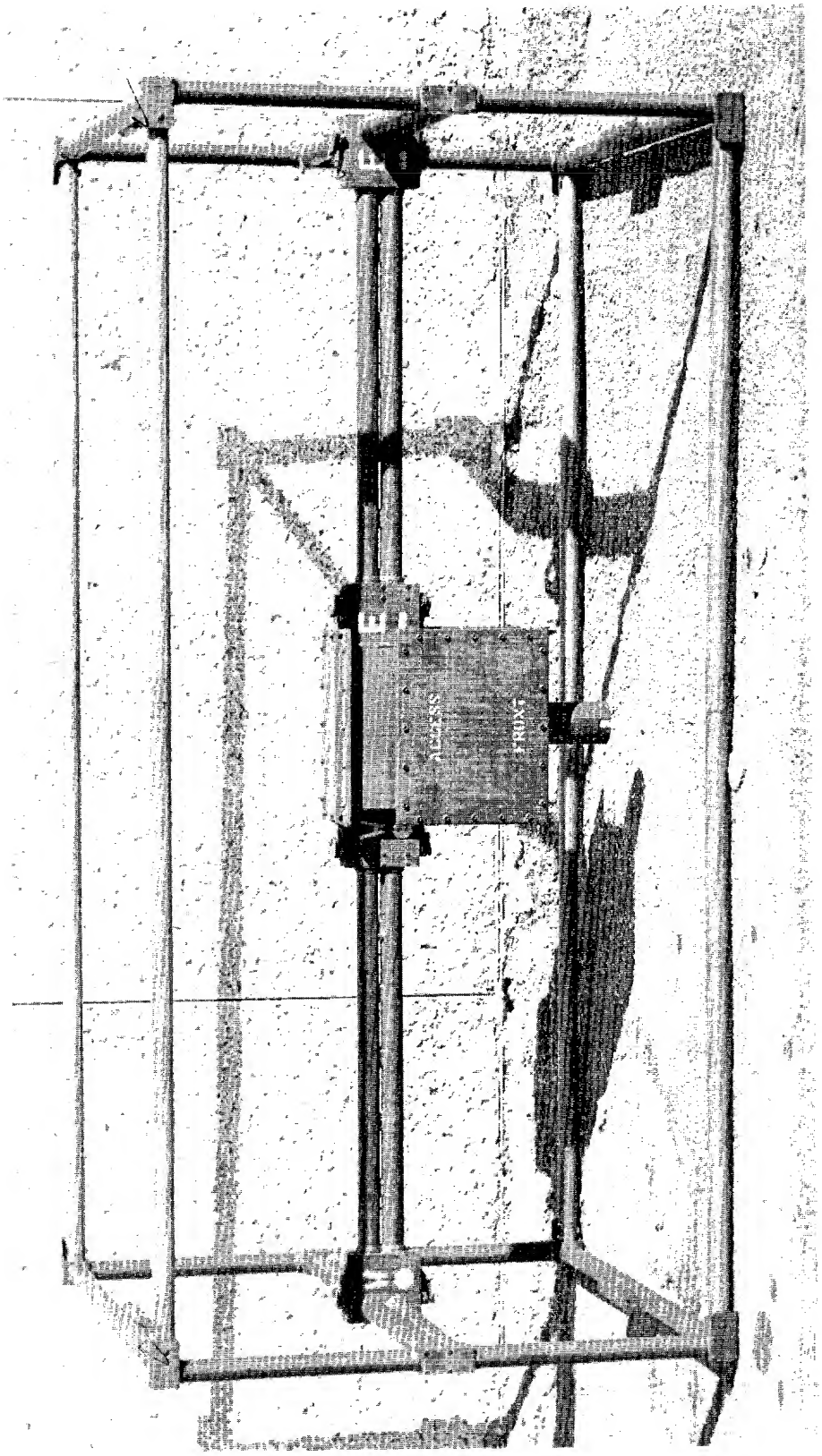

FIGURE 18
ASSEMBLED PORTABLE HF SPACED LOOP ANTENNA

installed between opposing corners of the two loops to establish the required spaced loop geometry. As discussed in Paragraph 4.3.5, improved flange surfaces between the loops, boom elements, and center electronics housing probably would establish the required geometry without bracing. The mating parts of the antenna are marked with a code system so that they may be quickly assembled. The loops and boom elements are not interchangeable and are keyed so that they cannot be installed incorrectly.

The antenna is shown mounted 10 ft above the ground using the two 2-1/2-ft mast extension sections on the modified AN/PRD-7 and 8 pedestal in Figure 19.* This is the recommended operational configuration. The 10-ft height appears necessary to reduce site error from the single control cable.[3] Although a ground stake may be seen immediately below the center of the pedestal in Figure 19, physical grounds of the pedestal were avoided because of the portable requirement.

The schematic of the advanced development/feasibility model of an HF spaced loop is shown in Figure 20. The three-turn loops are fed through the boom assembly to the crossover switching assembly at the center of the antenna. The purpose of the crossover switching assembly is to reverse the antenna from a spaced loop mode to a simple loop mode by changing the connection between the loops from parallel opposition to parallel aiding. The output of the crossover switching network is fed to the tuning network and the FET source follower amplifier of Figure 21. The balanced broadband transistor amplifier of Figure 22 is used to raise the signal level so that the effects of stray pickup on the control cable will be eliminated. A balanced to unbalanced balun (T-1) is included as part of the broadband amplifier of Figure 22.

Tuning of the antenna is accomplished using the varactor diodes shown in Figure 21. The diodes tune the antenna inductive reactance over the lowest frequency band. For the higher frequency bands, the antenna is shunted with inductance to decrease the effective inductance.

The control circuitry is straightforward. The series voltage regulator of Figure 23 provides +16 volts DC ±0.5 volt DC for the amplifiers for primary supply variations of +18 to +32 volts DC. Sensitivity is independent of the battery pack voltage limitations for the limits given.

The circuit of Figure 23 differs slightly from the circuit in the antenna shipped to the U. S. Army. The 10-ohm resistors, R-704 and R-705, were not included in the unit but are recommended to prevent shunt circuit damage to the regulator circuit.

*It is essential that the control cable within each mast section be wired in accordance with Figure 15.

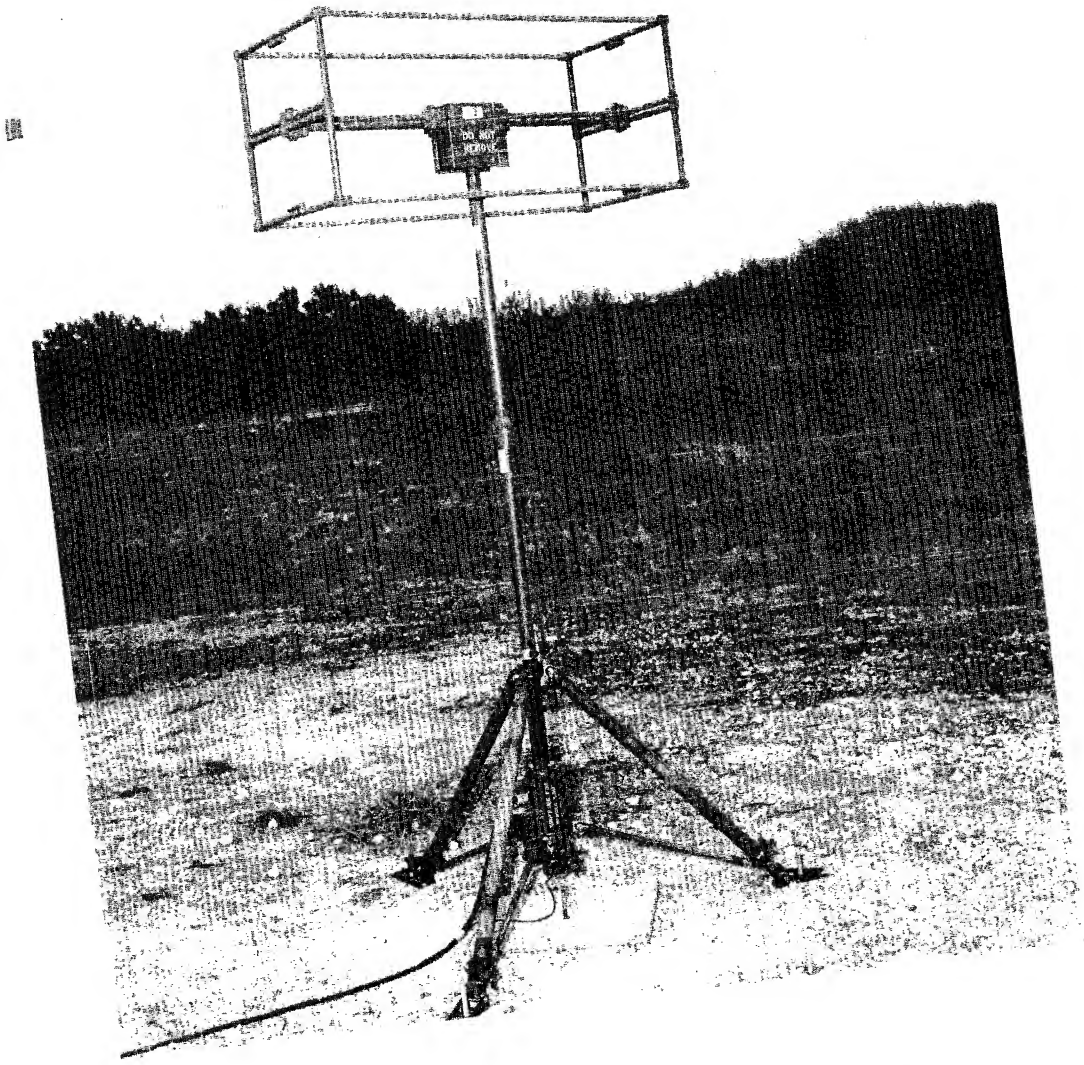

FIGURE 19
PORTABLE HF SPACED LOOP ANTENNA ON
THE MODIFIED AN/PRD-7 AND 8 PEDESTAL

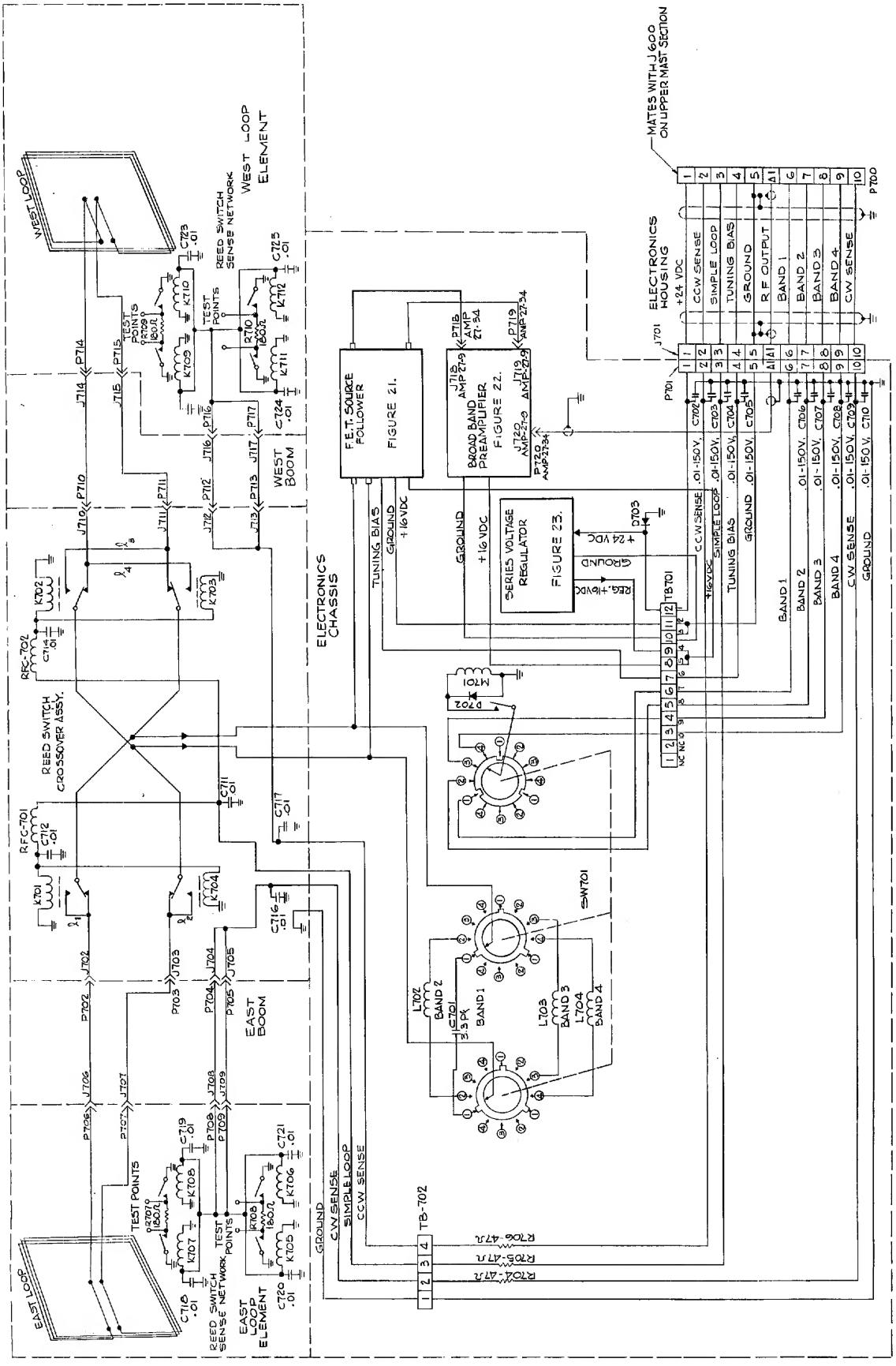

FIGURE 20
PORTABLE HF SPACED LOOP ANTENNA SCHEMATIC

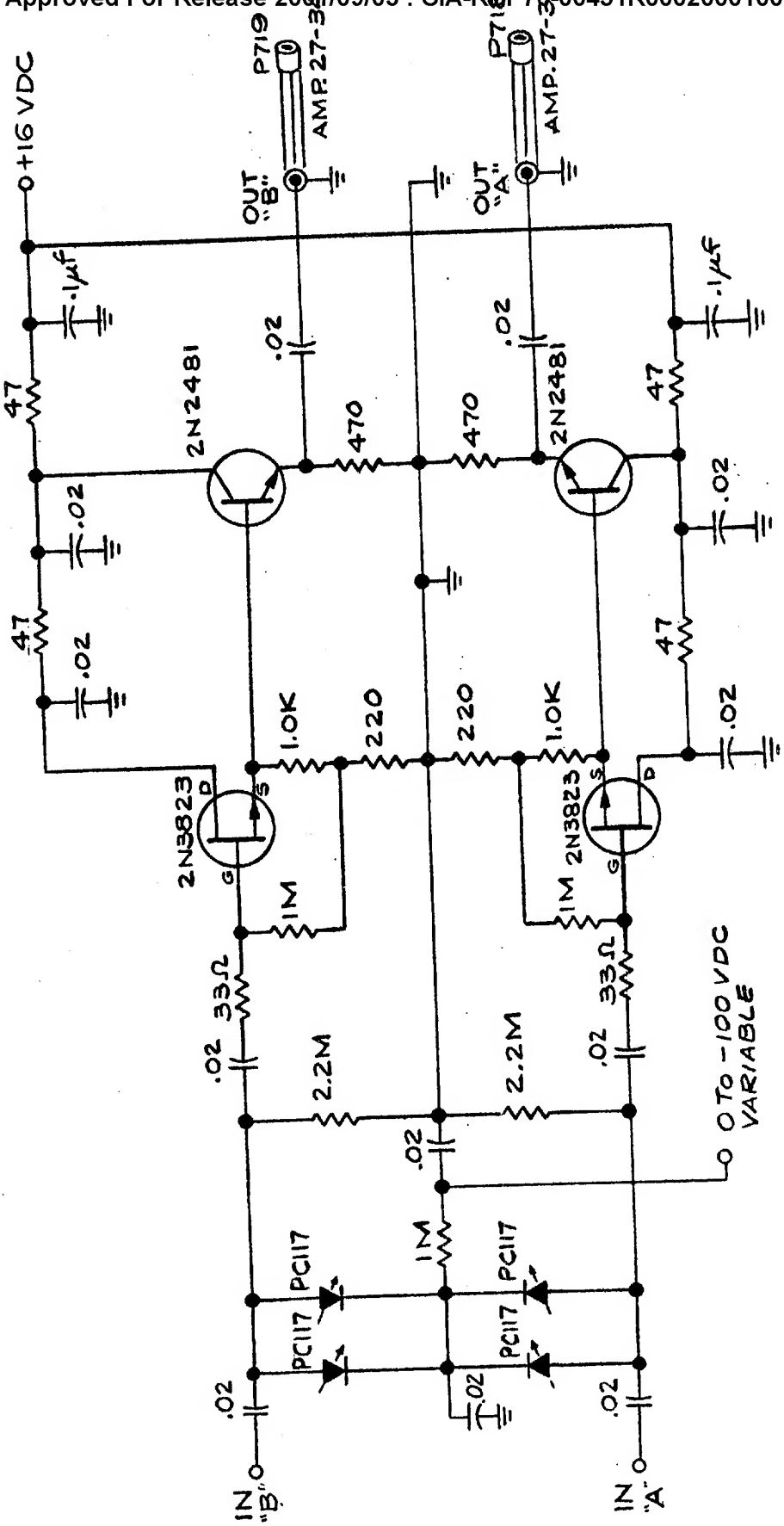

FIGURE 21. FIELD EFFECT TRANSISTOR SOURCE FOLLOWER SCHEMATIC

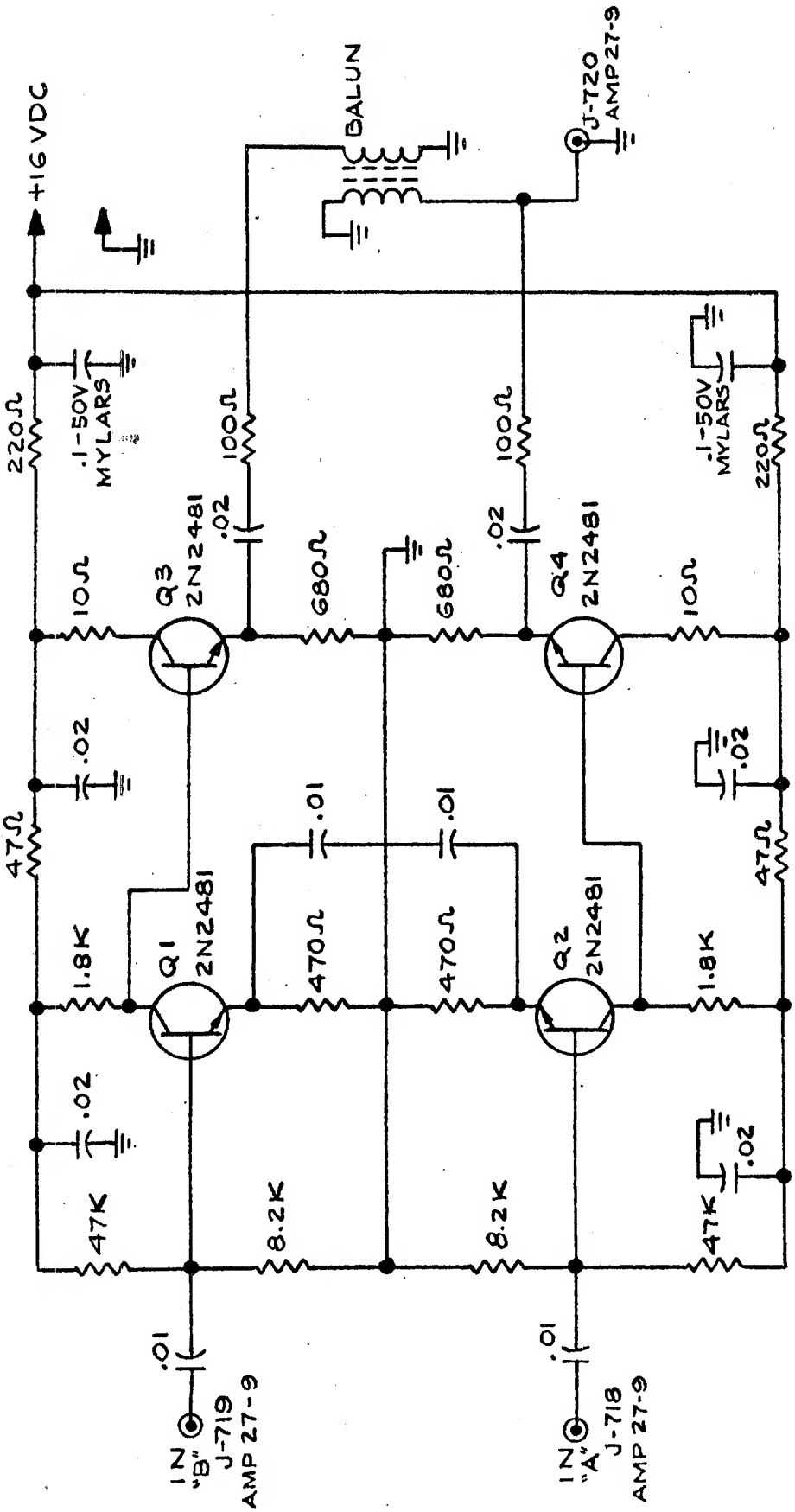

NOTES:
1. ALL RESISTORS 1/4 W. MATCHED PAIRS
2. ALL CAPACITORS DISC CERAMICS 150 VDC, UNLESS NOTED.

FIGURE 22. BROADBAND PREAMPLIFIER SCHEMATIC

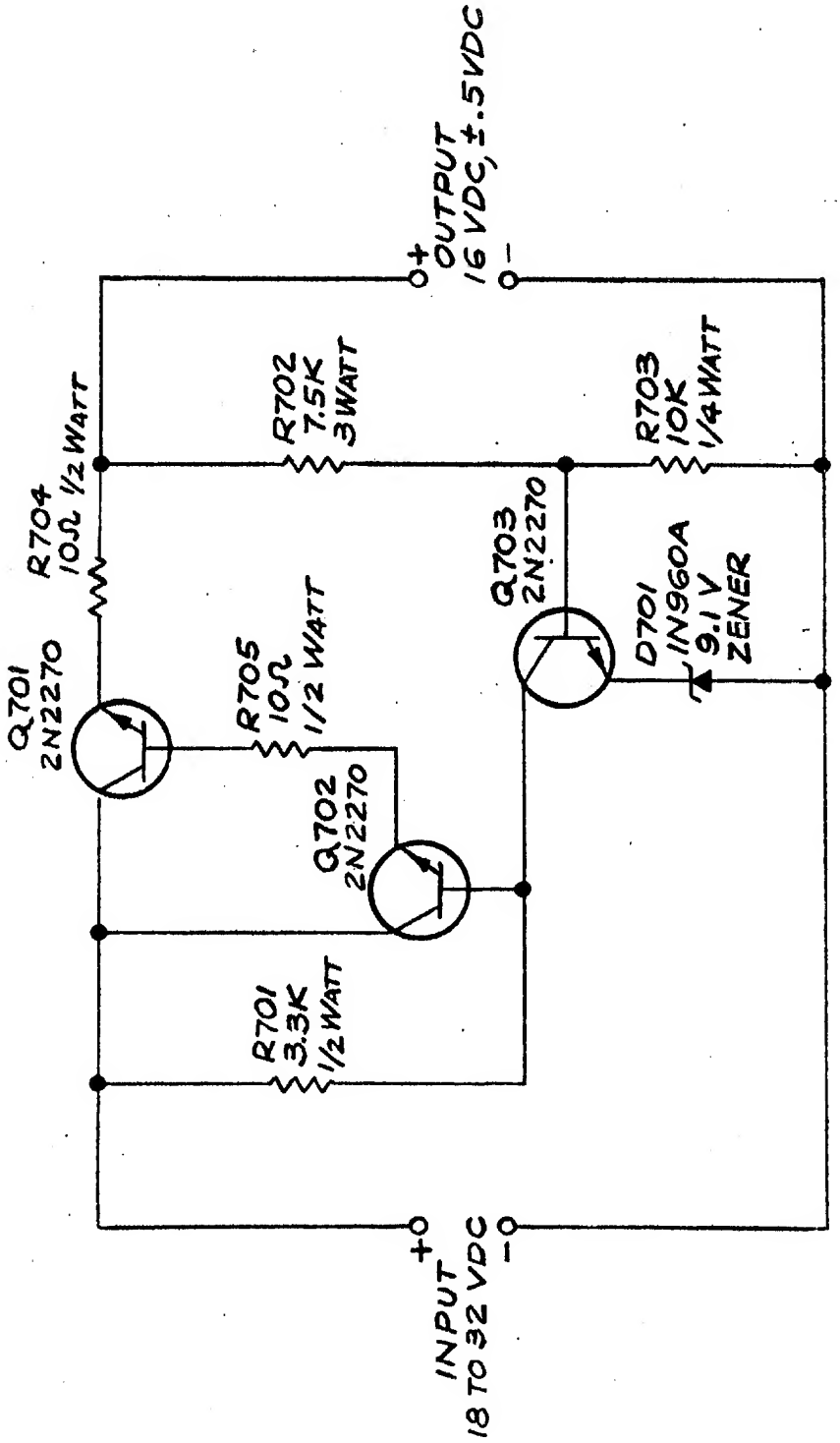

FIGURE 23. RECOMMENDED VOLTAGE REGULATOR SCHEMATIC FOR SwRI SPACED LOOP ANTENNAS

The reed switch sense networks in each loop schematic of Figure 20 are used to place sense resistors across the two shielded gaps of the loop for the sense mode. If resistors of the proper value are placed across the shield gaps of the east loop, the clockwise (CW) sense pattern is obtained. Resistors on the gaps of the west loop produce the counterclockwise (CCW) sense pattern. The normal sense mode discussed later is the CCW sense pattern with the normal DF indicator deflection plate connections from the reference resolver switched 90° counterclockwise. The sense mode is discussed further in the section on operations. The sense network assembly is further detailed in the section on maintenance. The electronics housing has two side access doors and a top access door. Because of the manner in which the electronics chassis is fastened to one side access door, this door has been marked "DO NOT REMOVE," as illustrated in Figure 17. If the other access door marked "ACCESS" is removed, then the electronics chassis can be seen as shown in Figure 24. The primary subassemblies of the electronics chassis are indicated in Figures 24 and 25. The antenna leads are fed to the source follower, which is also connected to the bandswitch assembly.

The removal of the electronics chassis from the electronics housing requires that leads to the crossover switching assembly be disconnected at terminal board TB-702. The antenna leads must be unsoldered at the point indicated in Figure 24, and the control cable connector J-701 must be disconnected. The four chassis retaining nuts and the side access door marked "DO NOT REMOVE" may be removed with the electronics chassis attached as shown in Figure 25. Reinstallation of the electronics chassis requires that leads from the crossover switching network be reconnected to TB-702, that the power connector control cable connector J-701 be connected to P-701, and that the antenna leads be resoldered to the output of the crossover switching network terminals as indicated in Figure 24.

Removal of the top access door provides access to the crossover switching assembly as shown in Figure 26. As discussed later in this report, this function has proven unnecessary in operation of the HF spaced loop antenna. However, the function is useful during the development and preliminary tests of a spaced loop antenna, and it provides a sensitive intercept mode. The sense control leads are routed up from TB-702 into this area and then to the connectors on the sides of the housing which mate with connectors on the boom elements.

The HF spaced loop antenna of this development was designed for 4 to 8 MHz. The upper frequency range was extended one band above 8 MHz to insure that distortion problems associated with stray pickup on

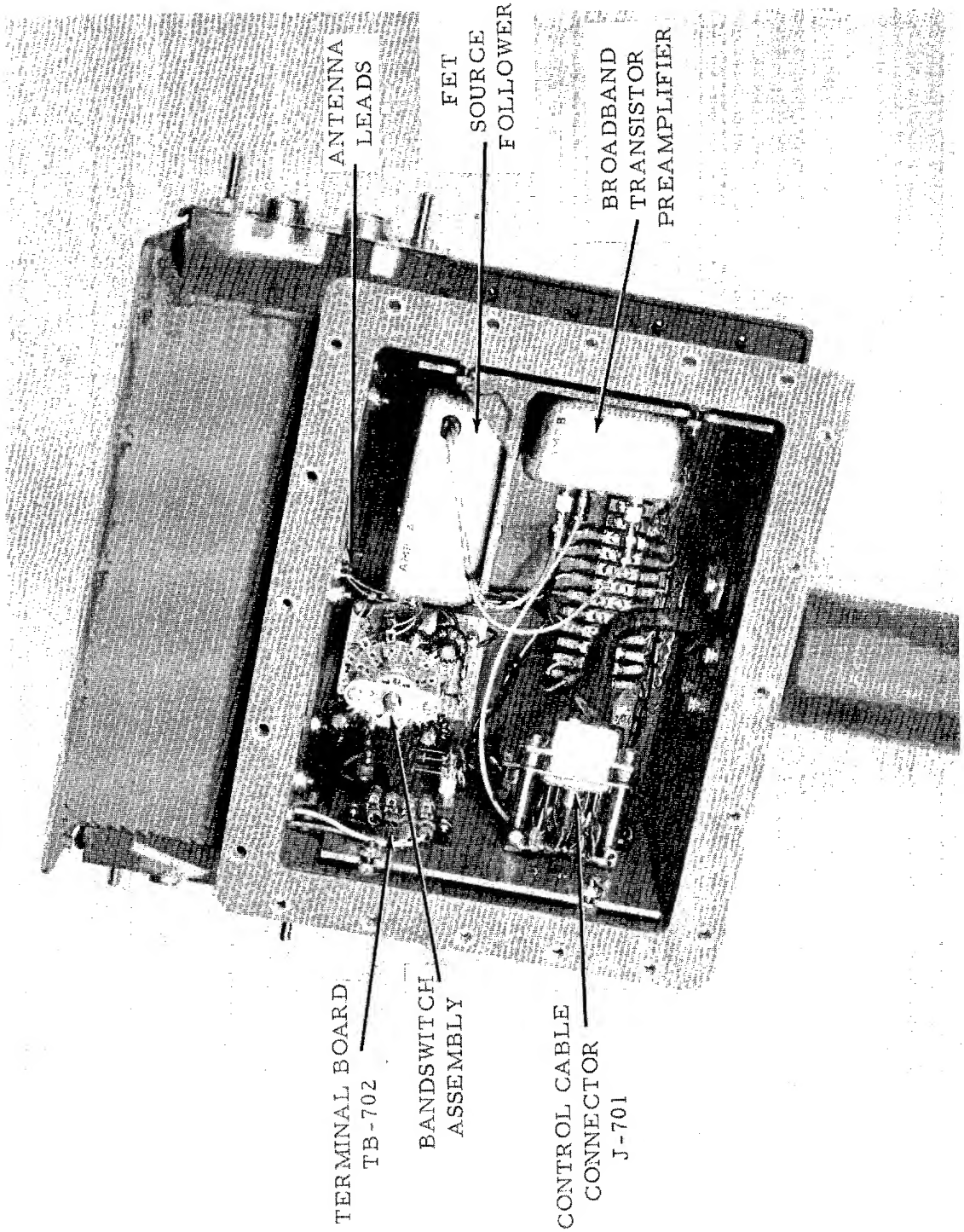

FIGURE 24
ELECTRONICS HOUSING WITH SIDE DOOR REMOVED
FOR ACCESS TO ELECTRONICS CHASSIS

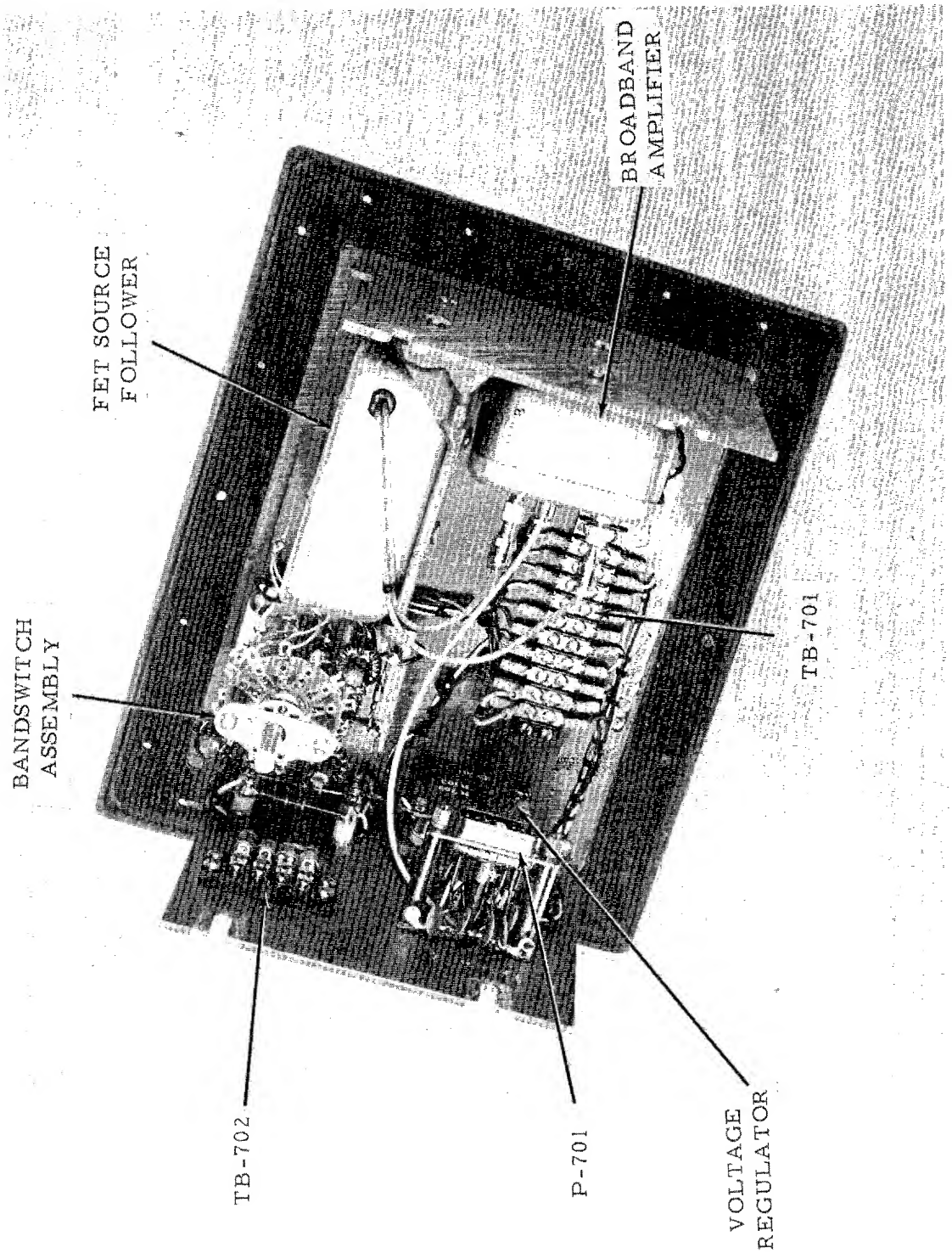

FIGURE 25
ELECTRONICS CHASSIS

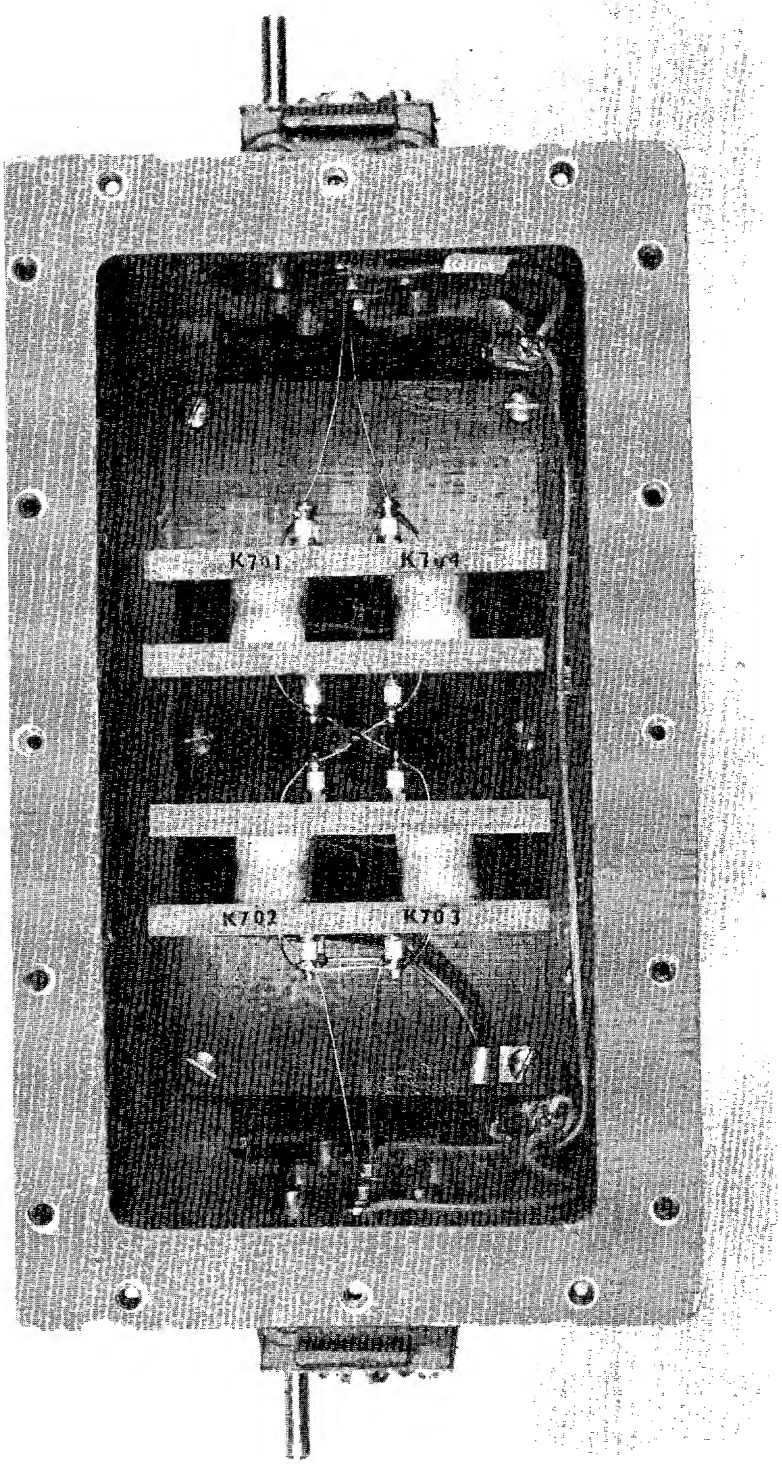

FIGURE 26
TOP ACCESS DOOR REMOVED FOR ACCESS TO CROSSOVER SWITCHING ASSEMBLY

control leads in the mast sections was not present. This problem occurred in the third breadboard model[3, 4] and in an HF spaced loop developed under contract DA 28-043 AMC-02368(E).[19] Tests of the final antenna above 8 MHz were restricted to those spaced loop pattern quality tests necessary to determine that the problem had not reoccurred in the final model.

The final tuning range of the four bands of the antenna is given below:

Band	Frequency Range
1	3.8 to 5.6 MHz
2	5.0 to 7.5 MHz
3	7.0 to 10.0 MHz
4	9.9 to 13.9 MHz

4.3.2.3 Rotation Pedestal

The AN/PRD-7 and 8 rotation pedestal was selected for use with the HF spaced loop antenna because previous experience had indicated that this pedestal could be easily modified to be compatible with the spaced loop antenna. In addition, the work under contract DA 28-043 AMC-01633(E) had proven that the unit was very reliable.

The rotation pedestal furnished under this program was purchased from American Electronics Laboratories. The pedestal was ordered as an original AN/PRD-7 and 8 unit with certain modifications to make the unit compatible with spaced loop antennas in the HF and VHF frequency ranges. The pedestal is shown in Figure 27 with the carrying bag open with the pedestal and the 100-ft antenna control cable removed. In addition to the pedestal and control cable, a compass is enclosed in a side pocket.

The modifications to original AN/PRD-7 and 8 specifications were as follows:

First, the pedestal was completely rewired to include a 12-contact slip ring assembly in accordance with the schematic of Figure 28. This schematic is different from the schematic of the AN/TRQ-23 pedestal unit now being produced for the U. S. Army which also has a 12-contact slip ring. It will be noted that all control leads are bypassed. This has proven necessary to avoid uncontrollable stray pickup on the control leads. The wiring of the reference resolver is identical to the original AN/PRD-7 and 8 reference resolver wiring. The coaxial shield and the

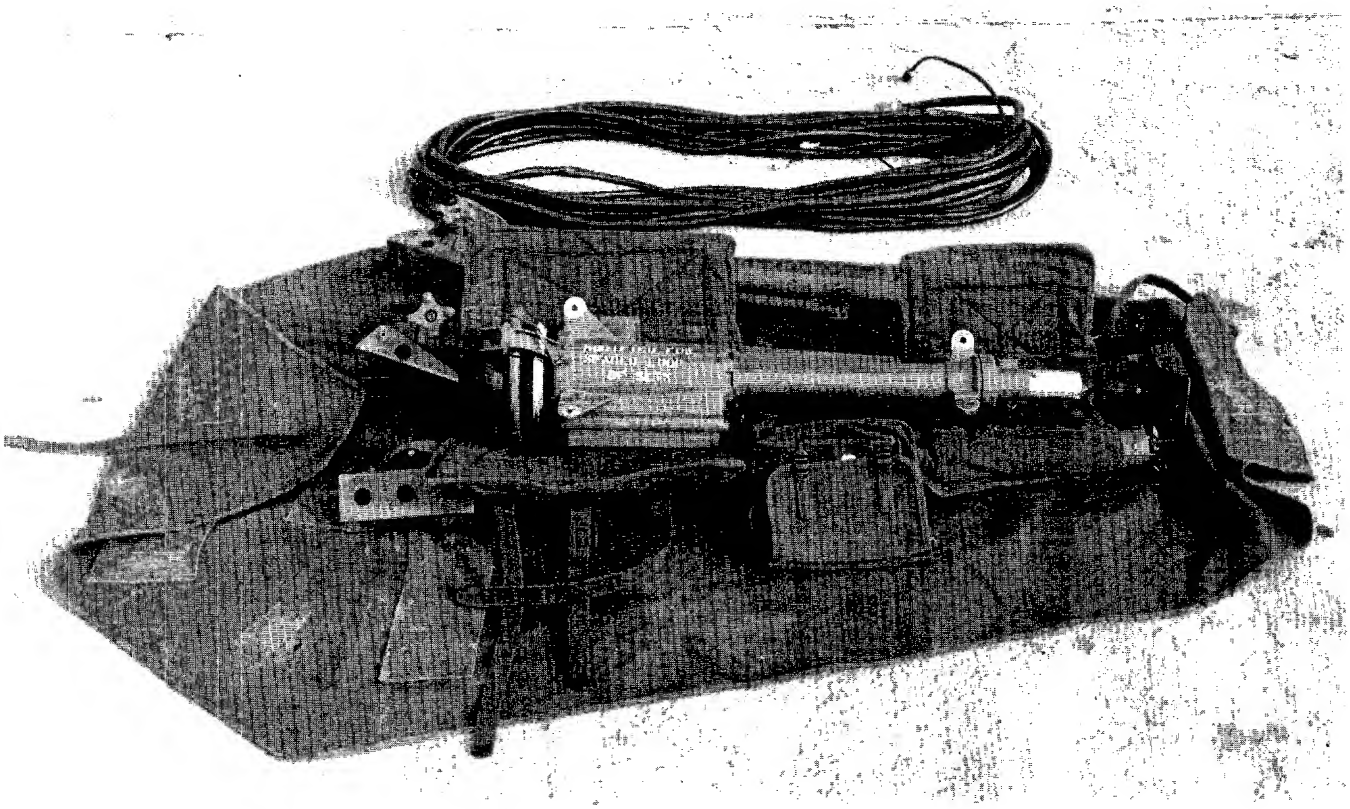

FIGURE 27

PEDESTAL AND CONTROL CABLE
REMOVED FROM CARRYING BAG

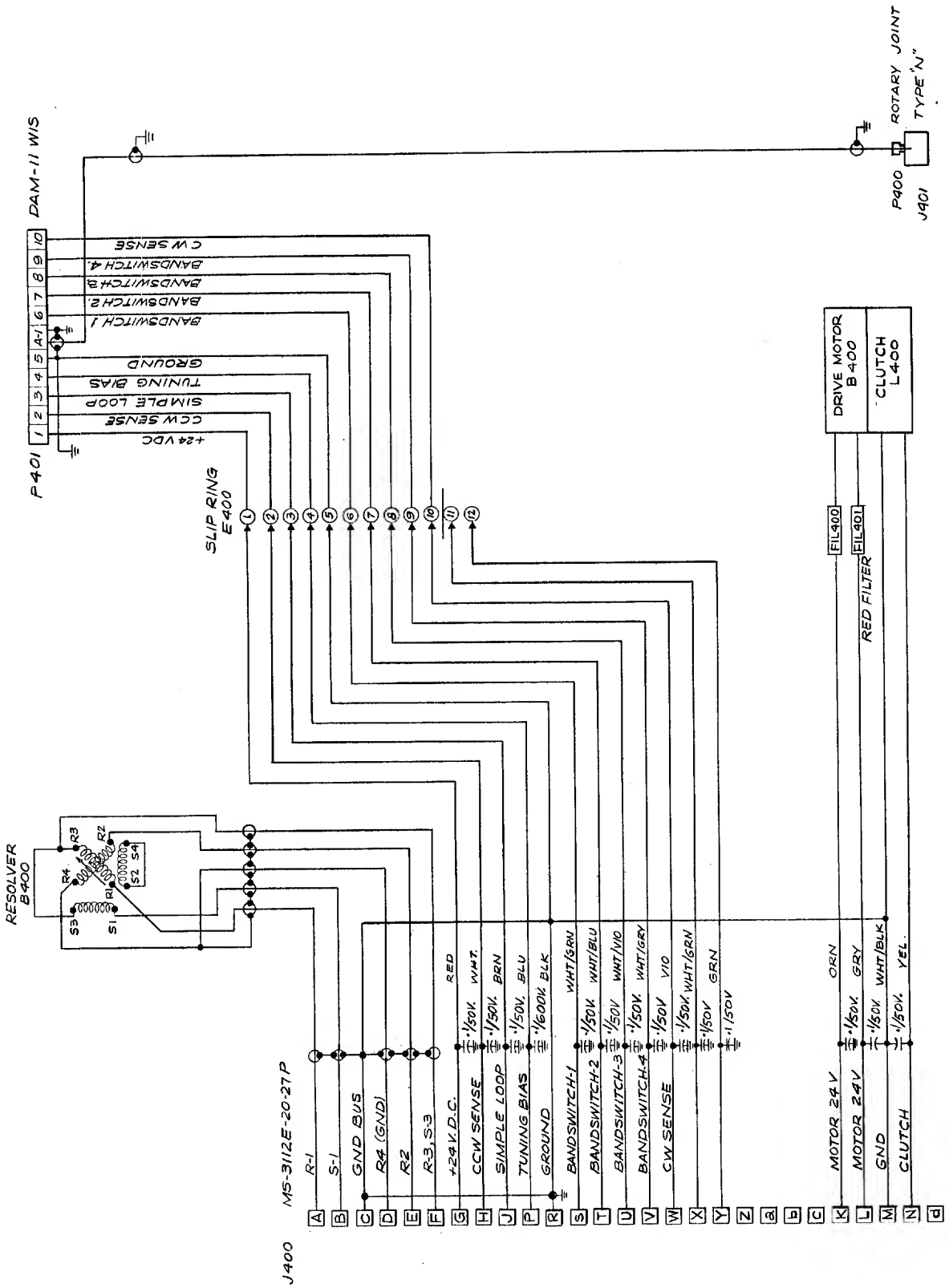

FIGURE 28. PEDESTAL WIRING SCHEMATIC

ground lead are physically tied to the rotating mast near the connector which mates with the mast extension sections.

Second, the rotary joint in the original pedestal unit was insulated from the rotating mast and from the fixed portion of the pedestal. Plastic parts normally used to accomplish the insulation were replaced by metal components so that the rotary joint was grounded to the rotating inner mast section and to the fixed portion of the pedestal. This is necessary to maintain a low VSWR across the joint and to avoid stray pickup within the pedestal. Sage Model 305W rotary joints with serial numbers higher than 1500 were used. All new rotary joints have developed an intermittent after 20 to 40 hours. Cleaning at this point usually yielded a life of 200 hours or more before additional maintenance is required.

Third, the specification for anodized surfaces at the flange which mates with the mast section was removed. The mast sections are unfinished in the areas where they mate with the antenna, each other, and the pedestal. This prevents the mast section from becoming isolated from RF ground and increases the effectiveness of the mast as a shield for the control leads.

Fourth, the rotation motor was changed from a 30-rpm to a 70-rpm motor. The 70-rpm motor specified was a Globe Model 25A677 with a Kinetics Instrument Corporation Model GM 915-016D gear head as used in the AN/TRQ-23 pedestals. However, this 70-rpm motor proved unsatisfactory because of low torque for the HF spaced loop antenna, high power requirements, and mechanical problems within the gear train of the speed reducer. The 70-rpm motor was replaced with the original AN/PRD-7 and 8 drive motor (Globe Model 102A254). Work to date to obtain a low power and high torque substitute 70-rpm motor has been unsuccessful. The motor requirements are discussed in greater detail in Section 4.3.3.6.

The modified pedestal retains all of the features of the original 30-rpm AN/PRD-7 and 8 pedestal. This includes continuous 30-rpm clockwise rotation, variable slow speed operation (between 1 to 15 rpm) in either direction, or manual rotation using the handwheel. Installation and alignment of the pedestal utilizing the combination level and compass remain unchanged.

4.3.2.4 Antenna and Pedestal Control Unit

The control functions for the modified AN/PRD-7 and 8 rotation pedestal and the HF spaced loop antenna have been combined into a common control unit. The control unit and the control unit to DF indicator control cable are shown in the carrying bag in Figure 29. The unit as furnished

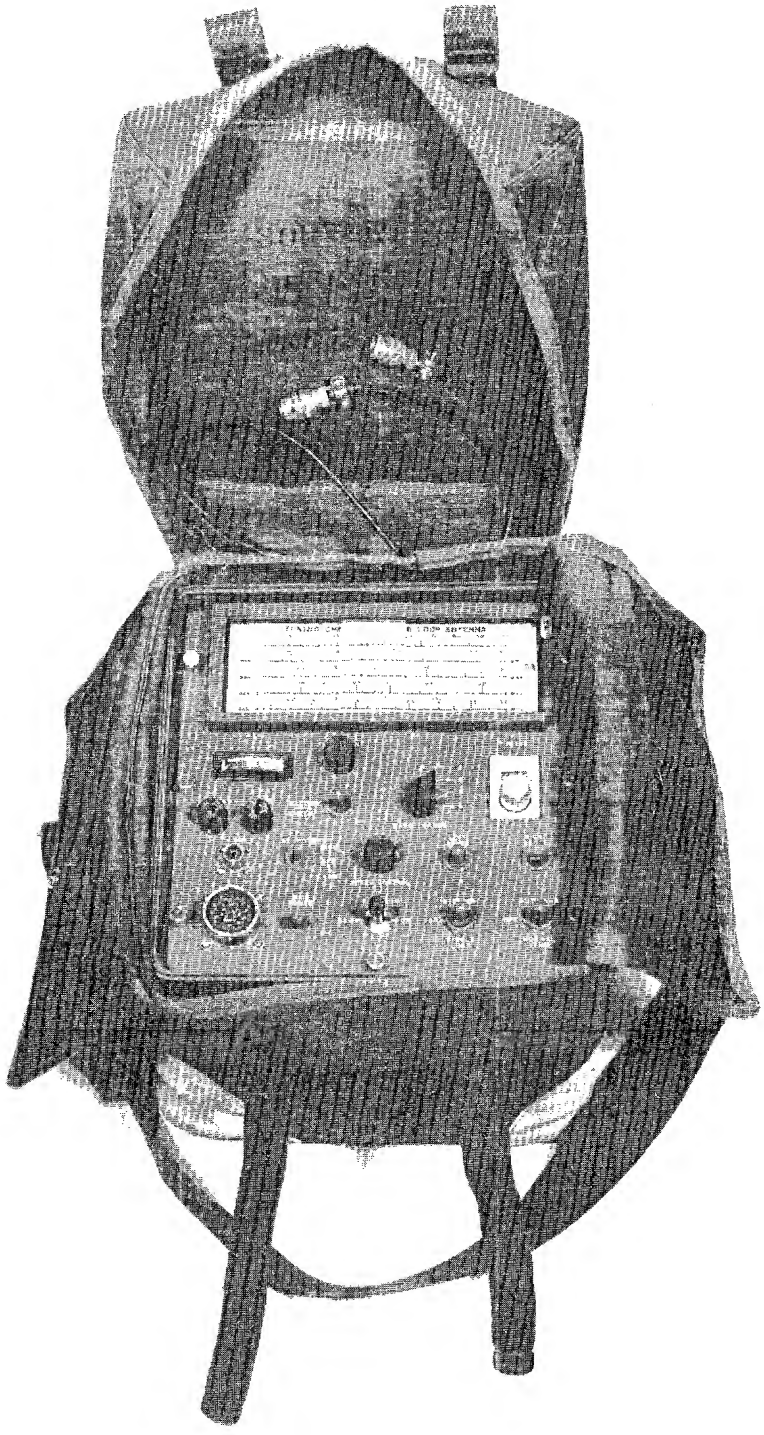

FIGURE 29
CONTROL UNIT IN CARRYING BAG

to the U. S. Army is designed specifically to control the HF spaced loop antenna. However, the design philosophy is very similar to that used in the control units for the VHF spaced loop antennas developed under Contract DA 28-043 AMC-01633(E).[18]

The schematic of the control unit for the HF spaced loop antenna is given in Figure 30. A close-up view of the front panel of the unit is given in Figure 31. The purpose and general operation of the functions of the control unit are outlined in Table 3. The description of the individual functions is referenced to the schematic of Figure 30 and the front panel nomenclature of Figure 31.

The portions of the instruction book covering the control unit for the VHF spaced loop direction finder set will be helpful in using this unit.[20] The two units are very similar. In detail, the differences include a change from a 90-volt DC bias battery to a 135-volt DC bias battery to supply the 100-volt DC bias as compared to 60-volt DC bias in the VHF unit for varactor diode tuning. A different tuning chart is also used. The only other major differences are the additional sense functions. The inclusion of the left sense (CCW) and right sense (CW) functions and provisions for an automatic left-right mode were designed into the unit midway in the program when the decision as to the best method of bearing and sense display was in doubt. Automatic left-right sensing which was illustrated in Quarterly Report No. 1[3] was a possibility. The intersections of the two sense patterns provide the same information as the spaced loop pattern. For this reason, a switch position for automatic left-right mode was included. (The circuitry for the mode is not included in the control unit.) Left (counterclockwise) and right (clockwise) sense functions were provided to investigate the intersection scheme. The normal sense switch is a momentary down switch which provides the sense mode with deflection plate switching. This was the only sense function provided in the VHF antennas[18] and probably is the only function necessary unless the more sophisticated left-right circuitry is fully developed. However, as suggested in Section 4.3.5, the automatic left-right mode could be an effective means of improving response time in a slow rotating spaced loop.

4.3.2.5 Requirements for Equipments Not Furnished to the Contractor

4.3.2.5.1 DF Indicator

The technical guidelines specified that the equipment furnished under this program should be compatible with the DF indicator for the AN/TRD-20 or its equivalent. The evaluation of the final antenna and the

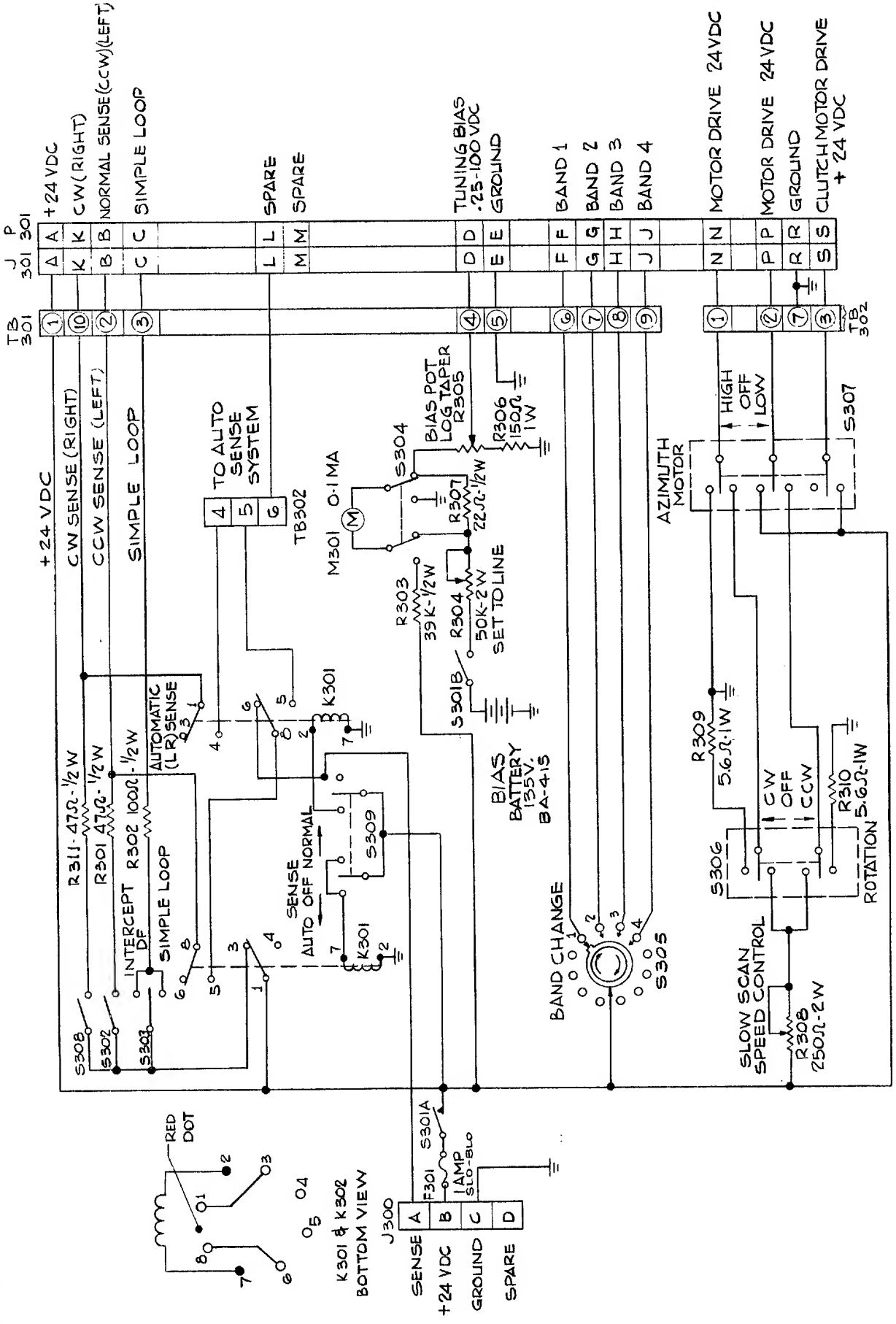

FIGURE 30. CONTROL UNIT SCHEMATIC

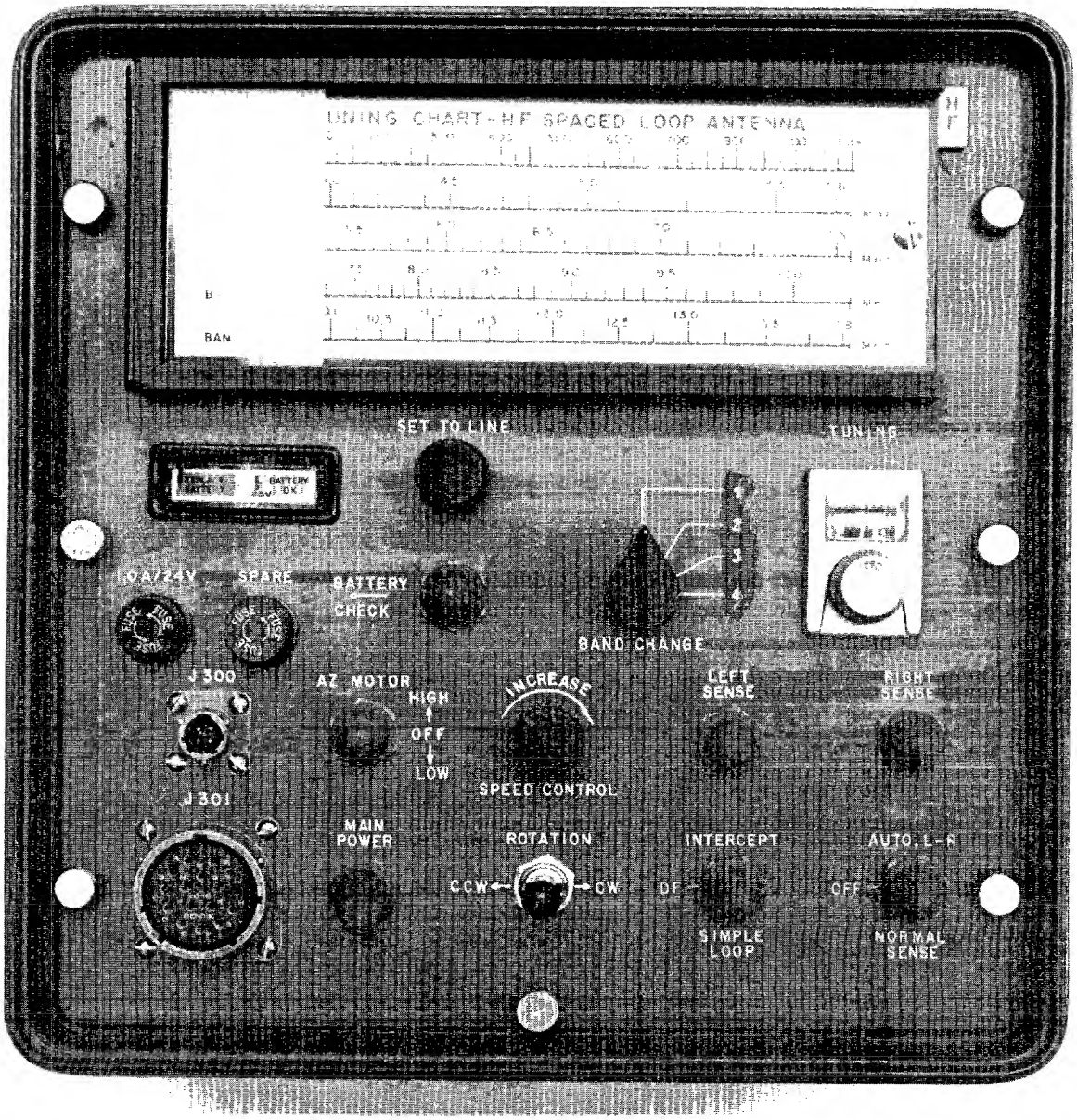

FIGURE 31
CONTROL UNIT FRONT PANEL

TABLE 3. DESCRIPTION OF CONTROL UNIT FUNCTIONS

Designation	Function
J301 (connector)	Provides for connection of 100-ft. antenna control cable to supply power to pedestal unit.
J300 (connector)	Provides for connection of +24 VDC power from and sense circuit control to visual indicator.
MAIN POWER (Switch S301)	Connects +24 VDC power to all controls. Connects internal battery for tuning bias to internal circuit.
AZ Motor (Switch S307) (High-Off-Low)	The HIGH position connects azimuth drive motor to +24 VDC for high speed rotation. Center position (OFF) disconnects azimuth motor. Down position (LOW) connects SPEED CONTROL for variable low speed, bidirectional azimuth motor operation with the CCW-CW ROTATION switch. In LOW position, main drive clutch draws power continuously.
SPEED CONTROL (Knob K308)	Azimuth speed control for low speed operation energized in AZ Motor-LOW position. CW rotation increases the speed of the antenna rotation.
ROTATION (Switch S306) CCW-CW	Energized in AZ Motor-LOW position CCW rotates antenna counter-clockwise. Center position stops antenna rotation. CW rotates antenna clockwise.
BATTERY CHECK - TUNING CHECK (Switch S304)	Held toward battery check position (momentary contact), connects meter to the battery pack to check quality of batteries. Good battery condition; pointer in green section. Bad condition; pointer in red section.

NOTE: If equipment is connected in reverse polarity, pointer will swing to left of zero position.

Approved For Release 2001/09/03 : CIA-RDP76-00451R000200010013-1

Table 3. (Continued)

Designation	Function
	Returned to the normal position maintains contact with the internal tuning battery.
SET TO LINE (Knob K304)	With BATTERY CHECK - TUNING CHECK switch in normal position, the control sets the tuning voltage to the calibration line as shown on the meter face.
BAND CHANGE (Knob S305)	Selects the proper band for the antenna as shown on the tuning chart mounted above.
TUNING (Knob K305)	Adjusts tuning voltage applied to the antenna tuning network. Dial count selected from tuning chart mounted above.
1.0 A/ 24V (Fuse F301)	Protects all equipments against overloads and short circuits.
INTERCEPT - DF - SIMPLE LOOP (Switch S303)	Locked in up position (INTERCEPT) connects more sensitive simple loop mode in antenna for search or intercept. Held down (momentary contact - SIMPLE LOOP) allows momentary simple loop operation which is used to resolve ambiguities of spaced loop pattern. Center off position (DF) must be used for all DF operation. This is only position which allows spaced loop mode of operation.
SENSE AUTO-OFF-NORMAL (Switch S-390)	Held down (momentary contact) applies power to sense networks in antenna and activates relay in indicator to switch deflection plates for sense pattern. Lock up for automatic left-right sense operation when provided with automatic switching circuit not now installed.

Approved For Release 2001/09/03 : CIA-RDP76-00451R000200010013-1

Table 3. (Continued)

Designation	Function
LEFT SENSE (Switch S-303)	Momentary contact switch to sense networks for counterclockwise rotation of desired spaced loop null.
RIGHT SENSE (Switch S-302)	Momentary contact switch to sense networks for clockwise rotation of desired spaced loop null.

Approved For Release 2001/09/03 : CIA-RDP76-00451R000200010013-1

experimental work were accomplished using the DF indicator for the AN/PRD-5. This indicator is similar to the AN/TRD-20 indicator with the exception of the input and output cable connector configuration.

Most of the HF spaced loop antenna work was performed with the AC deflection trace of the AN/PRD-5 DF indicator blanked. This produces the exact antenna pattern, whereas, without blanking of the trace, the pattern is produced twice in one revolution. In the sense mode, the indicator has provisions for blanking because sense patterns are usually unsymmetrical.

U. S. Army personnel requested that tests be conducted on the final antenna without blanking in the DF function. The AN/PRD-5 indicator was modified by the installation of a DPDT toggle switch which allowed the option of blanking or not blanking the AC deflection trace in the DF mode as shown in Figure 32. Experiments indicated that from the standpoint of pattern study the blanked trace was preferred. However, for unskilled operators using the 30-rpm rotating antenna pattern on skywave signals, the unblanked or normal trace was preferred. The unblanked trace (normal DF mode) yields a symmetrical pattern after 180° of antenna rotation for almost all skywave signals. In addition, both the forward null and the reciprocal spaced loop nulls are displayed at the correct bearing. If the operator had sensed the signal as a first step, then the use of the unblanked trace decreased the time necessary to obtain a bearing. Without the sense mode, the normal or unblanked trace simplified the process of obtaining a bearing with a 180° ambiguity.

It is suggested that this modification be performed on the DF indicator used to test the HF spaced loop antenna. The personnel evaluating this antenna for the first time should operate the equipment with blanking on the trace in the DF mode so that the character of the spaced loop pattern may be understood. After a period of operation in this mode, it is suggested that operation without blanking, or the normal mode, be performed. It is felt that as experience with the two techniques is gained, the operator's preference will be for the unblanked or normal deflection trace.

The spaced loop pattern requires greater linearity in the cathode ray tube indicator than the simple loop antenna. Both AN/PRD-5 indicators furnished to this laboratory have required maintenance to improve the linearity. Problems at this laboratory with nonlinearity involved bias of the first video amplifier Q-200, and a shift of the resonant frequency of the high voltage multivibrator.

It is recommended that the initial check-out procedure in the evaluation include a comparison of the spaced loop antenna pattern for a vertically

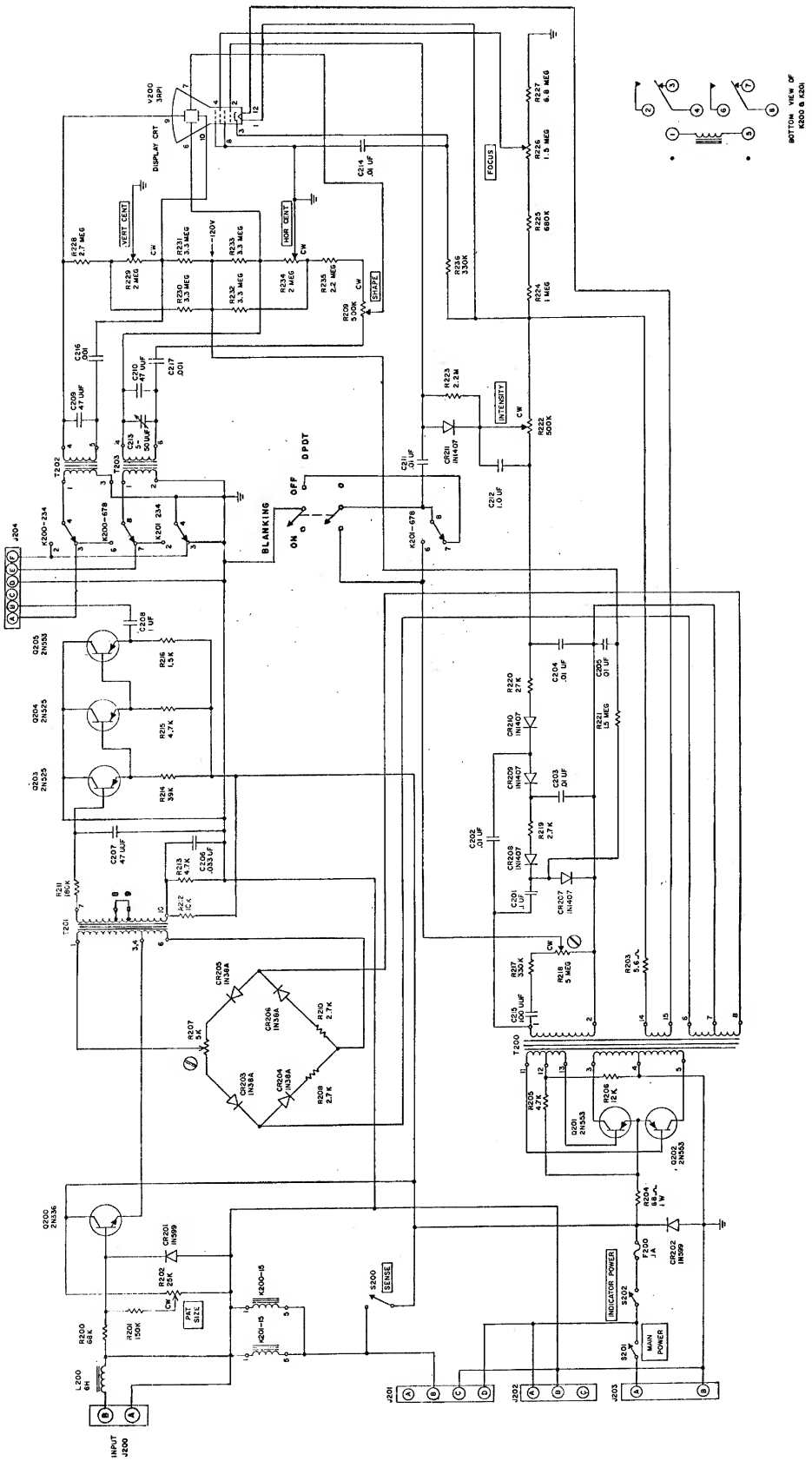

FIGURE 32
DF INDICATOR SCHEMATICS WITH MODIFICATIONS

polarized signal with the theoretical patterns of Figure 3. Blunt nulls are evidence of nonlinearity. (This condition should not be confused with blurred nulls.) Reference 20 gives a number of spaced loop patterns which can result with poor indicator linearity. This reference also illustrates the results when the video DC level is not properly set for the AN/PRD-5 indicator. Once a receiver and video detector are chosen, it is necessary to set the DC level for the best pattern linearity. This condition, once established, is a constant.

4.3.2.5.2 The Receiver

The HF spaced loop direction finder set is designed to be compatible with the R-901/PRD based upon the information available to this laboratory. Because this information may not be up to date, it is recommended that control cable wiring of Figure 15 be compared with the receiver used. The R-901/PRD does have a DF video detector. Dependent upon the version of the DF indicator used, it may be necessary to set the video DC level for the best possible pattern linearity.[20]

An R-390A receiver has been used for all work with the HF spaced loop at this laboratory. The R-390A receiver does have a diode output of the proper polarity for use with the DF indicator. However, this diode output can only be used when the receiver BFO is off. It has been the experience of the personnel at this laboratory that the use of the diode output of the R-390A to drive the DF indicator requires that the receiver performance be compromised (no BFO for CW signals, for example) to obtain proper conditions of DC level and video amplitude for the AN/PRD-5 indicator. To avoid this problem, the recommended procedure is to provide a separate DF IF amplifier and video detector unless the receiver has a diode output designed specifically for the DF indicator used with the system.

The schematic of the DF IF amplifier and detector used in the majority of tests at this laboratory is shown in Figure 33. When the R-390A was first aligned, this circuit was adequate. However, low IF outputs later in the program required frequent receiver realignments or more IF gain. The symptom of this condition is the inability to display the DF pattern for weak signals. The addition of a 10-dB IF amplifier or a second IF amplifier stage to Figure 33 is recommended if the receiver IF output is below 3 volts RMS. [The AN/PRD-5 indicator furnished this laboratory under Contract DA 28-043 AMC-01633(E) requires a 4.8-volt peak to peak video level.]

A one-time adjustment of the series and shunt potentiometers at the output of the video detector of Figure 33 is required for a given receiver

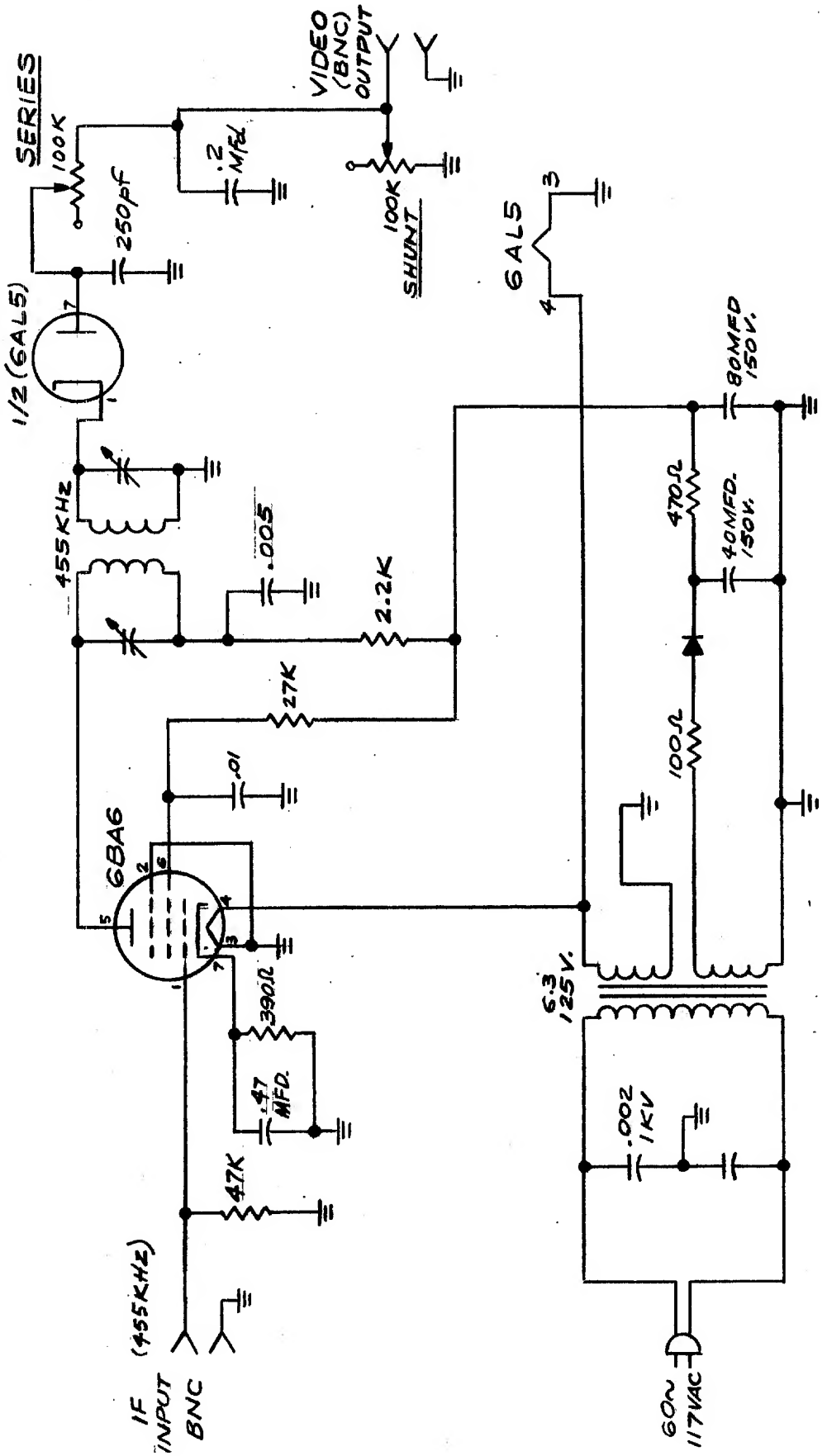

FIGURE 33. DF IF AMPLIFIER AND VIDEO DETECTOR SCHEMATIC (TUBE TYPE)

and DF indicator. A local vertically polarized target transmitter should be used. The series and shunt potentiometers are then adjusted to obtain the theoretical vertical polarized spaced loop pattern of Figure 3 or the photographs of the vertically polarized spaced loop patterns of Figure 33, 34 or 35.

The schematic of a second 455-kHz IF amplifier and DF detector used at this laboratory is shown in Figure 34. This transistorized circuit includes a simple voltage regulator for operation from portable battery packs over a 18 to 30-VDC range. The circuit was built to provide a DF IF amplifier and video detector compatible with the 26-volt DC battery pack.

The circuit of Figure 34 does clip pattern maximums slightly. However, for null displays, the distortion is not visible on the DF indicator. Linearity over the null is excellent. The circuit includes a gain control and video DC level controls. As in the previous circuit, the DC level controls should be set in a one-time adjustment for best pattern linearity. The gain control should be set in a one-time adjustment for an adequate DF display at a convenient RF gain setting of the receiver.

The DF receiver must have a nominal input impedance of 50 ohms to match the 50-ohm coaxial cable routed from the antenna. (The antenna RF output of the antenna preamplifiers was set at 50 ohms.) A high VSWR at the receiver input can create distortion of the antenna patterns. Resistive loading of the R-390A was necessary when the high impedance input was used.

4.3.3 Evaluation of the Equipment

4.3.3.1 Field Site and Equipment

The field site and general equipment used in the development and the evaluation of the HF spaced loop antenna is similar to that used in the work with the VHF spaced loop antenna. The field site and facilities for elevating the modified DAQ target transmitter for multipolarization tests was detailed in Quarterly Report No. 1.[3] This site has also been described in detail in the Final Report for Contract DA 28-043 AMC-01633(E).[18]

All equipment except the pedestal and antenna was located in a portable shelter at the field site which was described in the two references of the previous paragraph. (The antenna and pedestal have been previously shown in the field test configuration of Figure 19.) The equipment used in the shelter for the evaluation of the final HF spaced loop antenna is shown in Figure 35. This equipment shown in Figure 35 necessary for operation of

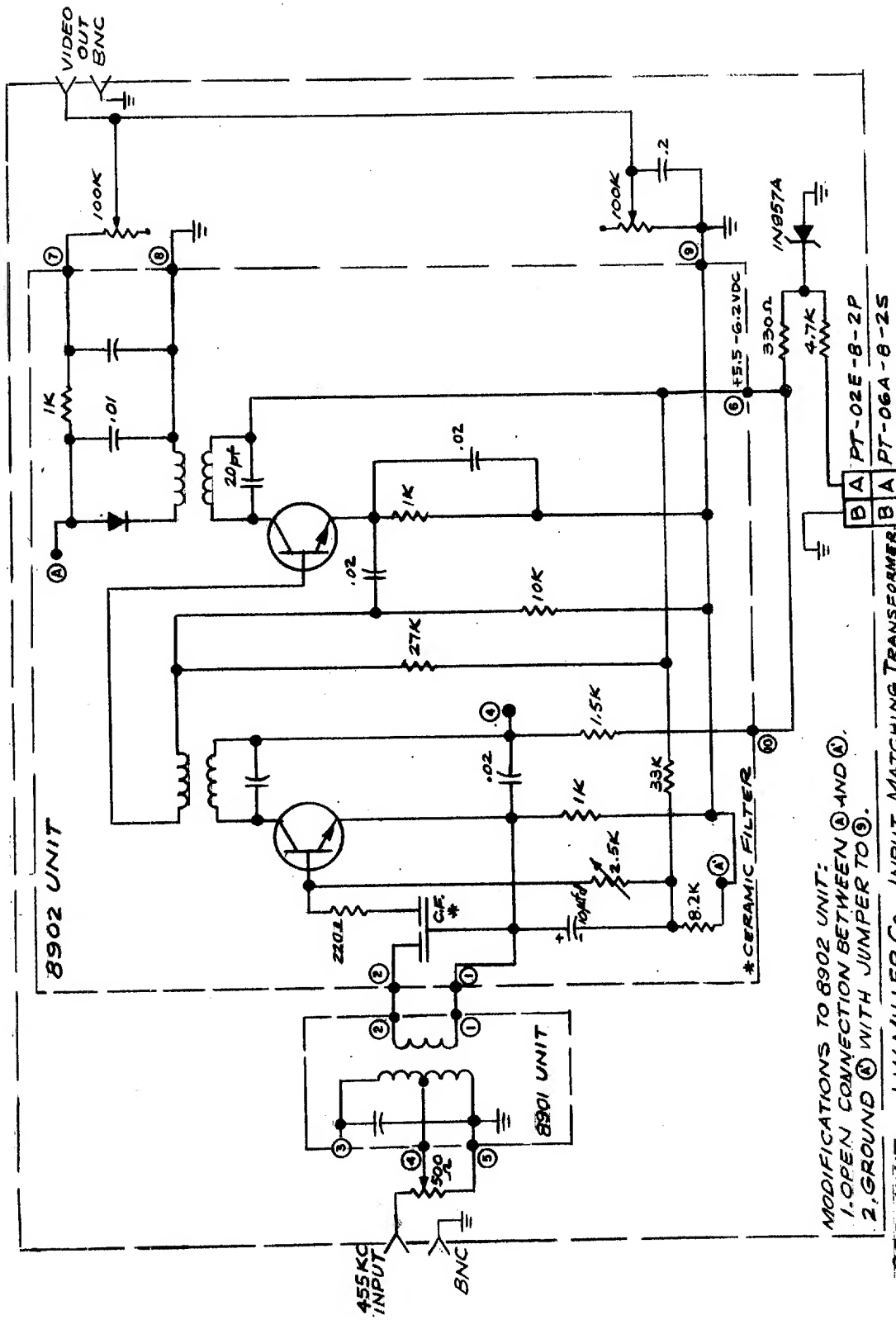

FIGURE 34. DF IF AMPLIFIER AND VIDEO DETECTOR (TRANSISTOR)

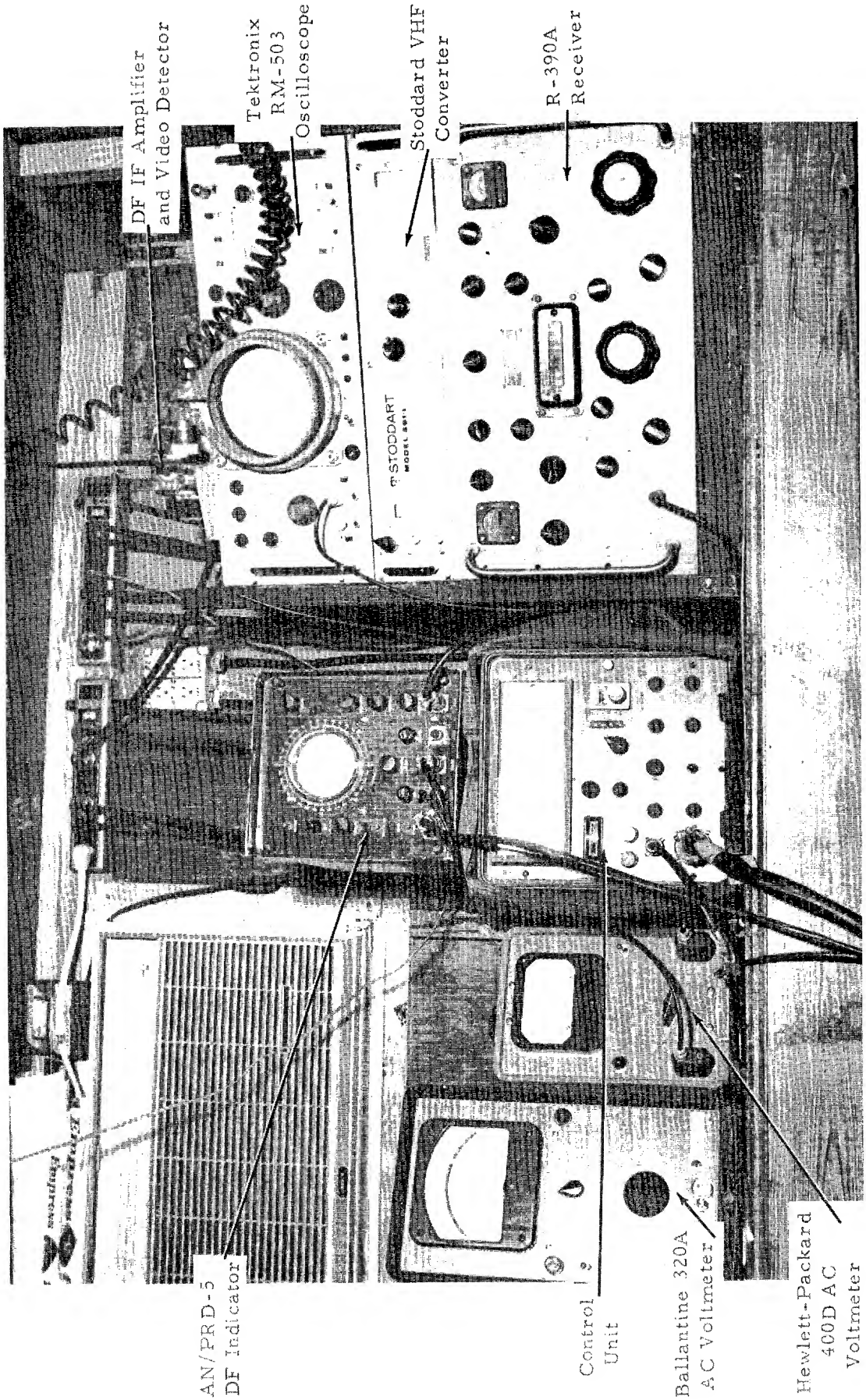

FIGURE 35
EQUIPMENT USED IN EVALUATION OF HF SPACED LOOP

the spaced loop antenna includes the AN/PRD-5 DF indicator, the control unit, the R-390A receiver, the DF and IF amplifier and video detector. Not shown are AC to DC power supplies and DC batteries for use when power cables to the shelter are removed for maximum accuracy tests. (The Stoddard VHF converter was employed in tests of VHF antennas and was not associated with the HF antenna.)

Other equipment shown in Figure 35 was used in various tests during the evaluation of the antenna. The Tektronix 532 oscilloscope was used to monitor the video output of the DF detector. The Ballantine Model 320A AC voltmeter was used to measure audio and IF outputs in sensitivity measurements. The Hewlett-Packard 400D AC voltmeter was also used in the sensitivity measurements and as a 10-dB IF amplifier for the R-390A receiver late in the program when the receiver needed realignment.

4.3.3.2 Sensitivity

The field test of the final advanced development/feasibility model of an HF spaced loop conducted to determine sensitivity followed a standard technique used on previous HF spaced loop antennas.[3, 19] A target transmitter with a vertically polarized antenna was located approximately 1,000 ft away from the DF antenna. The output of this target transmitter was controlled to yield the desired field strength at the DF antenna. The field strength was measured using a Stoddard Model 191 tuned rod antenna over the recommended ground plane feeding an Empire Devices NF-105 field strength meter. Calibration of the field strength equipment was made at each frequency for each field strength using a Hewlett-Packard Model 606 signal generator. The accuracy of the field strength measurement is, therefore, as good as the calibration accuracy of the signal generator.

With care, a clear frequency could be found where the noise and on-the-air signal strength was less than 1.5 μv/m. With a field strength of 10 μv/m, the signal plus noise to noise ratios of the spaced loop mode, simple loop mode, and sense mode were measured at the pattern maximums at both the IF output and at the audio output of the R-390A receiver using a Ballantine Model 320A AC vacuum tube voltmeter. The measurement was taken at a pattern maxima for each mode. (400-Hz modulation was used on the target signal for the audio measurement.) The signal was turned off to measure the noise level for both IF and audio measurements. The receiver bandwidth was 4 kHz for all tests. The test data are summarized in Table 4. The spaced loop mode approaches the 10-μv/m design goal. The sense mode is less sensitive; however, experience has shown that this mode requires less sensitivity to provide adequate sense. The mode is used only to resolve ambiguities and need not have pattern

TABLE 4

Summary of Final Sensitivity Data on the Final Advanced Development/Feasibility Model of the HF Spaced Loop Antenna at 4-kHz Receiver Bandwidth

Frequency	Spaced Loop		Sense		Simple Loop	
	IF S+N/N Ratio	Audio S+N/N Ratio	IF S+N/N Ratio	Audio S+N/N Ratio	IF S+N/N Ratio	Audio S+N/N Ratio
4 MHz	9 dB	7 dB	5 dB	4 dB	25 dB	28 dB
5 MHz	10 dB	7 dB	4 dB	4 dB	20 dB	18 dB
6 MHz	11 dB	8 dB	9 dB	7 dB	24 dB	28 dB
7 MHz	13 dB	10 dB	7 dB	5 dB	29 dB	30 dB
8 MHz	10 dB	8 dB	6 dB	6 dB	18 dB	24 dB

Approved For Release 2001/09/03 : CIA-RDP76-00451R000200010013-1

quality of the DF mode. The data of Table 4 also indicate that the tuned simple loop mode is extremely sensitive, probably being limited by the ambient noise. The greater sensitivity of the simple loop mode does indicate that the spaced loop mode sensitivity is not noise limited, justifying sensitivity improvements of the spaced loop mode.

Sensitivity improvements can, of course, be obtained by narrowing bandwidth. This method was used in the bearing accuracy evaluation of the antenna on weak on-the-air skywave signals.

4.3.3.3 Performance for a Local Target

The most effective method of demonstrating correct performance of a multipolarization antenna at low angles of elevation has been the use of an elevated controlled polarization target transmitter. A 1.5 to 30-MHz DAQ battery powered target transmitter was modified by replacing the monopole antenna of the unit with a balanced dipole antenna for tests of the HF spaced loop antenna. The grounded side of the output coil was removed from ground and connected to one side of the dipole. The other half of the dipole was connected to the original RF output. Antenna loading coils in each half of the dipole were used to increase the efficiency of the transmitter antenna. The target transmitter was located 5 ft above the top deck of the 60-ft Navy DF tower as shown in Figure 12 of Quarterly Report No. 1.[3] An offset mast installed on the tower to test a Navy DF antenna has eliminated some of the polarization control formerly available from a target transmitter on the tower and increased bearing error for certain polarizations.[19] However, the site is still more than adequate to evaluate spaced loop performance as a function of polarization.

Figures 36, 37 and 38 are typical pattern photographs obtained with the final antenna at 4 MHz, 6 MHz, and 8 MHz. The target dipole was rotated 180° from horizontal counterclockwise (CCW) in 15° steps through a vertical position to horizontal clockwise (CW). The spaced loop patterns, the normal sense patterns (the CCW sense pattern with deflection plate switching), a double exposure of the spaced loop and simple loop patterns to demonstrate that the simple loop nulls lie on top of the unwanted loop nulls of the spaced loop pattern, and a double exposure showing both the clockwise and counterclockwise patterns to demonstrate the principle of left-right DF are given in each of the three illustrations. Similar pattern and accuracy observations were made at 5 MHz and 7 MHz without photographing the patterns. It will be noted that the intersections of the two sense patterns in Figures 36, 37, and 38 agree in position with the spaced loop null. Furthermore, the slopes of the patterns are opposite. There is sufficient information to obtain a bearing with no

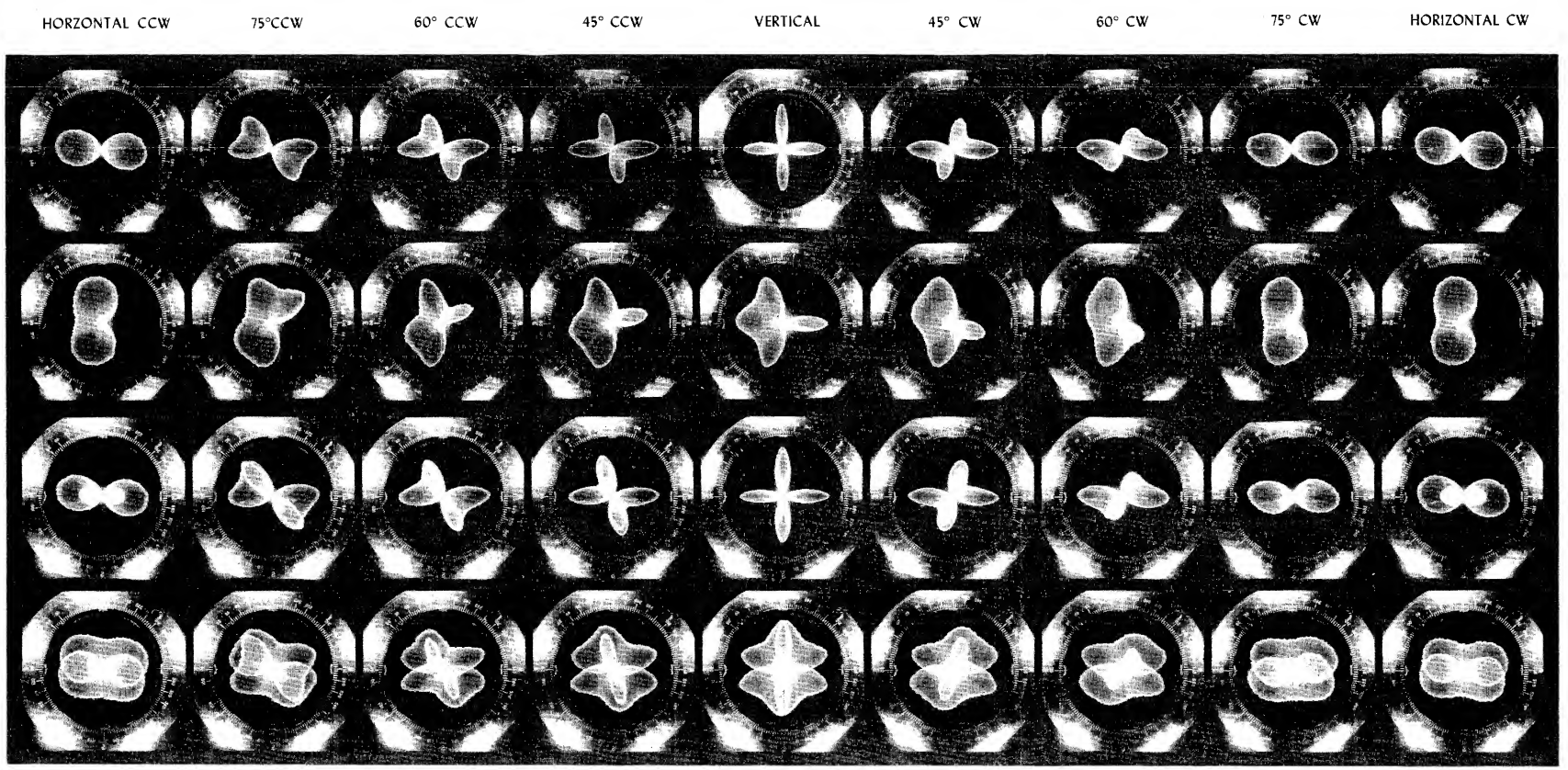

Approved For Release 2001/09/03 : CIA-RDP76-00451R000200010013-1

FIGURE 36

SPACED LOOP, SIMPLE LOOP, AND SENSE PATTERNS
FOR ADVANCED DEVELOPMENT/FEASIBILITY MODEL HF SPACED LOOP ANTENNA
AS A FUNCTION OF SIGNAL POLARIZATION θ = 82° (8° ABOVE THE HORIZONTAL)

TARGET DIPOLE

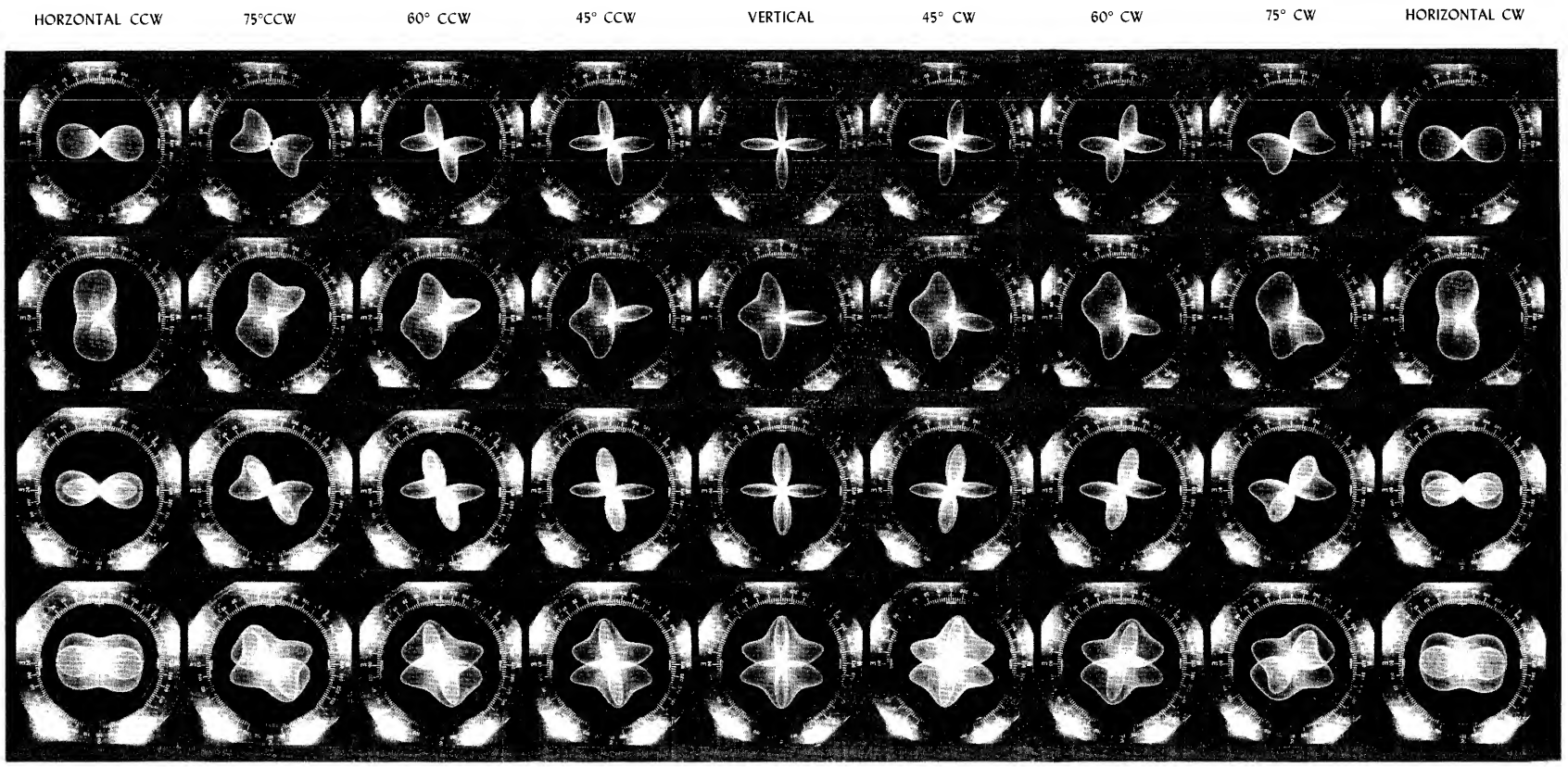

FIGURE 37

SPACED LOOP, SIMPLE LOOP, AND SENSE PATTERNS
FOR ADVANCED DEVELOPMENT/FEASIBILITY MODEL HF SPACED LOOP ANTENNA
AS A FUNCTION OF SIGNAL POLARIZATION θ = 82° (8° ABOVE THE HORIZONTAL)

Approved For Release 2001/09/03 : CIA-RDP76-00451R000200010013-1

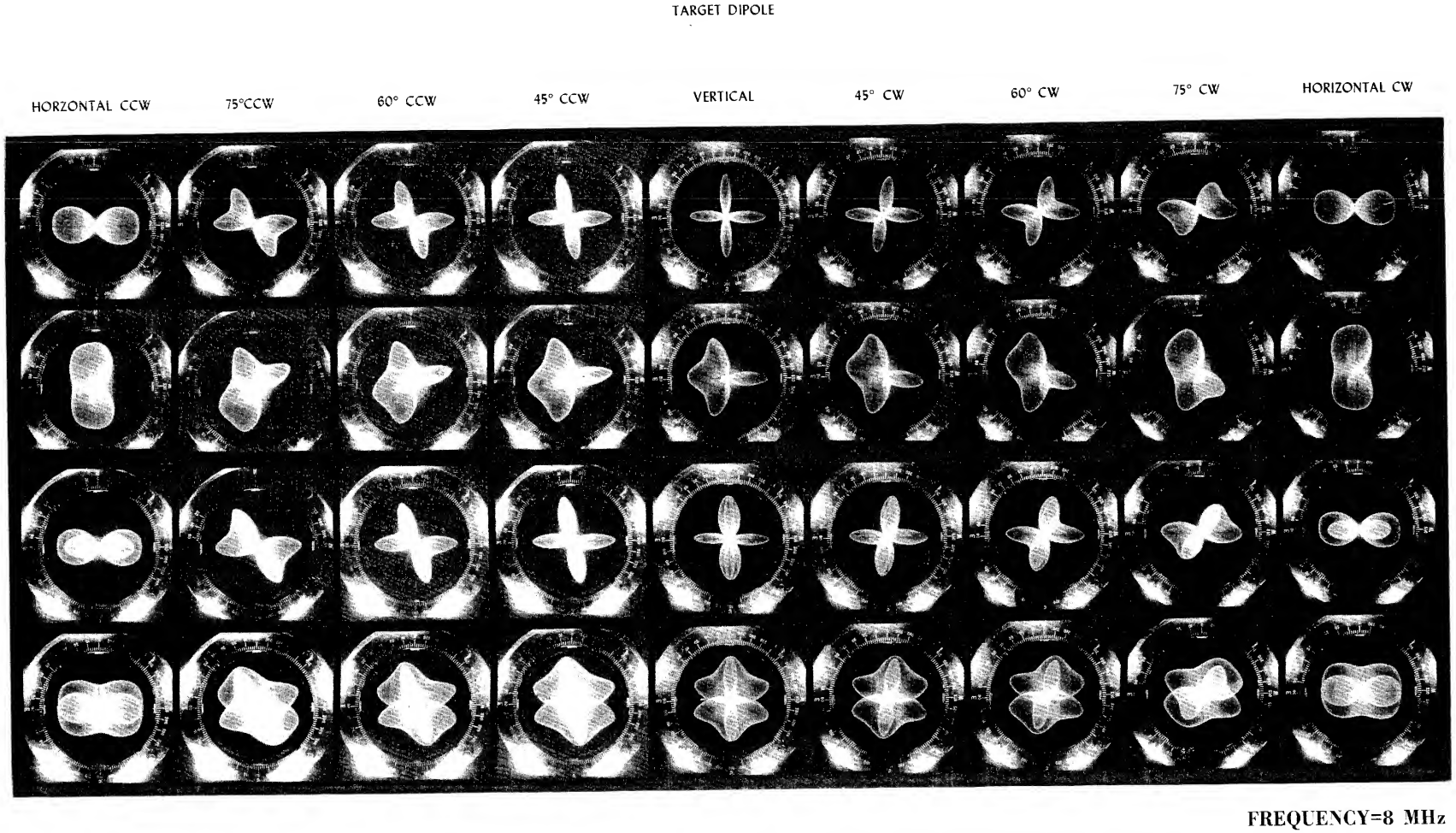

FIGURE 38

SPACED LOOP, SIMPLE LOOP, AND SENSE PATTERNS
FOR ADVANCED DEVELOPMENT/FEASIBILITY MODEL HF SPACED LOOP ANTENNA
AS A FUNCTION OF SIGNAL POLARIZATION θ = 82° (8° ABOVE THE HORIZONTAL)

Approved For Release 2001/09/03 : CIA-RDP76-00451R000200010013-1

ambiguities. In practice, the normal sense pattern and the spaced loop pattern are all that are required for a bearing. The simple loop is not necessary but it is useful in initial tests of the spaced loop and provides a sensitive intercept mode.

Bearing error occurred near the horizontal CW polarization condition at all frequencies. This was traced to the offset mast. The spaced loop patterns at 60° CW and 75° CW in Figures 36, 37, and 38 show blurred loop nulls as a result of elliptical polarization. There was not time on this program or on the Navy program to determine the exact extent of the bearing error from the offset mast. Comparison of patterns obtained with the third breadboard model before and after the offset mast was installed indicated that most of the elliptical polarization and bearing error were a result of the mast.

The patterns of Figures 36, 37, and 38 indicate that the final antenna approaches the theoretical patterns of Figure 4 at a low angle of elevation. High angle tests were not conducted with the local target transmitter because the data are invalid as the target transmitter comes into the near field. Far field test requirements restrict the elevation angle to 8° and the distance from the target to the DF antenna to approximately 600 ft using 60-ft Navy tower.

The 400-ft diameter calibration track around the spaced loop site is not adequate for far field calibration curves between 4 and 8 MHz. * However, calibration curves were taken at 1-MHz intervals for vertical polarization on this track for both the spaced loop and simple loop modes with all power cables removed from the site. The results were essentially as given in Figure 6 of Quarterly Report No. 2 with spaced loop accuracy approximately twice that of the simple loop.

The 10-ft antenna height minimizes error as a result of the single unsymmetrical control cable. A symmetrical ground plane is not recommended at this time. The effect of ground planes on the spaced loop has not been fully studied in theory or in practice.

4.3.3.4 Performance Using an Aircraft-Mounted Target Transmitter

The use of an aircraft-mounted target transmitter was very effective in determining DF accuracy at elevation angles up to 85° in the development of the breadboard antennas, as discussed in Quarterly Reports No. 2 and No. 3.[4, 5] The technique permits rapid changes in polarization, frequency, and elevation angle. The coaxial spaced loop serves as relative polarimeter while being tested for accuracy.

*See Figure 10 of Quarterly Report No. 1.[3]

These tests proved that the third breadboard model of the spaced loop antenna was accurate with ±3° for various signal polarizations to an angle of elevation of 85° at three test frequencies. The tests also allowed the selection of a single value of sense resistor (180 ohms) which yielded good sense patterns for signals arriving along the horizontal and at signal elevation angles up to 85°. (The initial theoretical investigation had indicated the need for a change in sense resistors between the low angle signals and high angle signals. The 180-ohm value was selected by trial and error in repeated tests.)

In tests of the final antenna, the same procedure was followed with DF accuracy runs and sense pattern quality runs at 3.995 MHz, 6.325 MHz, and 7.240 MHz. The target transmitter and aircraft dipole resonance were adjusted to yield a large amount of horizontal polarization for the tests. Approximately 4 to 6 accuracy runs and 4 to 6 sense runs were completed at each test frequency. In the most successful runs, the aircraft flew directly overhead and could be tracked both with the transit used to measure azimuth and elevation angle and with the DF antenna. Bearing accuracy was ±2° for the final antenna in these tests. The 180-ohm sense resistors proved to be the proper value for all angles of elevation.

The test data were recorded on a tape recorder. The character and volume of the data, when transcribed, make it impractical to reproduce in this report. The results, when edited for clarification, would be similar to the data given on the third breadboard model on pages 14 - 22 of Quarterly Report No. 2.[4]

4.3.3.5 Performance on Skywave Signals

4.3.3.5.1 Description of the Tests and Procedures

The most important aspect of performance of a rotating coaxial spaced loop antenna is the ability of the antenna to yield accurate bearings on groundwave signals when skywave components are also present. The coaxial spaced loop antenna has a null directly overhead for both vertical and horizontal polarization, as illustrated in Figure 2. However, both the third breadboard spaced loop antenna and the final spaced loop antenna have been successfully used to DF on skywave signals arriving at angles of elevation up to 85°. The performance of these antennas has been excellent. With the excellent data, some of the limitations of a small aperture DF antenna remain. For example, with two signals on the same frequency, receiver bandwidth and tuning become major tools to obtain an accurate bearing. The 30-rpm rotation is also a limitation in obtaining a bearing in a short period of time.

Skywave signals are intercepted in random signal DF tests as signals of opportunity. It cannot be denied by anyone performing a random bearing test that some unintentional selection process occurred. If the bearing is to be meaningful in terms of a standard deviation, then the signal must be identified so that the great circle bearing and distance may be determined. For this reason, signal selection begins immediately. If the operator cannot identify the signal in a reasonable length of time, he begins looking for a new signal. This could be eliminated by repeated bearings on known stations. However, then the chances of operator bias are greatly increased. Operator bias in the tests of the final antenna was reduced to some extent by setting the reference resolver to a new reference frequently with this fixed error not given to the operators or recorded on bearing data sheets until a new reference was used.

It is felt that the tests of this section were run as objectively as possible. Factors such as competition between operators, fatigue, remaining operator bias, exact propagation conditions, etc., are not known. Only experience in the field using typical operators will ultimately establish the accuracy of the spaced loop antenna.

The tests on the third breadboard antenna were partially summarized in Quarterly Report No. 2.[4] The results for this antenna are included in this section for comparison with the final antenna. The skywave tests of the final model were conducted for two weeks on a 24 hour per day basis using random on-the-air signals between 4 and 8 MHz which could be identified. A controlled target transmitter with a horizontal dipole was employed at one site at 30 miles and at one site at 100 miles to obtain high angle signals. * In addition, the data for a commercial station at 210 miles were sorted from the first tests to obtain a data sample at this distance.

The operators were instructed to operate the HF spaced loop DF set in the INTERCEPT mode (simple loop mode) with the DF antenna rotating at 30 rpm until a signal was identified. After the operator identified a signal, he would record the call sign and time. Switching to the DF mode, the operator would sense the signal as a first step using the NORMAL SENSE switch. At 30 rpm, the normal sense pattern would sense a ±30°, or tighter, sector. After a bearing was obtained, the bearing data sheet was completed.

*Three transmitting antennas were used in the 30-mile and 100-mile tests with one antenna resonant at 4, 6, and 8-MHz frequencies used. The half-wave dipole antennas were aligned broadside to the direction to the DF antenna and were approximately 30 feet above the ground.

Figure 39 is a typical continuous rotation bearing data sheet. Material in Figure 39 was typed from an original handwritten data sheet. Above the first dark line, the operator completed all information after a bearing was obtained determining such factors as frequency and bandwidth from the receiver. He then completed information below the second dark line by checking the appropriate block on sense pattern quality, receiver bandwidth, and type of emission. He observed the signal to determine the rate of amplitude fade, amount of noise, modulation level, and interference from other signals.

On signals which were not keyed or pulsed, he was asked to determine the number of antenna rotations necessary for a symmetrical pattern with a blanked deflection trace. The number of sweeps to obtain a symmetrical pattern should indicate to some extent the rate of polarization change and the presence of multipath and other propagation phenomena. With slow rotation, the number of sweeps observation is a relative indication of propagation conditions. However, individual phenomenon cannot be identified.

Reference antenna readout and instrument calibration were recorded on the bearing data sheet by personnel other than the operator. The space at the bottom of the page was used to process the station and bearing until true bearing and distance could be determined by computer calculation using coordinates obtained from the Bern listing. This portion of the page was completed in steps as the data were processed.

The space between the first two dark lines was used to record all information in the form necessary for punching an IBM data card for the statistical analysis.

The operator indicates both A-0 and FS-CW as the emission in Figure 39. The FS-CW signal was unmodulated during some portion of the observation period.

A typical data sheet for an A-1 or CW signal is given in Figure 40. The data are obtained by the same method. For a signal class, aural null is indicated. The rotation speed of 1 also indicates the bearing was taken by aural null techniques. The operator also placed a +2° by the observed bearing. This means he determined final antenna position for the null by using the blanked trace on the AN/PRD-5 indicator. There was a 2° lag between the 30-rpm and slow speed mode with the equipment used at this laboratory.

The test procedure was modified to some extent as the test progressed. With skywave signal patterns as shown in Figure 41 for

Call Sign	Freq. Indicated	Log	Observed Bearing	Apparent Polarization	Time 24h CST	Date Mo Da Yr	Observer No.
WID 36	6775		95°	E	0500	1 7 67	23

Skip	TB	Skip	OB	Skip	Call #	Skip	Cal	Skip	$
	97.6 (3–7)		95.0 (10–14)		523 (17–20)		0.0 (23–27)		(32)

Skip	Mo	Da	Skip	Time	Oper	Antenna	Polarization	Freq.	Emiss	Noise	Mod	Fade	Int.	Elev.	Skip	Distance	INTC Time	Call Sign	BW	Class	Speed	Sense	Page No.
	01	07		0500	23	02	E	6802	43	2						1148		WID36		4431	F	440	
	34	38		44		48									57		65		73		77	80	

SIGNAL CLASS — Sweeps for a Symmetrical Pattern

1	Aural Null A-1, SSB	
2	CLASS A (Every Sweep)	
3	CLASS B (2-3 Sweeps)	
4	CLASS C (4-6 Sweeps)	✓
5	CLASS D (7-9 Sweeps)	
6	CLASS E (>9 Sweeps)	
7	CLASS F (No Sym Pat)	

Band Width-kc/s: 4

Type Emission: A-Ø, FS-CW

AMPLITUDE FADE

1	2	3	4	5	6
NONE	SLIGHT	MOD	EXTREME	N/A	CW SSB
		✓			

SENSE

1	2	3	4
EXCEL	GOOD	FAIR	NONE
✓			

SIGNAL DATA

	1/None	2/Avg	3/Extreme	4/Not Applic
Noise		✓		
Mod.				✓
Intfrnce		✓		

Reference Antenna Readout: 0° °

Comments:

Instrument Calibration: +2° for aural null

Intercept To Bearing Time: Not taken

ROTATION SPEED: 3 RPM (3-30) (6-60) (7-70) (1-AURAL NULL)

TRANSMITTER DATA:

Nominal Location: Miami, Florida — Authority: — Bern listing

Coordinates: Long. 80° 12m W; Lat. 25° 29m N — Authority: — Bern listing

Calculated True Bearing And Distance: 97.6 Degrees; 1,148 Miles

OTHER COMMENTS:

TELETYPE TAPE SAMPLE:

CRT Photo If Available
Photo No. ____
1 Photo/Day/Station

* TO NEAREST .1 DEGREE

Name of Test: Final antenna

Observed Bearing *	95.0°
True Bearing	97.6°
Gross Error	-2.6°
Instrument Error	0°
Net Error	-2.6°

∈Gross = OB − TB

∈Net = ∈Gross − ∈Instr.

Call No. ____

FIGURE 39. SAMPLE SKYWAVE BEARING DATA SHEET (CONTINUOUS ROTATION)

Page F-304

Call Sign	Freq. Indicated	Log	Observed Bearing	Apparent Polarization	Time 24h CST	Date Mo	Da	Yr	Observer No.
CLA	8.707		108° +2	AN	1045	1	4	67	12

Skip	TB	Skip	OB	Skip	Call #	Skip	Cal	Skip	$
	109.5 (3–7)		110.0 (10–14)		4 (17–20)		0.0 (23–27)		32

Skip	Mo	Da	Skip	Time	Oper	Antenna	Polarization	Freq.	Emiss	Noise	Mod	Fade	Int.	Elev.	Skip	Distance	INTC Time	Call Sign	BW	Class	Speed	Sense	Page No.
	01	04		1045	12	02		0871	2	4	2	1				1090		CLA	4	1	1	1	F304
	34	38		44				48								57		65		73		77	80

SIGNAL CLASS — Sweeps for a Symmetrical Pattern

1	Aural Null A-1, SSB	✓
2	CLASS A (Every Sweep)	
3	CLASS B (2-3 Sweeps)	
4	CLASS C (4-6 Sweeps)	
5	CLASS D (7-9 Sweeps)	
6	CLASS E (>9 Sweeps)	
7	CLASS F (No Sym Pat)	

Band Width-kc/s: 4

Type Emission: A-1

AMPLITUDE FADE

1	2	3	4	5	6
NONE	SLIGHT	MOD	EXTREME	N/A	CW SSB
	✓				

SENSE

1	2	3	4
EXCEL	GOOD	FAIR	NONE
✓			

SIGNAL DATA

	1 None	2 Avg	3 Extreme	4 Not Applic
Noise		✓		
Mod.				✓
Intfrnce	✓			

Reference Antenna Readout: 0° °

Comments:

Instrument Calibration: +2° for aural null

Intercept To Bearing Time:

ROTATION SPEED: 1 RPM (3-30) (6-60) (7-70) (1-AURAL NULL)

TRANSMITTER DATA:

Nominal Location: Habana, Cuba — Authority: T-2

Coordinates: Long. 82° 21 m W — Authority: T-2

Lat. 23° 09 m N

Calculated True Bearing And Distance: 109.5 Degrees, 1,090 Miles

TELETYPE TAPE SAMPLE:

OTHER COMMENTS:

CRT Photo If Available

Photo No.

1 Photo/Day/Station

Name of Test: Final antenna

* TO NEAREST .1 DEGREE

Observed Bearing *	108°
True Bearing	109.5°
Gross Error	-1.5°
Instrument Error	+2°
Net Error	+.5°

∈Gross = OB − TB

∈Net = ∈Gross − ∈Instr.

Call No. 40

FIGURE 40. SAMPLE SKYWAVE BEARING DATA SHEET (AURAL NULL)

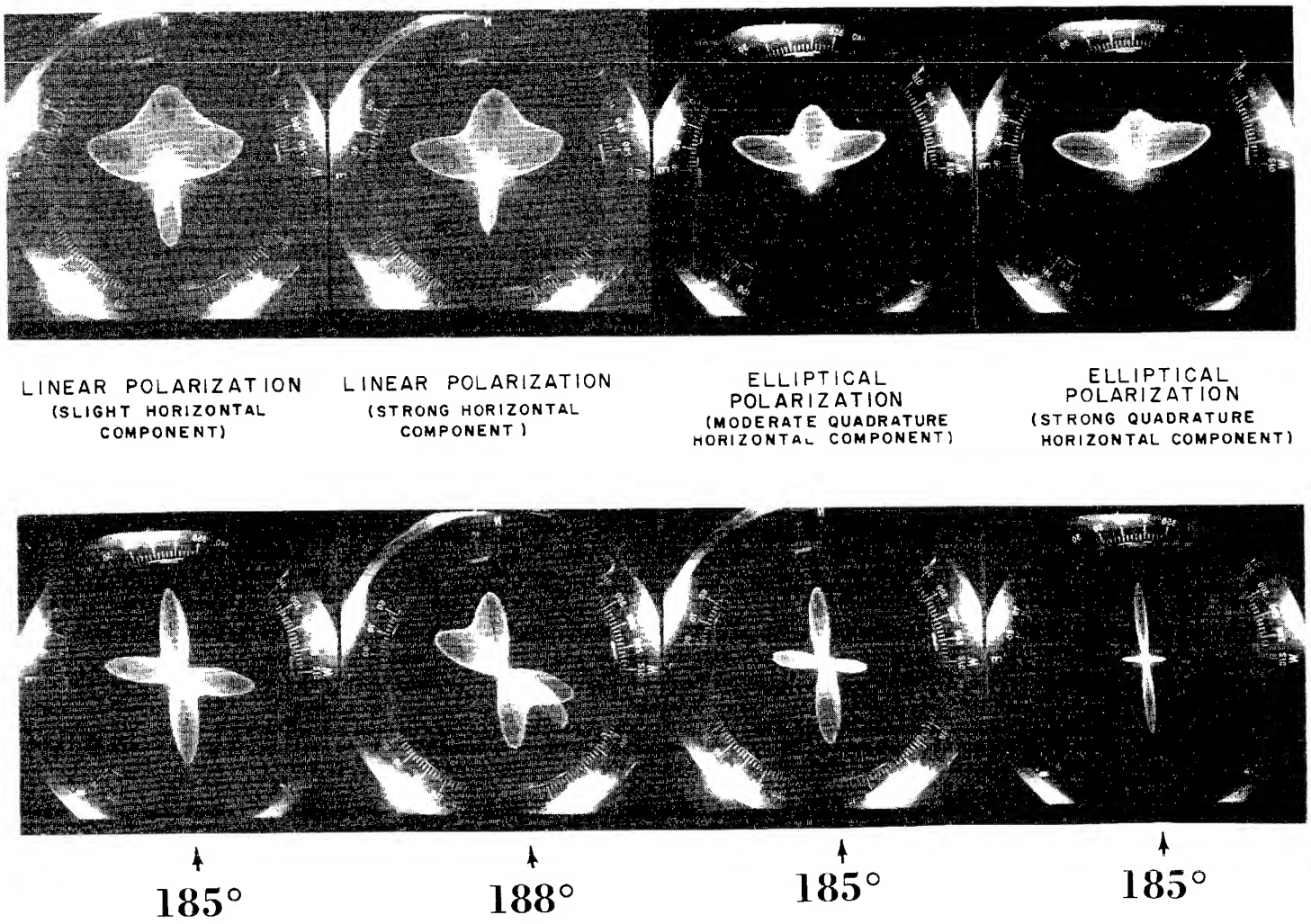

FIGURE 41. TYPICAL SKYWAVE PATTERNS-AMPLITUDE MODULATION (A3)

Approved For Release 2001/09/03 : CIA-RDP76-00451R000200010013-1

amplitude modulation (A-3), there is little doubt of the result. The four sense patterns all indicate that the bearing is at the bottom of the cathode ray tube indicator. The true bearing was 185°; however, for one DF pattern photograph in Figure 41, a bearing of 188° was obtained. The exposure for this 188° bearing DF pattern was slightly more than one antenna rotation, and one of the unwanted loop nulls appears at a new azimuth indicating a polarization change in the 2-second period.

The skywave sense and DF patterns for frequency shift CW (F1) are given in Figure 42 where the polarization is near vertical for all patterns. The effects of modulation on the pattern are slight, indicating careful receiver tuning. Tuning for frequency shift CW signals and teletype signals is critical for the slow speed spaced loop. With practice, the operator learns to tune across the signal for a best DF pattern.

The polarizations adjacent to the DF patterns given in Figures 41 and 42 are relative because the angle of arrival is not known. The relative polarizations as given do indicate the random changing polarization of a skywave signal.

The unmodulated carrier (A-0) patterns of Figure 42B indicate mixed linear polarization for the top set of patterns and circular polarization for the bottom set. It was obvious in tests of the antenna that elliptical polarization simplified pattern interpretation by blurring the unwanted nulls.

The occurrence of the symmetrical patterns as presented in Figures 41 and 42 is rare at 30 rpm. Most of the time after obtaining a sector to observe with the sense pattern, the operator is forced to wait for a pattern with a sharp null in that sector. Sometimes, as in the class F signals (no symmetrical patterns), a full pattern never develops because propagation conditions never stabilize for a 2-second period. The operator then must take the first sharp null in the sensed sector.

Experience late in the program with the normal (unblanked) deflection trace on the AN/PRD-5 DF indicator pointed out that the resulting pattern was an aid because more symmetrical patterns are obtained. The moving and blurring unwanted loop nulls were easier to locate. Furthermore, both the forward and reciprocal spaced loop nulls were being displayed in the sensed sector. This reduced response time for the signals with rapid changing polarization.

Patterns obtained on CW signals (A-1) at 30 rpm are given in Figure 43. The CW sense pattern is difficult to photograph, but, with practice, an operator learns to use the sense pattern. As the signal is

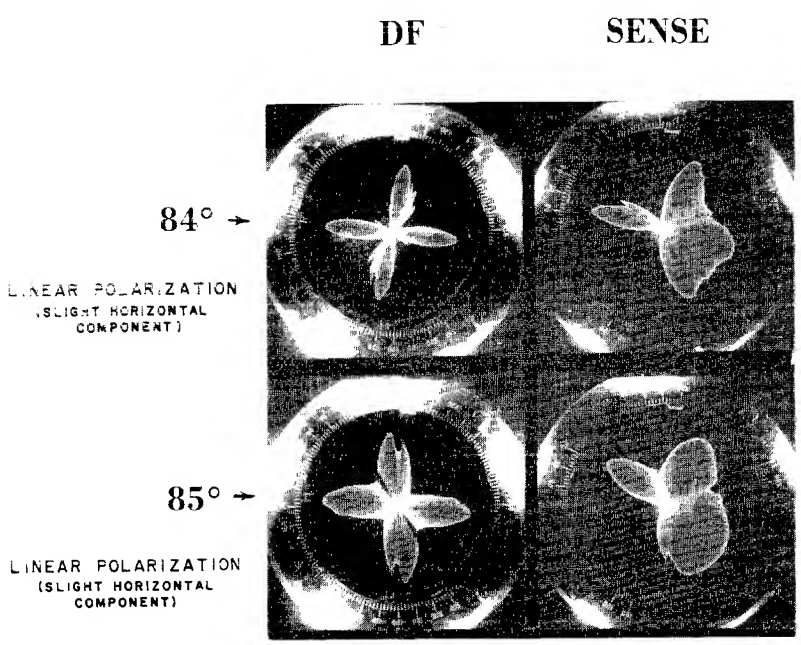

FIGURE 42A.

TYPICAL SKYWAVE PATTERNS

FREQUENCY SHIFT CW (F1)

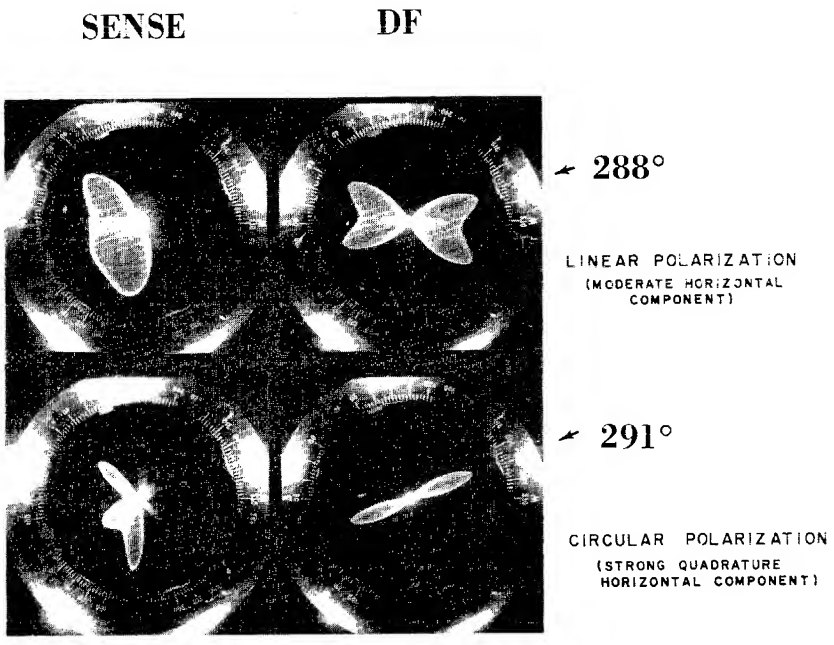

FIGURE 42B.

TYPICAL SKYWAVE PATTERNS

UNMODULATED CARRIER (A0)

Approved For Release 2001/09/03 : CIA-RDP76-00451R000200010013-1

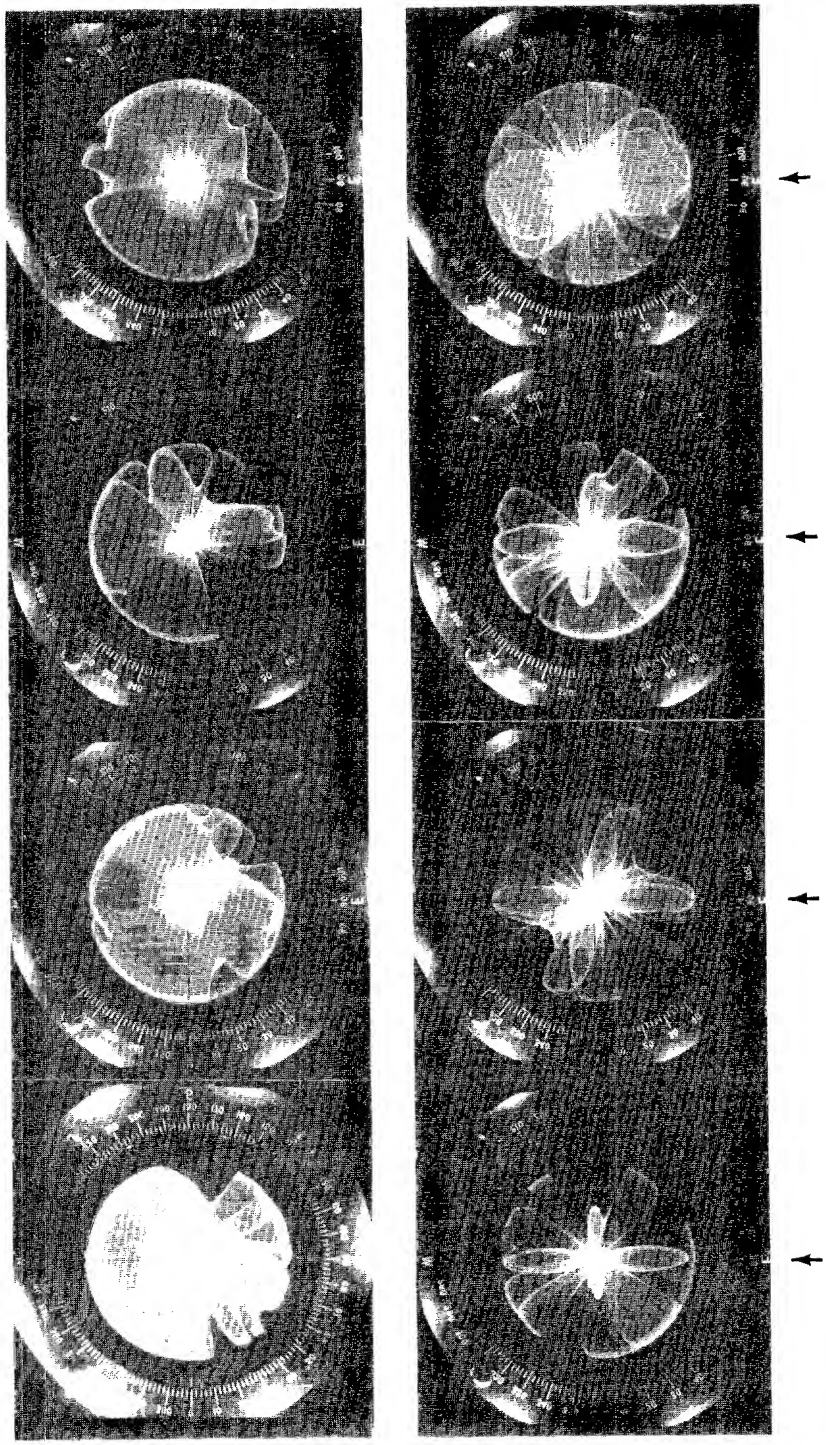

FIGURE 43. TYPICAL SKYWAVE PATTERNS-CW (A1)-AT 30 RPM

keyed, the sense pattern is driven towards the center sector of the correct bearing. At least two (2) and as many as eight (8) rotations of the antenna were required for positive sense on CW signals. The DF patterns of Figure 43 were obtained by 4 to 8 seconds exposure. For the majority of the CW signals, the operator used aural null techniques. After sensing the pattern, the operator would search the sensed sector in the low speed CW-CCW pedestal rotation mode for the fixed spaced loop null using the ear or DF indicator as a detector.

By operating the pedestal in the slow speed mode, but locked in 5 to 10-rpm continuous rotation, the improved results of Figure 44 were obtained. By slowing the antenna rotation to a rate where multiple keying occurs, the sense pattern and DF pattern can be developed as shown in Figure 44 at the expense of response time.

The patterns of Figures 43 and 44 show the limitation of a slow rotation rate for CW and SSB signals. Aural null techniques are accurate and effective, but time consuming.

4.3.3.5.2 Test Results

The skywave bearing data for the third breadboard model was partially reported in Quarterly Report No. 2.[4] A total of 301 bearings was taken with this antenna. Of the 301, the true bearings for 21 could not be determined. Two (2) bearings were eliminated because of obvious data recording errors.

The true bearing for individual stations and the statistical analysis of this and all subsequent bearing samples were performed using a computer program derived in work on other contracts. The basic equations for the statistical analysis were given in Quarterly Report No. 2 for this contract[4] and were previously given in the Final Report for Contract DA 36-039 AMC-02346(E).[21] The computer program is described in detail in a report covering work on the Beverage Antenna for the Navy Department under Contract NObsr-89345.[22]

A histogram of the error distribution of the 278 bearing sample for all data on the third breadboard model is given in Figure 45. The mean error is -0.15° and the standard deviation is 2.58°. Of the 278 bearings, 188 were taken on signals where the pedestal was operated at 30-rpm continuous rotation. These data for the third breadboard model are summarized in the histogram of Figure 46 where the mean error is -0.07° and the standard deviation is 2.79°.

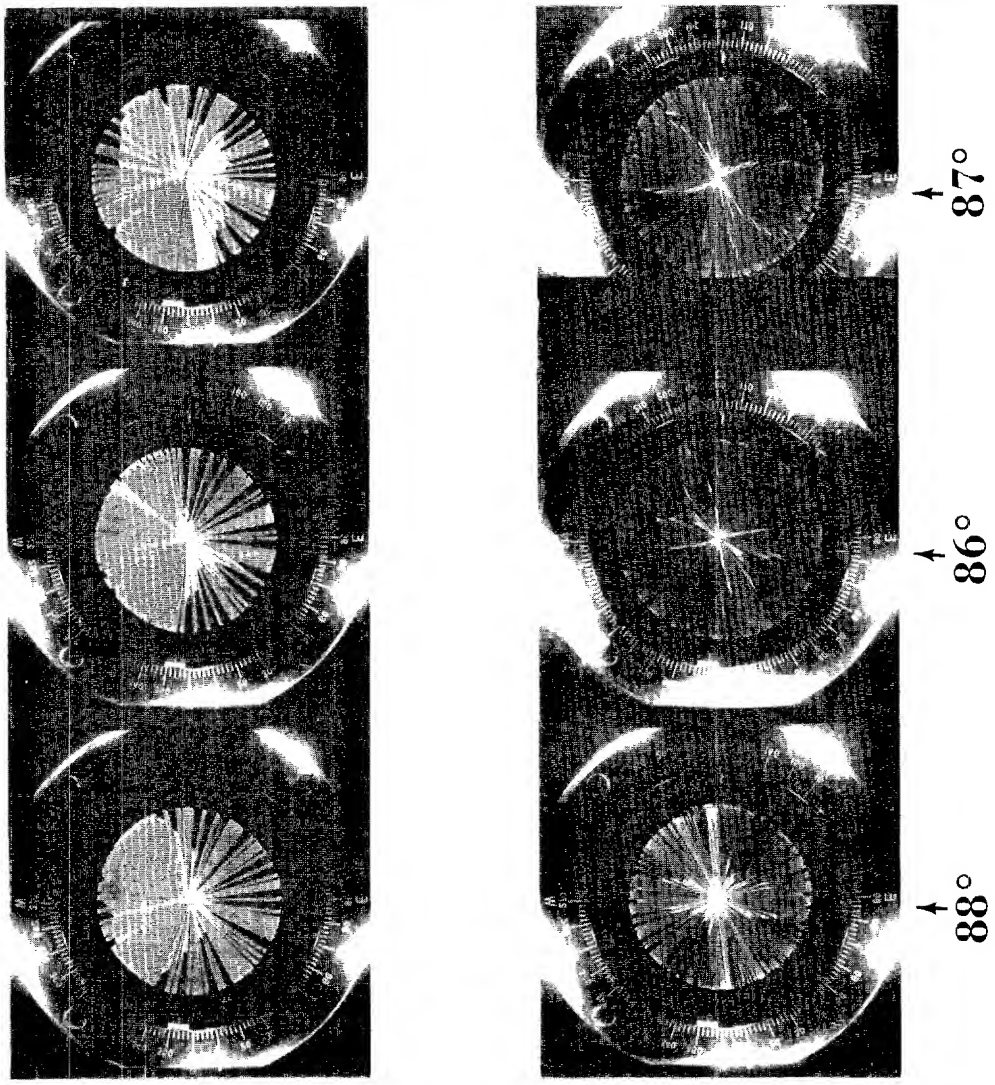

FIGURE 44. TYPICAL SKYWAVE PATTERNS-CW (A1) -5 TO 10 RPM

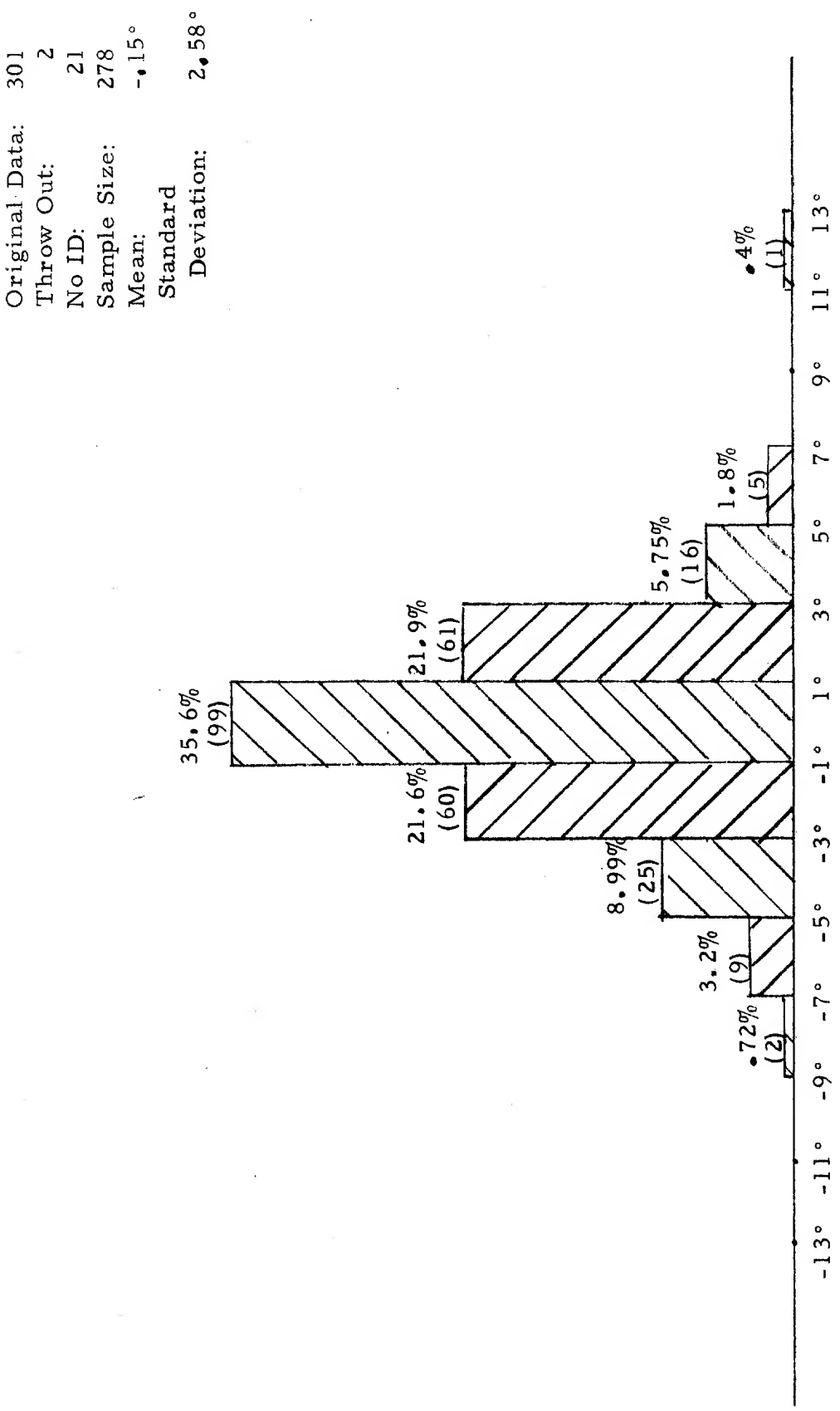

FIGURE 45
HISTOGRAM OF BREADBOARD ANTENNA SKYWAVE BEARING DATA - TOTAL SAMPLE

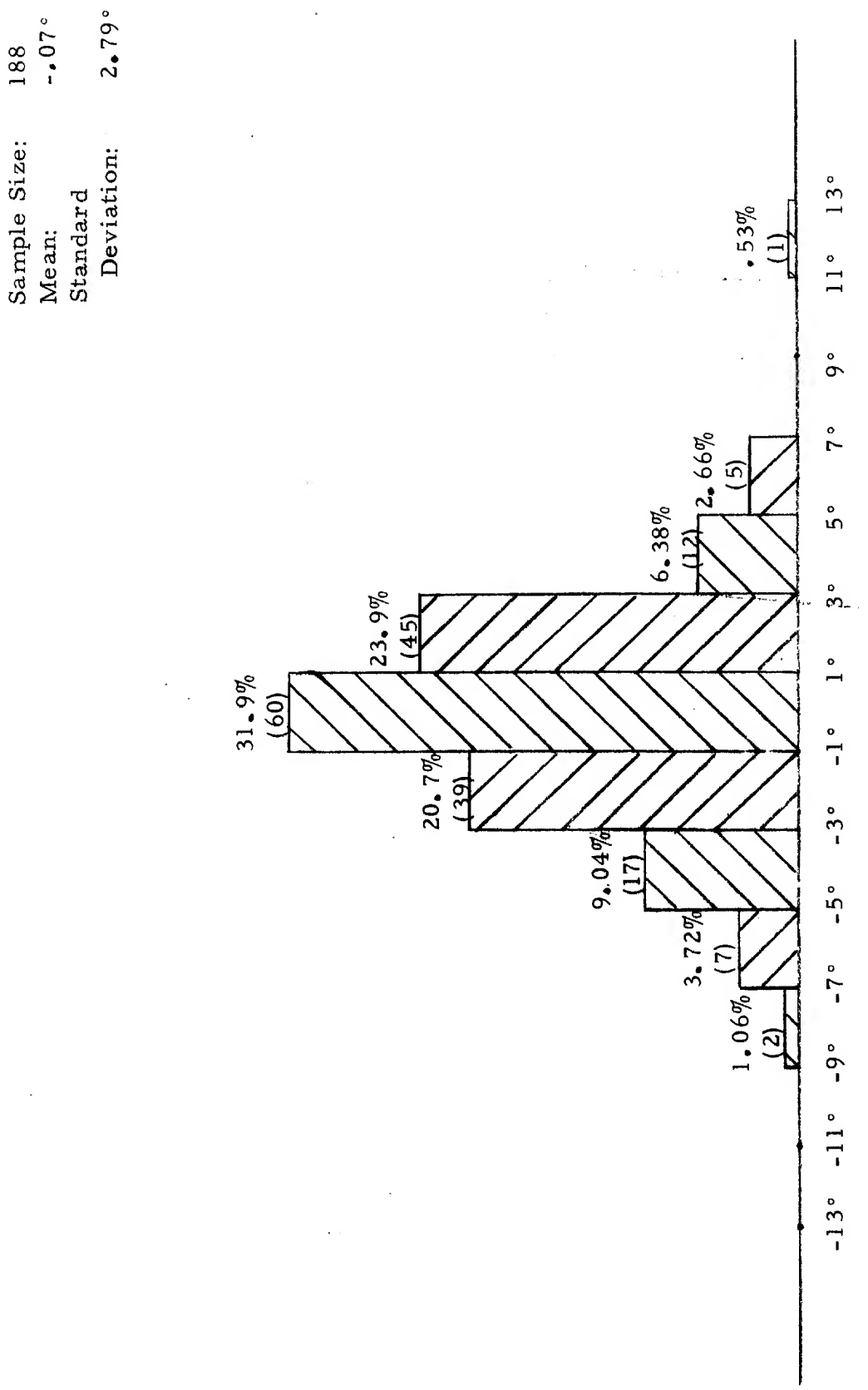

FIGURE 46
HISTOGRAM OF BREADBOARD ANTENNA SKYWAVE BEARING DATA -
CONTINUOUS 30 RPM MODE

Ninety (90) bearings of the total sample for the breadboard antenna were taken by aural null techniques using the low speed CW-CCW rotation function of the AN/PRD-7 and 8 pedestal. The histogram for the breadboard aural null data with a mean error of -0.32° and a standard deviation of 2.06° is given in Figure 47. Fifty-seven (57) bearings of the breadboard antenna samples were obtained on stations at distances less than 300 miles. The histogram of Figure 48 for these data shows a mean error of -0.3° and a standard deviation of 3.48°.

A list of the stations used for the breadboard data is given in Table 5. The number of bearings taken on each station is given along with location, coordinates, computer call number for the station, distance, and true bearing of the station.

For the final antenna, a total of 703 intercepts was made (station call letters determined) in the 24 hour per day tests. As summarized in Figure 49, a bearing was not obtained on 41 signals for various reasons. (Signal too weak in the DF mode, signal went off the air, and interference too severe are a few of the reasons.) The location of stations for 27 bearings could not be determined. Of the remaining, six (6) data sheets were eliminated because of inconsistencies or obvious errors in the data sheet.

The statistical analysis of the remaining 561 bearings for stations at distances greater than 300 miles resulted in a mean error of 0.27° and a standard deviation of 2.67° as given in Figure 49.

The 561 bearings have further been analyzed by signal class. The histogram of Figure 50 indicates that 243 bearings were taken by aural null techniques with a resulting mean error of 0.55° and a standard deviation of 2.70°.

Histograms for the data for the other signal classes for signals greater than 300 miles on the final antenna are given in Figures 51 to 56. The results are summarized in Table 6.

Response time is related to the signal class but less time was required to obtain a bearing than to obtain a symmetrical pattern at the 30-rpm rotation rate. The significance of the data of Table 6 is that standard deviation did increase for signals where propagation conditions were rapidly changing. With the signal sensed, the operator is forced to take the first sharp null that appears in the correct sector for the Class E and F signals. For the class A signals where a symmetrical pattern is obtained every sweep, the standard deviation is probably higher because the operator took a bearing on the spaced loop pattern with less averaging.

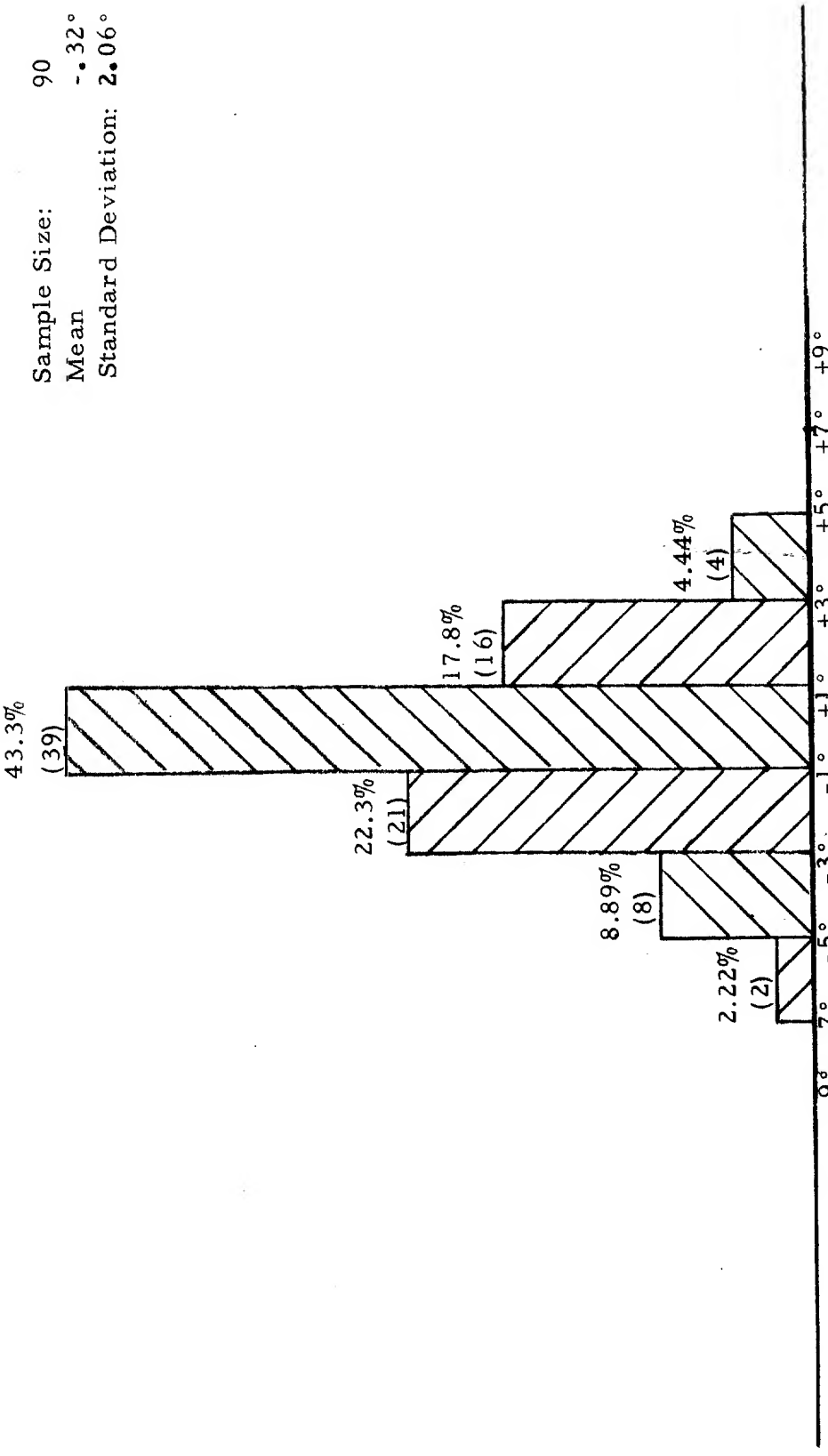

FIGURE 47
HISTOGRAM OF BREADBOARD ANTENNA SKYWAVE BEARING DATA -
AURAL NULL MODE

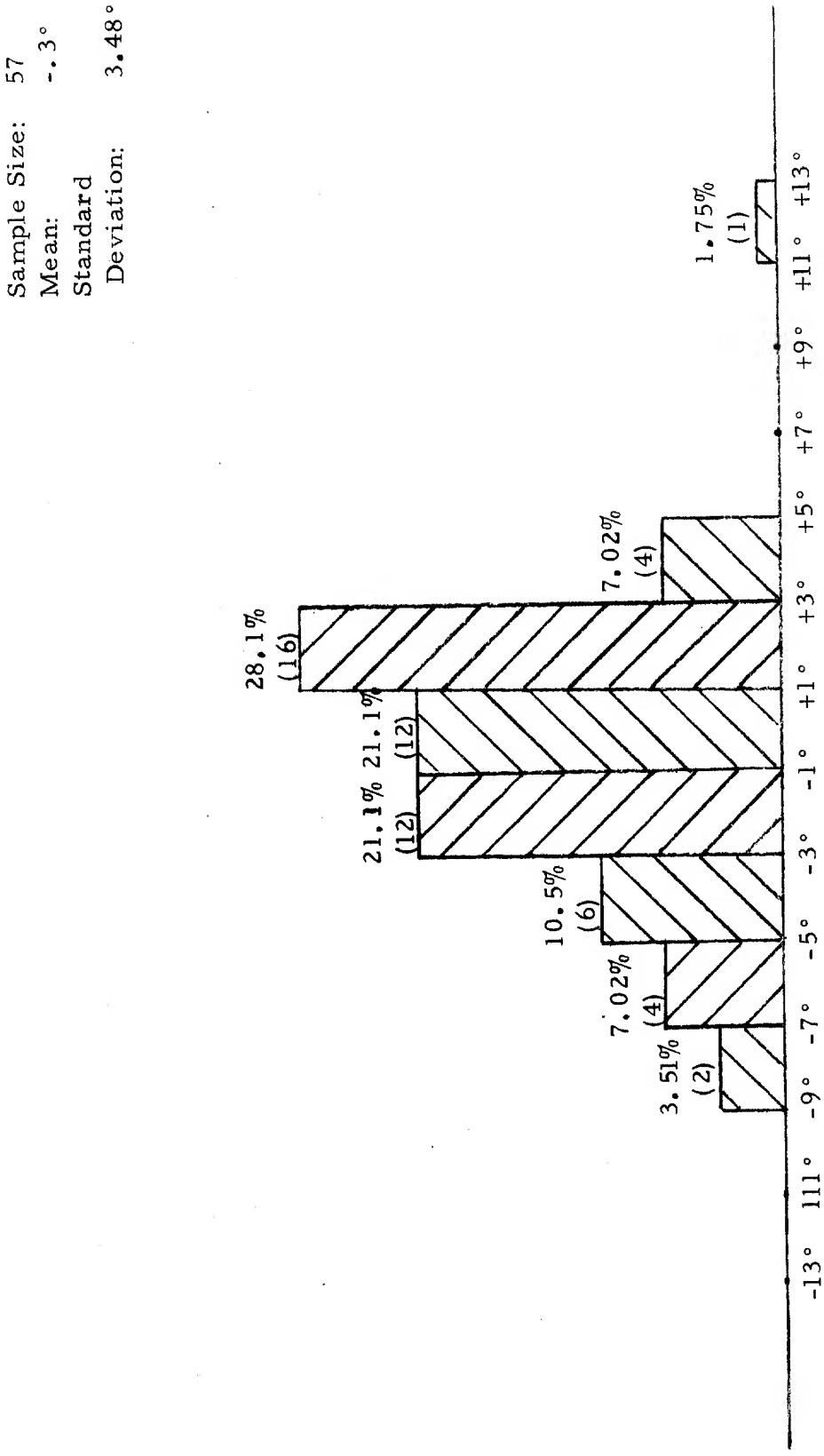

FIGURE 48
HISTOGRAM OF BREADBOARD ANTENNA SKYWAVE BEARING DATA -
STATIONS LESS THAN 300 MILES

TABLE 5. LIST OF STATIONS USED IN THE BREADBOARD ANTENNA SKYWAVE BEARING TESTS

Frequency MHz	Call Sign	Location	Coordinates Long.	Coordinates Lat.	Distance Miles	True Bearing	Comp Call	No. of Bearings
4.352	NBA	Balboa, PNZ	79W21	8N22	1919	135.5	495	2
4.367	WCC	South Chatham, Mass.	70W01	41N40	1804	54.3	488	1
4.590	AFA4RPP	Ft. Worth, Texas	97W27	32N46	240	16.4	757	1
4.590	AF5BOY	Corpus Christi, Texas	97W24	27N46	137	147.0	521	4
4.590	AFB5EIB	Houston, Texas	95W26	29N50	193	81.0	421	4
4.590	AF5FHW	Ft. Worth, Texas	97W21	32N40	235	18.2	754	1
4.590	AFB5FLM	Tulsa, Oklahoma	95W52	36N09	491	18.2	780	1
4.590	AFA5FOB	El Paso, Texas	106W25	31N54	490	288.0	781	2
4.590	AFB5GGN	Bristow, Oklahoma	96W25	36N44	521	13.5	763	1
4.590	AFB5HAP	Houma, Louisiana	90W44	29N35	474	86.8	782	2
4.590	AF5HBI	Losano, Texas	97W32	26N11	234	163.2	783	2
4.590	AFA5HKE	Wesson, Louisiana	90W47	31N22	486	72.0	756	1
4.590	AFB5HXH	Harlingen, Texas	97W41	27N11	165	165.5	499	1
4.590	AFA5INU	San Benito, Texas	97W37	26N08	236	164.7	518	1
4.590	AFA5IQZ	Sulphur, Louisiana	93W22	30N13	320	79.0	307	3
4.590	AF5JL	Corpus Christi, Texas	97W23	27N45	139	146.9	785	1
4.590	AF5JLI	Beaumont, Texas	94W06	30N06	275	79.2	786	2
4.590	AF5JWL	Gurdon, Arkansas	93W10	33N56	446	44.5	755	3
4.590	AF5KBY	Oklahoma City, Oklahoma	97W34	35N23	416	8.2	761	3
4.590	AFA5LEP	Houston, Texas	95W32	27N47	187	81.9	508	3
4.590	AFB5LHR	Austin, Texas	97W42	30N00	79	38.5	788	4
4.590	AF5LPZ	Tyler, Texas	95W09	32N18	288	45.3	305	2
4.590	AFA5LYP	Brady, Texas	99W20	31N07	124	339.8	497	7
4.590	AFA5QBU	Edgewater Park, Miss.	89W00	30N25	580	80.9	758	1
4.590	AF5QYO	Garland, Texas	96W52	32N44	250	24.0	511	1
4.590	AFA5UTE	Yazoo City, Miss.	91W05	33N24	523	56.4	762	2
4.590	AF5YCQ	Houston, Texas	95W29	29N18	189	92.0	810	1
4.590	AFA5ZPC	Dallas, Texas	96W52	32N44	250	24.0	306	2
4.590	AFØAIG	Mt. Vernon, Missouri	93W50	37N07	598	26.2	338	2
4.590	AFAØLFI	Independence, Missouri	94W27	39N05	708	18.5	220	2
4.590	AFBØLNM	Great Bend, Kansas	98W52	38N21	616	358.8	752	4
4.590	AFØMKJ	Arnold, Missouri	90W24	38N25	778	35.0	759	1
4.786	WID64	Miami, Florida	80W12	25N59	1148	97.5	411	9
4.985	WKA24	New Orleans, Louisiana	89W44	30N17	534	81.5	1	6
5.000	WWV	Beltsville, Maryland	76W50	38N59	1402	56.2	2	18
5.000	WWV	Ft. Collins, Colorado	105W02	40N40	857	336.7	775	3
5.096	CFH	Halifax N.S., Canada	63W59	44N58	2168	50.7	561	4
5.780	HQL2	La Lima, Honduras	87W55	15N50	1160	141.8	627	4
5.790	TGA	Barcenas, Guatemala	90W37	14N32	1149	151.9	678	5
5.870	NSS	Annapolis, Maryland	76W27	38N59	1422	56.5	413	4
6.376	WCC	South Chatham, Mass.	70W02	41N40	1802	54.3	3	2
6.425	CFH	Halifax, Nova Scotia	63W59	44N58	2163	50.7	562	2

TABLE 5. LIST OF STATIONS USED IN THE BREADBOARD ANTENNA SKYWAVE BEARING TESTS (Cont'd)

Frequency MHz	Call Sign	Location	Coordinates Long.	Coordinates Lat.	Distance Miles	True Bearing	Comp Call	No. of Bearings
6.446	WLO	Mobile, Alabama	88W02	30N42	637	79.5	581	6
6.448	WPA	Port Arthur, Texas	93W58	29N50	281	83.2	455	3
6.481	NSS	Annapolis, Maryland	76W27	38N59	1422	56.2	10	1
6.495	WNU	Slidell, Louisiana	89W44	30N17	534	81.5	11	2
6.502	WSC	Tuckerton, New Jersey	74W18	39N38	1545	56.4	12	4
6.512	CLA	Havana, Cuba	82W21	23N09	1090	109.5	147	6
6.770	WKA46	New Orleans, Louisiana	89W44	30N17	534	81.5	587	6
6.778	WID36	Miami, Florida	80W12	25N29	1148	97.6	523	9
6.785	WKA	New Orleans, Louisiana	89W44	30N17	534	81.5	15	23
6.832	CLA	Havana, Cuba	82W21	23N09	1090	109.5	602	8
7.335	CHU	Ottawa, Canada	75W43	45N24	1659	42.0	16	5
7.351	CLA211	Havana, Cuba	82W21	23N09	1090	109.5	806	4
7.508	CLA9	Havana, Cuba	82W21	23N09	1090	109.5	807	4
7.600	YNA3	Managua, Nicaragua	86W26	12N10	1427	144.2	157	2
7.665	TIO	Las Pavas, Costa Rica	84W52	09N50	1620	143.9	156	5
7.980	HPC	Panama	79W28	09N02	1876	134.8	808	2
8.479	TIO	Las Pavas, Costa Rica	84W52	09N50	1620	143.9	809	1
8.486	WOE	Lakeworth, Florida	80W06	26N23	1144	95.5	22	3
8.531	WAX	Hialeah, Florida	80W12	25N59	1149	97.6	24	2
8.550	WPA	Port Arthur, Texas	93W58	29N50	281	83.2	152	10
8.570	WNU	Slidell, Louisiana	89W44	30N17	535	81.5	27	4
8.586	WCC	South Chatham, Mass.	70W02	41N40	1802	54.3	29	1
8.590	KOK	Clearwater, California	118W09	33N54	1188	290.0	30	1
8.630	WCC	South Chatham, Mass.	70W02	41N40	1804	54.3	198	1
8.642	KPH	Bolinas, California	122W44	37N54	1499	299.3	196	1
8.666	KLC	Galveston, Texas	95W08	29N24	210	89.8	208	2
8.714	WLO	Mobile, Alabama	88W02	30N42	637	79.5	39	7
8.714	CLA	Havana, Cuba	82W21	23N09	1090	109.5	40	1
9.083	TIV	Las Pavas, CTR.	84W52	09N50	1620	143.9	502	1
9.425	NSS	Annapolis, Maryland	76W27	38N59	1422	56.2	44	1
10.000	WWV	Beltsville, Maryland	76W50	38N59	1402	56.2	48	9
10.008	HRX6/25	La Lima, Honduras	87W55	15N50	1160	141.8	805	2
10.270	HPD	Panama	79W28	09N02	1876	134.8	49	1
10.470	WKB3Ø	New Orleans, Louisiana	89W44	30N17	534	81.5	53	1
10.492	WFE5Ø	Brentwood, New York	73W15	40N49	1624	54.3	568	2
10.515	WFE5Ø	New York City	73W15	40N40	1623	54.6	383	4
10.636	XDA138	Mexico D. F.	99W02	19N22	696	182.2	650	3
12.993	KOK	Clearwater, California	118W09	33N54	1188	290.0	85	1
15.000	WWV	Ft. Collins, Colorado	105W02	40N40	857	336.7	778	3

Approved For Release 2001/09/03 : CIA-RDP76-00451R000200010013-1

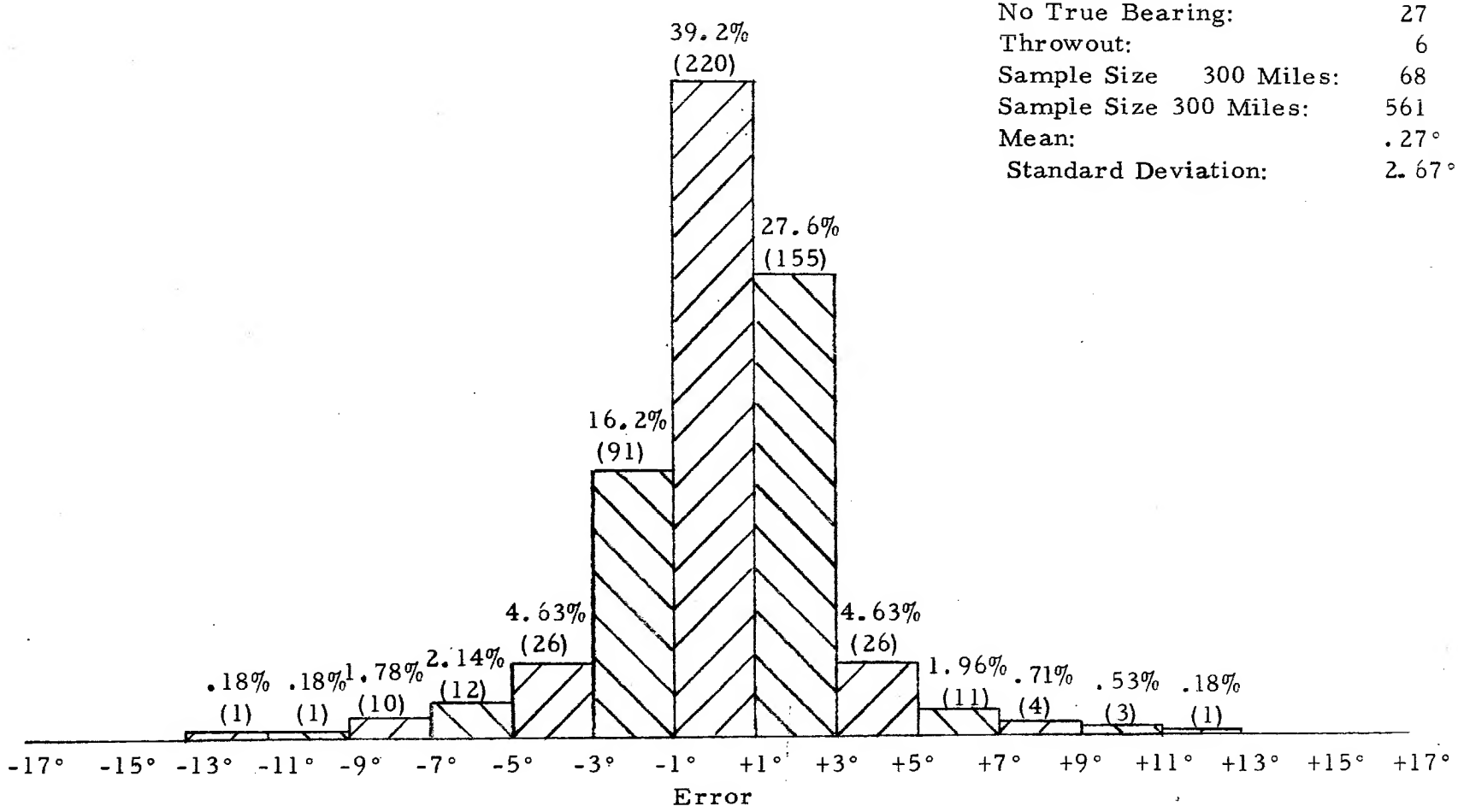

FIGURE 49
HISTOGRAM OF FINAL ANTENNA SKYWAVE BEARING DATA -
ALL DATA GREATER THAN 300 MILES

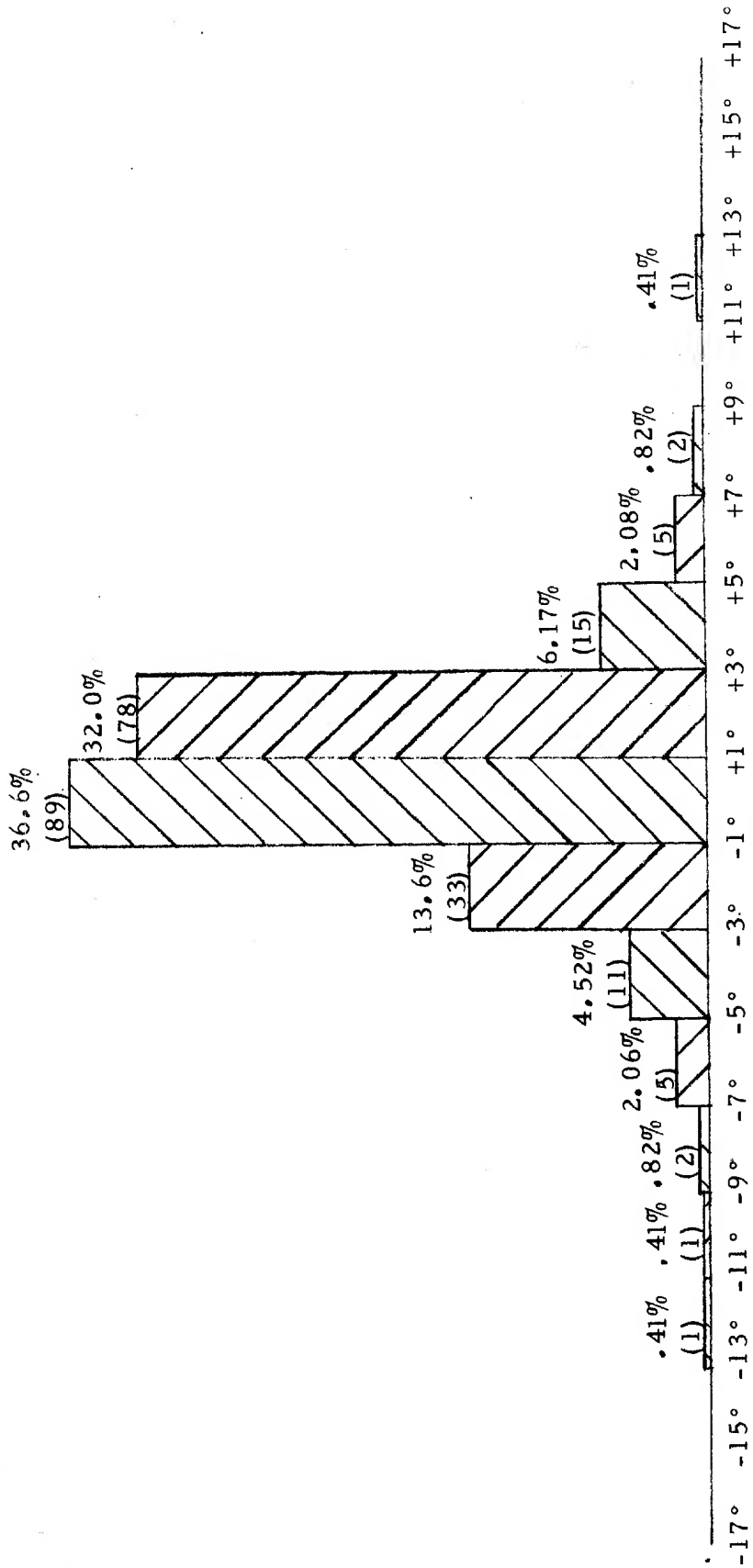

FIGURE 50
HISTOGRAM OF FINAL ANTENNA SKYWAVE BEARING DATA -
AURAL NULL GREATER THAN 300 MILES

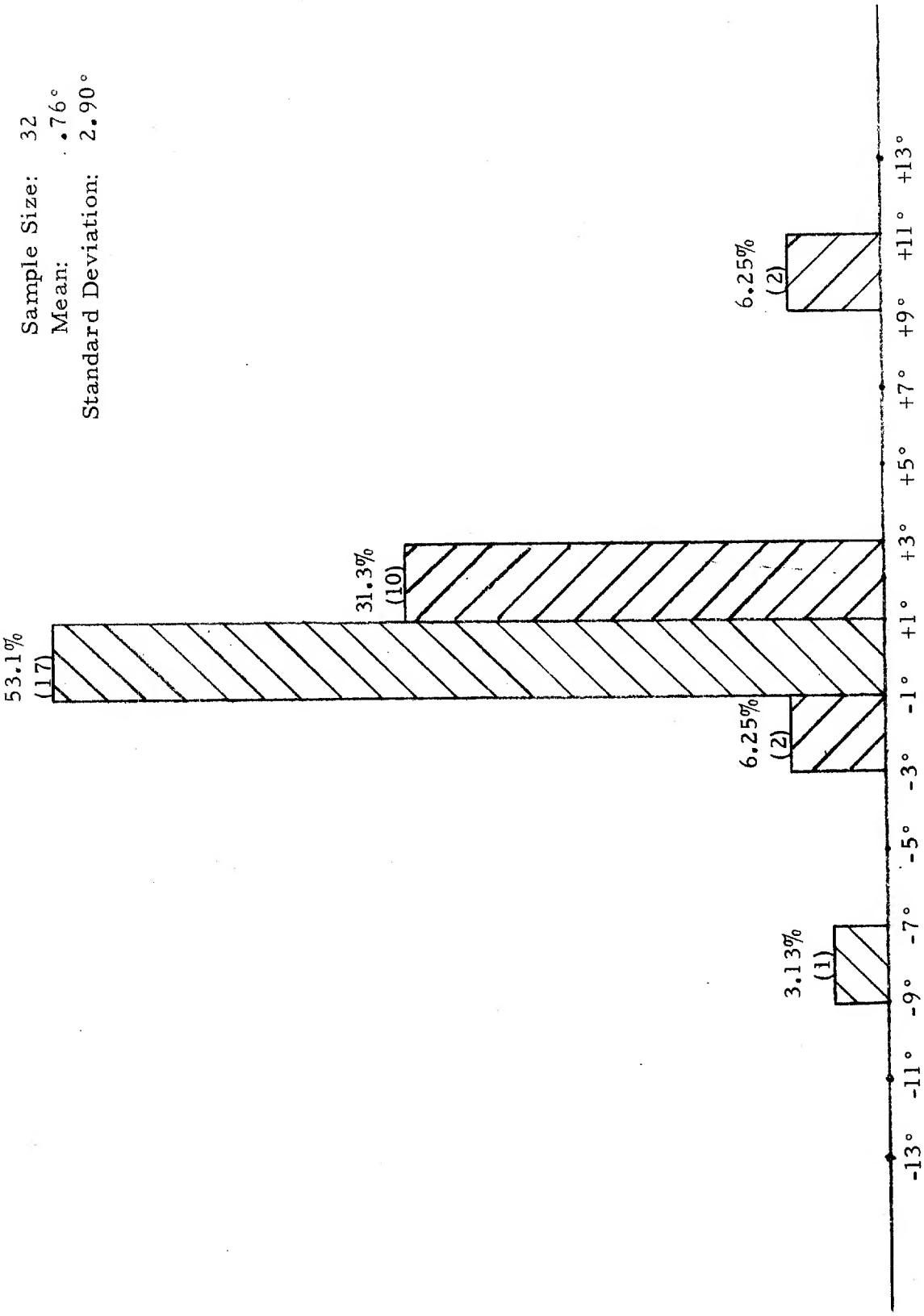

FIGURE 51
HISTOGRAM OF FINAL ANTENNA SKYWAVE BEARING DATA -
CONTINUOUS ROTATION GREATER THAN 300 MILES -
CLASS A OR SYMMETRICAL PATTERN EVERY SWEEP

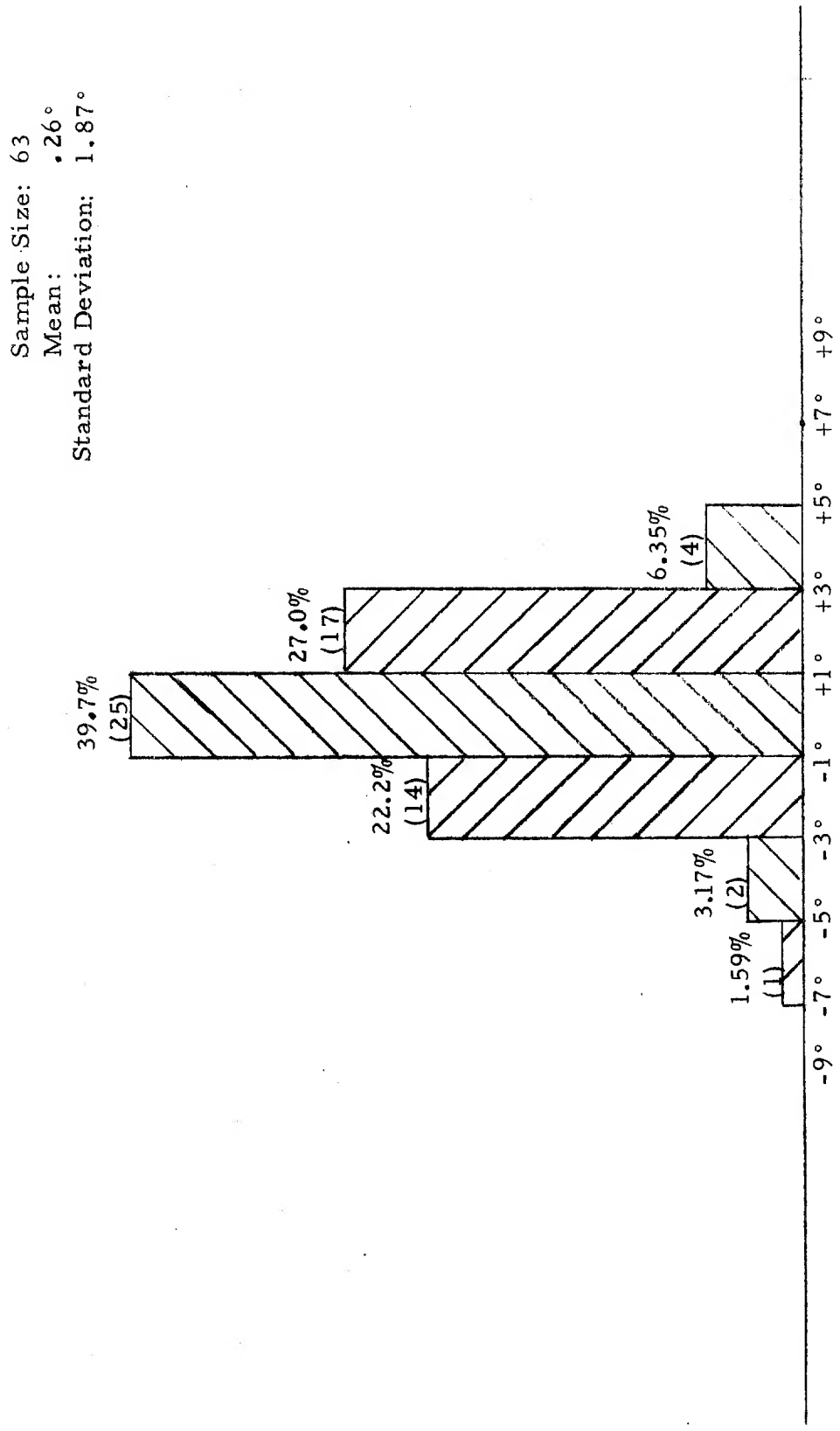

FIGURE 52
HISTOGRAM OF FINAL ANTENNA SKYWAVE BEARING DATA -
CONTINUOUS ROTATION GREATER THAN 300 MILES
CLASS B OR SYMMETRICAL PATTERN EVERY 2 to 3
SWEEPS

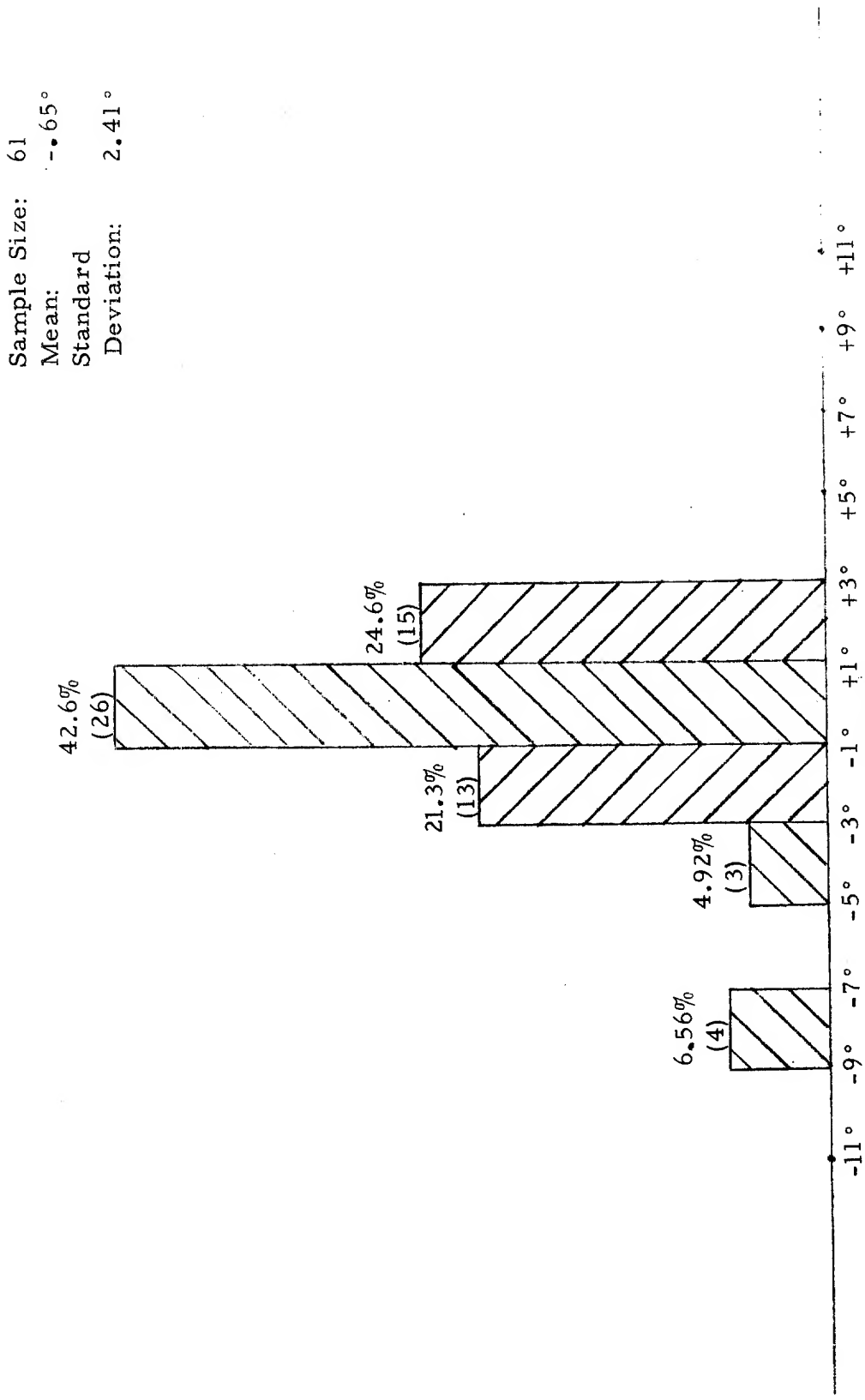

FIGURE 53
HISTOGRAM OF FINAL ANTENNA SKYWAVE BEARING DATA -
CONTINUOUS ROTATION GREATER THAN 300 MILES -
CLASS C OR SYMMETRICAL PATTERN EVERY 4 TO 6 SWEEPS

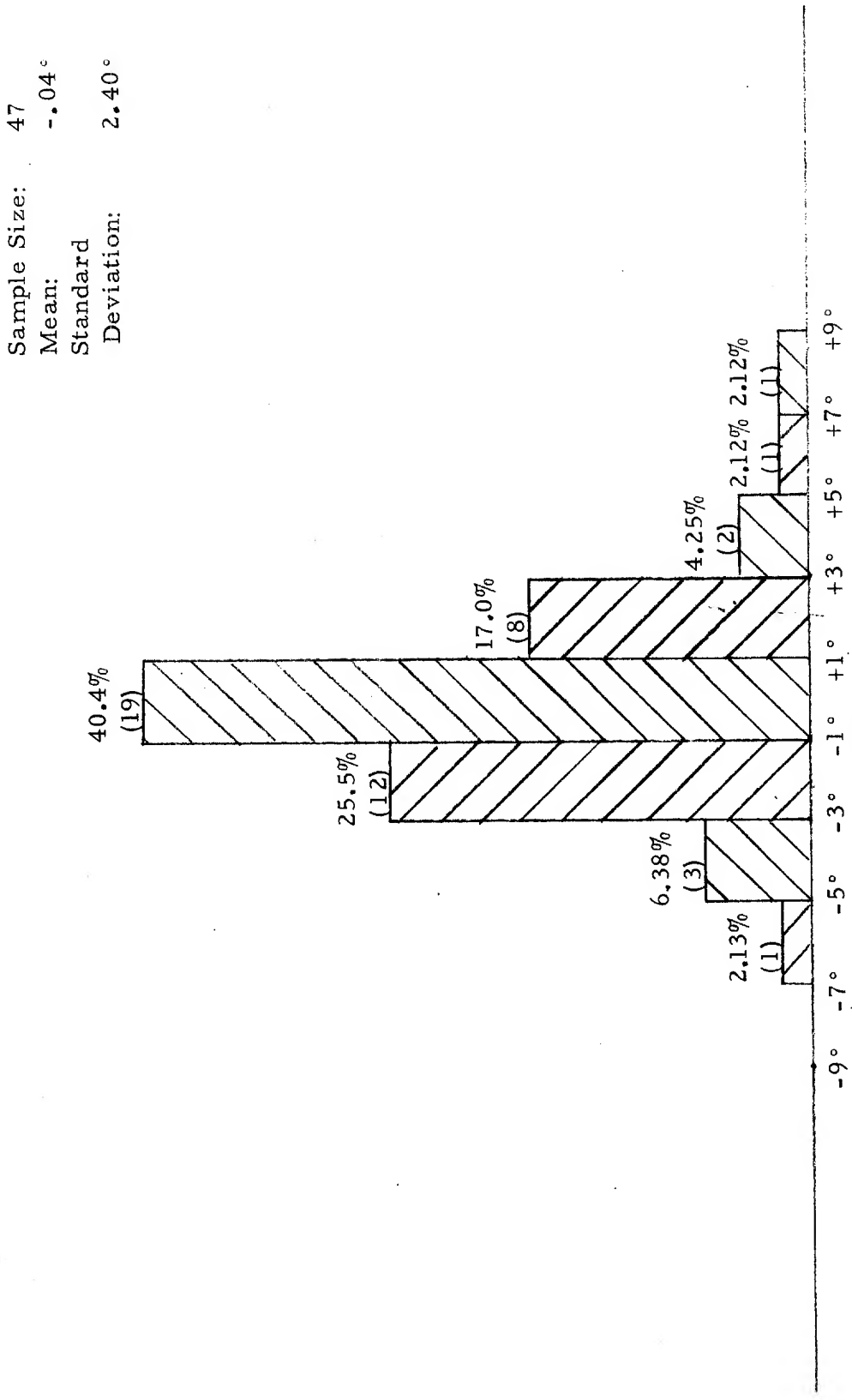

FIGURE 54
HISTOGRAM OF FINAL ANTENNA SKYWAVE BEARING DATA -
CONTINUOUS ROTATION GREATER THAN 300 MILES -
CLASS D OR SYMMETRICAL PATTERN EVERY 7 TO 9 SWEEPS

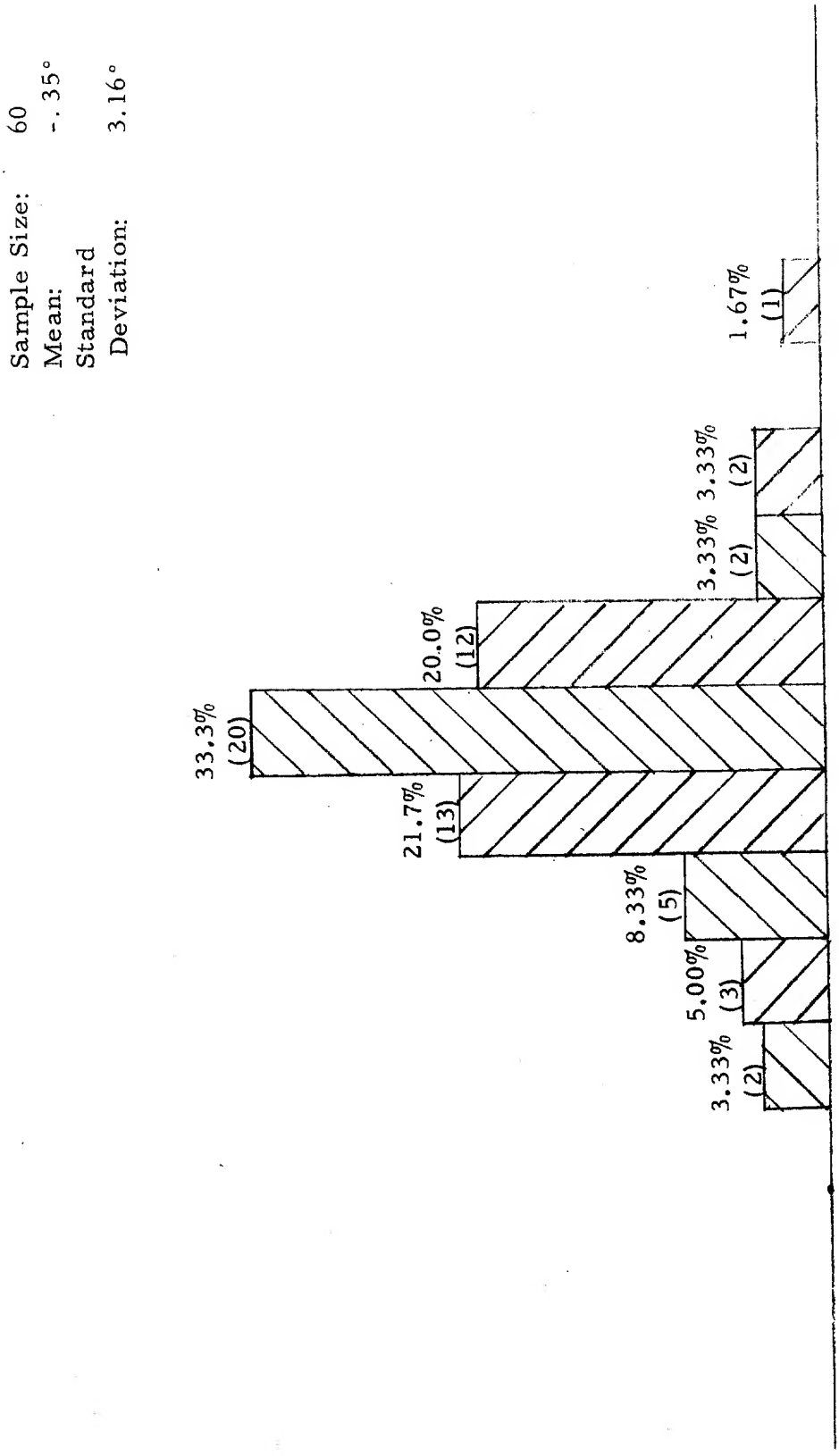

FIGURE 55
HISTOGRAM OF FINAL ANTENNA SKYWAVE BEARING DATA -
CONTINUOUS ROTATION GREATER THAN 300 MILES -
CLASS E OR SYMMETRICAL PATTERN AFTER MORE THAN 9 SWEEPS

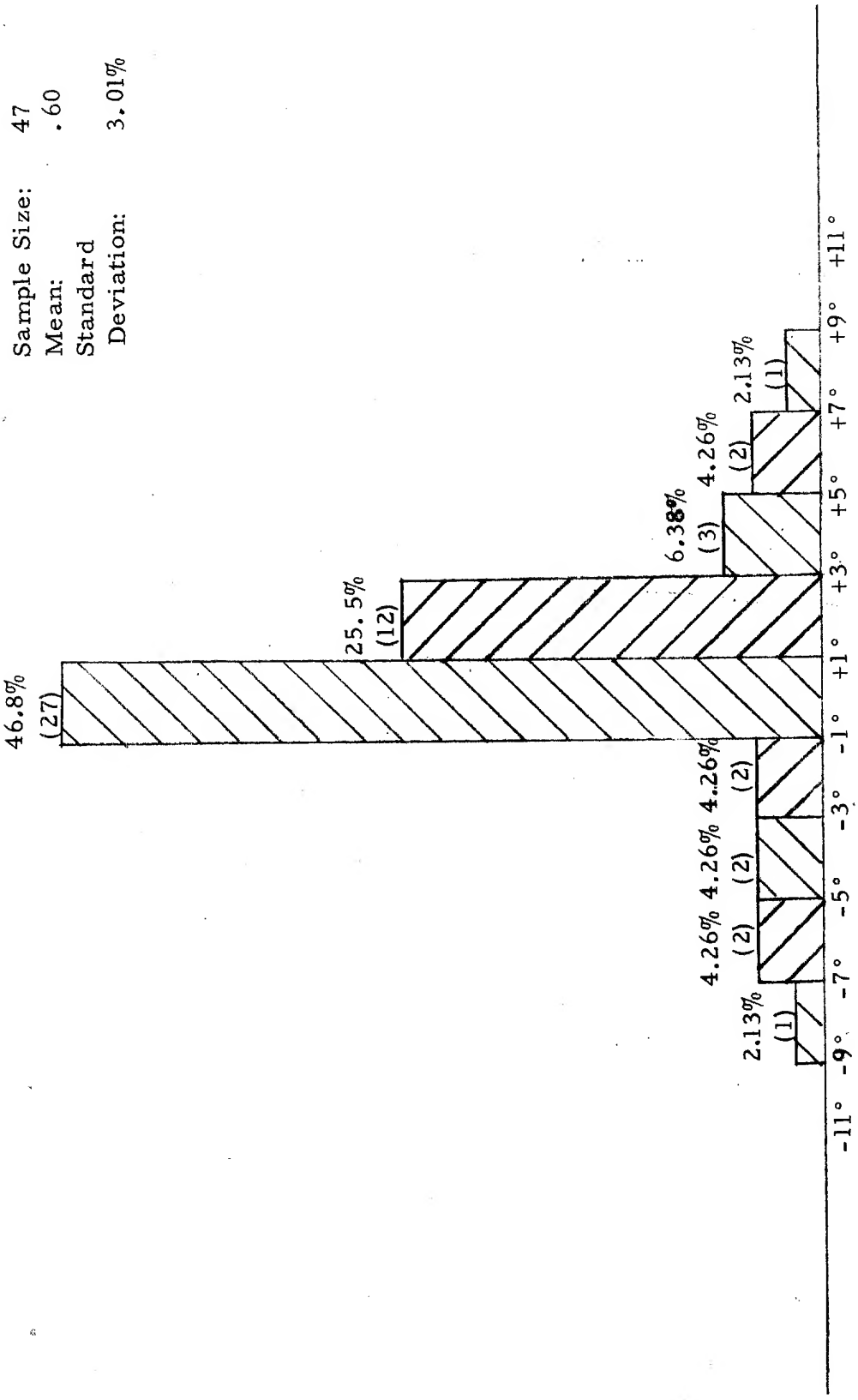

FIGURE 56
HISTOGRAM OF FINAL ANTENNA SKYWAVE BEARING DATA -
CONTINUOUS ROTATION GREATER THAN 300 MILES -
CLASS F OR SYMMETRICAL PATTERN NEVER OCCURRED

TABLE 6
Summary of Data as a Function of Signal Class
On the Final Antenna

Signal Class	Antenna Rotations Necessary For a Symmetrical Pattern	Sample Size	Mean Error	Standard Deviation
A	Every rotation	32	.76°	2.90°
B	2 to 3	63	.26°	1.87°
C	4 to 6	61	-.65°	2.41°
D	7 to 9	47	-.04°	2.40°
E	Greater than 9	60	-.35°	3.16°
F	Never	47	.60°	3.01°

A list of the stations at distances greater than 300 miles used in the sky-wave bearing tests of the final antenna is given in Table 7.

The histogram for 141 bearings taken on a controlled transmitter using a broadside horizontal half-wave dipole at Bandera, Texas (distance 35 miles and true bearing 306.5°) is given in Figure 57. The distribution with a mean error of 1.13° and a standard deviation of 8.85° is a typical distribution for signals arriving at a high angle of elevation.

The data of Figure 57 were taken over a 2-day period at 6.3 MHz and 8.5 MHz. The target transmitter was on for 20 seconds and off for 20 seconds. During eleven (11) of the 20-second transmissions, the sense and DF procedure could not be completed because of propagation conditions, signal fade, and other reasons. It is estimated that the signal angle of elevation was between 83° and 87° for these tests.

Both long-term and short-term bearings were observed, and it was obvious that the spaced loop zenith elevation null was being approached.

During a demonstration period (no data were recorded), the bearing of the 6.3-MHz signal slowly drifted to a -15° error. Over a 20-minute period while the signal was stable with little polarization change, the bearing slowly drifted through the correct bearing to a +17° error. A "slight tilt" of the ionosphere at high signal angles of elevation will produce large bearing errors.

Tests were also conducted with the target transmitter at Carrizo Springs, Texas (distance 96 miles and true bearing 229.5°). With the horizontal dipole broadside, bearings were attempted on 167 20-second unmodulated transmissions. Frequency was varied between 3.995 MHz, 6.300 MHz, and 8.500 MHz during the test to maintain a strong signal as propagation conditions changed.

The histogram of Figure 58 summarizes the data for the 150 bearings obtained. For this high angle signal, a mean error of 2.09° and a standard deviation of 6.68° were obtained. A larger bearing sample may have reduced the large mean error, although site error could be the source of the high mean error on this fixed azimuth test.

Data obtained on the only consistent 200-mile station are summarized in Figure 59. Most of the data were taken at 8.660 MHz during daylight hours. The standard deviation of 2.15° seemed too low for the distance. It was determined that the station uses a rhombic antenna directed toward this laboratory. It is suspected that this antenna reduces dispersion from

TABLE 7. LIST OF STATIONS USED IN THE FINAL ANTENNA SKYWAVE BEARING TESTS

Frequency MHz	Call Sign	Comp Call	Location	Coordinates Long.	Coordinates Lat.	Distance Miles	Bearing	No. of Bearings
4.005	NPG	210	San Francisco, California	122W16	38N05	1478	300.1	4
4.022	TEL5	720	Las Pavas, Costa Rica	84W52	09N50	1620	143.9	11
4.186	VCS	821	Halifax NS, Canada	63W37	44N28	2172	51.7	1
4.247	KPH	295	Bolinas, California	122W44	37N54	1498	299.3	2
4.271	CFH	505	Halifax, Nova Scotia	63W59	44N58	2163	50.7	1
4.274	KFS	468	Palo Alto, California	122W07	37N27	1454	298.5	2
4.283	PJK3	837	Suffisant Atw., Neth.	68W55	12N09	2249	115.8	1
4.284	PJK34/38	836	Suffisant Atw., Neth. App.	68W55	12N09	2249	115.8	5
4.292	VCS	654	Halifax NS, Canada	63W37	44N28	2171	51.7	2
4.300	WAX	811	Hialeah, Florida	80W12	25N59	1149	97.5	5
4.310	WNV	200	Slidell, Louisiana	89W44	30N17	535	81.5	4
4.343	WSL	461	Amagansett, N. Y.	72W03	41N00	1688	54.6	1
4.350	CLA	211	Habana, Cuba	82W21	23N09	1090	109.5	7
4.352	NBA	495	Balboa, PNZ.	79W21	8N22	1919	135.5	4
4.360	CFH	812	Halifax NS, Canada	63W59	44N58	2163	50.7	4
4.367	WCC	488	South Chatham, Mass.	70W01	41N40	1804	54.3	5
4.448	NPO	831	Manila, Philippines	120F59	14N36	2605	315.2	1
4.466	HPA	830	Panama, Canal Zone	79W28	09N02	1877	134.7	3
4.519	NKA	844	Asmara, Ethiopia	38E50	15N15	8245	48.4	1
4.525	NPM	464	Pearl Harbor	157W58	21N22	3705	276.0	6
4.615	MLU	852	Gibraltar, Gibraltar	05W25	36N10	5216	56.3	1
4.786	WID64	411	Miami, Florida	80W12	25N59	1148	97.5	21
4.808	YNA2	686	Managua, Nicaragua	86W14	12N10	1434	143.7	3
4.810	YNA2	478	Managua, Nicaragua	86W26	12N10	1427	144.2	3
4.957	NPN	813	Guam, Guam	144E47	13N29	7279	295.6	1
4.985	WKA24	1	New Orleans, Louisiana	89W44	30N17	534	81.5	19
5.000	WWV	2	Beltsville, Maryland	76W50	38N59	1402	56.2	1
5.000	WWVH	410	Maui, Hawaii	156W27	20N46	3630	274.6	2
5.000	WWV	776	Ft. Collins, Colorado	105W02	40N40	857	336.7	30
5.131	HRE1Ø	630	Tegucigalpa, Honduras	87W20	14N15	1270	143.0	10
5.280	HPJ	483	Panama, PNC.	79W29	9N02	1877	134.8	3
5.450	NBA	477	Balboa, PNZ.	79W39	9N03	1866	135.1	1
5.779	WID36	823	Miami, Florida	80W12	25N59	1148	97.5	1
5.780	HQL2	627	La Lima, Honduras	87W55	15N50	1160	141.8	8
5.790	TGA	678	Barcenas, Guatemala	90W37	14N32	1149	151.9	4
5.870	NSS	413	Annapolis, Maryland	76W27	38N59	1422	56.5	6
5.975	TGA	820	Barcenas, Guatemala	90W37	14N32	1149	151.9	1
5.980	WKA24	817	New Orleans, Louisiana	89W44	30N17	534	81.5	2
6.136	HABANA	846	Habana, Cuba App.	82W21	23N09	1090	109.5	2
6.365	KFS	207	Palo Alto, California	122W07	37N27	1454	298.5	1
6.369	KLC	153	Galveston, Texas	95W08	29N24	210	89.8	2
6.369	KFS	635	Palo Alto, California	122W07	37N27	1454	298.5	1
6.376	WCC	3	South Chatham, Mass.	70W02	41N40	1802	54.3	6
6.382	EAD2	4	Aranjuez, Spain	3W36	40N01	5186	52.0	1
6.390	WAX	5	Hialeah, Florida	80W12	25N59	1149	97.6	5
6.411	WOE	6	Lakeworth, Florida	80W06	26N33	1144	95.5	6
6.411	KLB	648	Kent, Washington	122W11	48N02	1792	322.3	2
6.421	FFL3/4	559	Slys, France	1E24	43N25	5310	47.3	1
6.429	NPG	642	San Francisco, California	122W34	37N37	1485	298.7	2
6.446	CKN	8	Vancouver, B. C.	122W15	49N06	1839	324.2	5
6.446	WLO	581	Mobile, Alabama	88W02	30N42	637	79.5	2
6.448	WPA	455	Port Arthur, Texas	93W58	29N50	281	83.2	4
6.452	CFH	562	Halifax NS, Canada	63W59	44N58	2163	50.7	8
6.463	KOK	9	Clearwater, California	118W09	33N54	1188	290.0	4
6.477	KPH	205	Bolinas, California	122W44	37N54	1499	299.3	2
6.481	NSS	10	Annapolis, Maryland	76W27	38N59	1422	56.5	5
6.492	VRT	834	Bermuda, Bermuda	64W40	32N23	2015	75.4	1
6.493	VCS	493	Halifax, Nova Scotia	63W37	44N28	2171	51.7	5
6.495	WNU	11	Slidell, Louisiana	89W44	30N17	534	81.5	10
6.512	CLA	147	Habana, Cuba	82W21	23N09	1090	109.5	6
6.519	KFS	814	Palo Alto, California	122W07	37N27	1454	298.5	1
6.522	YVG	828	La Guaira, Venezuela	66W58	10N36	2419	115.9	1
6.770	WKA46	587	New Orleans, Louisiana	89W44	30N17	534	81.5	12
6.770	CLA	818	Habana, Cuba	82W21	23N09	1090	109.5	1
6.778	WID36	594	Miami, Florida	80W12	25N59	1148	97.6	2
6.782	WID36	523	Miami, Florida	80W12	25N59	1148	97.5	8
6.785	WKA	15	New Orleans, Louisiana	89W44	30N17	534	81.5	4
6.838	NNI	853	Napoli, Italy	14F15	40N50	5939	44.5	1
6.980	HPC	294	Panama, PNR	79W28	09N02	1876	134.8	4

TABLE 7. LIST OF STATIONS USED IN THE FINAL ANTENNA SKYWAVE BEARING TESTS (Cont'd)

Frequency MHz	Call Sign	Comp Call	Location	Coordinates Long.	Coordinates Lat.	Distance Miles	Bearing	No. of Bearings
6.996	CLX9	827	Casa Blanca, Cuba App.	82W21	23N09	1096	109.5	2
7.335	CHU	16	Ottawa, Canada	75W43	45N24	1659	42.0	3
7.508	CLA9	807	Havana, Cuba	82W21	23N09	1090	109.5	5
7.600	YNA3	157	Managua, Nicaragua	86W26	12N10	1427	144.2	13
7.665	TIO	156	Las Pavas, Costa Rica	84W52	09N50	1620	143.9	2
7.697	CLA2Ø	841	Havana, Cuba App.	82W21	23N09	1090	109.5	1
8.090	NSS	466	Annapolis, Maryland	76W27	38N59	1422	56.5	10
8.478	TIM	20	Limon, Costa Rica	83W01	10N00	1678	139.9	1
8.478	OST4	21	Ostende, Belgium	2E48	51N11	5112	39.7	1
8.484	VIS28	832	Sydney, NSW, Australia App.	151E03	33S46	6239	248.0	1
8.486	WOE	22	Lakeworth, Florida	80W06	26N33	1144	95.5	7
8.498	SAG4/6	688	Goeteborg, Sweden	11E56	57N28	5219	31.3	1
8.513	DAL	816	Noddeich, Germany	07E08	53N36	5190	36.2	1
8.514	WSL	23	Amagansett, New York	72W03	41N00	1688	54.6	3
8.527	CLA	603	Habana, Cuba	82W21	23N09	1090	109.5	1
8.531	WAX	24	Hialeah, Florida	80W12	25N59	1149	97.6	6
8.538	NPG	25	San Francisco, California	122W16	38N05	1478	300.0	4
8.545	PJK24	838	Suffisant Atw., Neth.	68W55	12N09	2249	115.8	1
8.546	KLB	649	Kent, Washington	122W11	48N02	1792	322.3	4
8.550	WPA	152	Port Arthur, Texas	93W58	29N50	281	83.2	17
8.556	FUF	833	Ft. de France, Mrt.	61W04	14N36	2600	104.9	1
8.558	KFS	26	San Francisco, California	122W07	37N27	1454	298.5	6
8.558	SPE4/6/8	839	Szczccin, Poland	14E34	53N28	5459	33.9	1
8.570	WNU	27	Slidell, Louisiana	89W44	30N17	535	81.5	11
8.581	WOF	591	Lantana, Florida	80W06	26N33	1144	95.5	1
8.582	KLB	28	Kent, Washington	122W17	47N23	1768	321.0	1
8.586	WCC	29	South Chatham, Mass.	70W02	41N40	1802	54.3	7
8.590	KOK	30	Clearwater, California	118W09	33N54	1188	290.0	9
8.610	WSC	32	Tuckerton, New Jersey	74W18	39N38	1545	56.4	8
8.614	NBA	183	Balboa, PNZ	79W39	09N03	1866	135.1	11
8.615	CKN	819	Vancouver, B. C.	122W15	49N06	1839	324.2	1
8.618	KPH	33	Bolinas, California	122W44	37N54	1499	299.3	11
8.620	EAD2/3	815	Aranjuez, Spain	03W36	40N01	5186	52.0	1
8.630	WCC	198	South Chatham, Mass.	70W02	41N40	1804	54.3	9
8.642	KPH	196	Bolinas, California	122W44	37N54	1499	299.3	11
8.650	DAF	547	Norddeich, Germany	07E08	53N36	5190	36.2	1
8.658	WSL	35	Amagansett, New York	72W03	41N00	1688	54.6	7
8.662	CFH	36	Halifax, Nova Scotia	63W59	44N58	2163	50.7	1
8.666	KLC	208	Galveston, Texas	95W08	29N24	210	89.8	6
8.674	FFP	37	Ft. De France, Martinique	61W04	14N35	2598	105.0	2
8.678	FFP2	843	Ft. De France, Martinique	61W04	14N35	2598	105.0	1
8.687	WMH	659	Baltimore, Maryland	76W32	39N15	1426	55.7	3
8.688	CLA	604	Habana, Cuba	82W21	23N09	1090	109.5	1
8.690	VCS	656	Halifax NS, Canada	63W37	44N28	2171	51.7	1
8.698	PJC	845	Curacao, Atn, Netherlands	68W55	12N08	2250	115.8	1
8.713	VCS	492	Halifax, Nova Scotia	63W37	44N28	2171	51.7	3
8.714	WLO	39	Mobile, Alabama	88W02	30N42	637	79.5	8
8.714	CLA	40	Habana, Cuba	82W21	23N09	1090	109.5	11
8.715	KFS	636	Palo Alto, California	122W07	37N27	1454	298.5	6
8.735	NMY	829	New York, New York	72W45	40N48	1651	54.6	1
10.000	WWVH	47	Maui, Hawaii	156W27	20N46	3630	274.6	2
10.000	WWV	48	Beltsville, Maryland	76W50	38N59	1402	56.2	2
10.000	WWV	777	Ft. Collins, Colorado	105W02	40N40	857	336.7	9
10.131	NAA	824	Cutler, Maine	67W17	44N38	2004	49.7	3
10.270	HPD	49	Panama	79W28	09N02	1876	134.8	1
10.299	AT&T	289	Oakland, California	121W47	38N25	1460	301.2	1
10.460	WKB2Ø	50	New Orleans, Louisiana	89W44	30N17	534	81.5	2
10.465	WIE3Ø	52	Miami, Florida	80W12	25N59	1148	97.5	2
10.470	WKB3Ø	53	New Orleans, Louisiana	89W44	30N17	534	81.5	1
10.492	WFE5Ø/WF	367	Brentwood, New York	73W15	40N49	1624	54.3	1
10,636	XDA138	650	Mexico D. F.	99W02	19N22	696	182.2	3
10.677	WMC	842	Oakland, California	121W47	38N25	1460	301.2	1
10.860	NSS	54	Washington, D. C.	77W01	38N59	1390	56.4	1
11.000	HRX6/25	522	La Lima, Honduras	87W55	15N50	1160	141.8	1
11.005	HRX6/25	628	La Lima, Honduras	87W55	15N50	1160	141.8	1
11.650	YND5	674	Managua, Nicaragua	86W14	12N10	1434	143.7	1

Test Transmissions	
Bearings Attempted:	152
Bearings Taken (Sample Size):	141
Mean:	1.13°
Standard Deviation:	8.85°

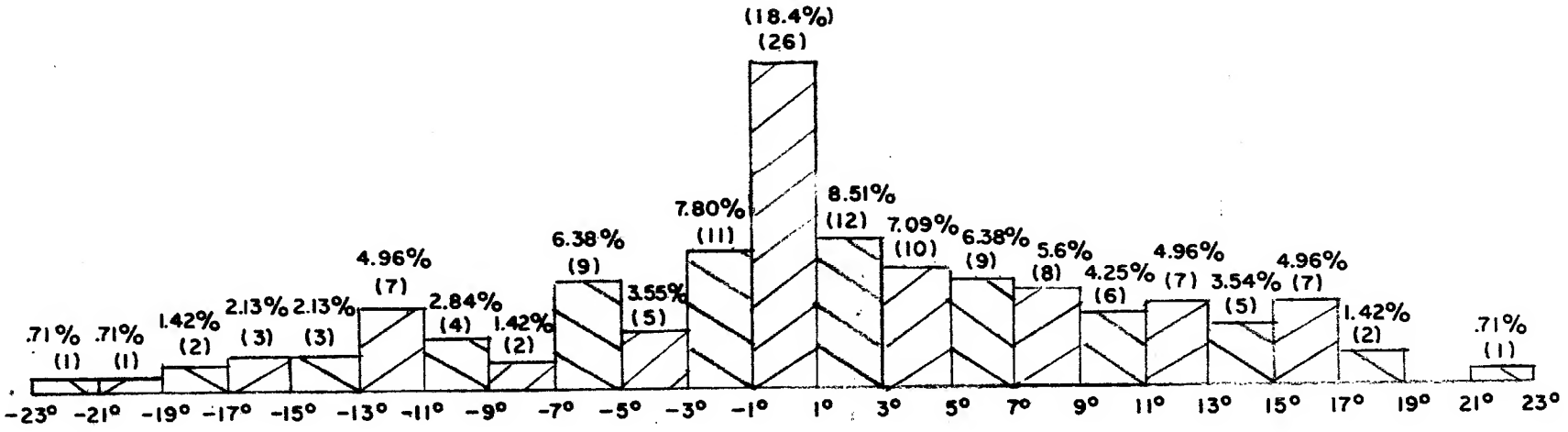

FIGURE 57
HISTOGRAM OF FINAL ANTENNA SKYWAVE BEARING DATA -
ALL 30 MILE DATA

Approved For Release 2001/09/03 : CIA-RDP76-00451R000200010013-1

Approved For Release 2001/09/03 : CIA-RDP76-00451R000200010013-1

Test Transmissions (Bearings Attempted):	167
Bearings Taken (Sample Size):	150
Mean:	2.09°
Standard Deviation:	6.68°

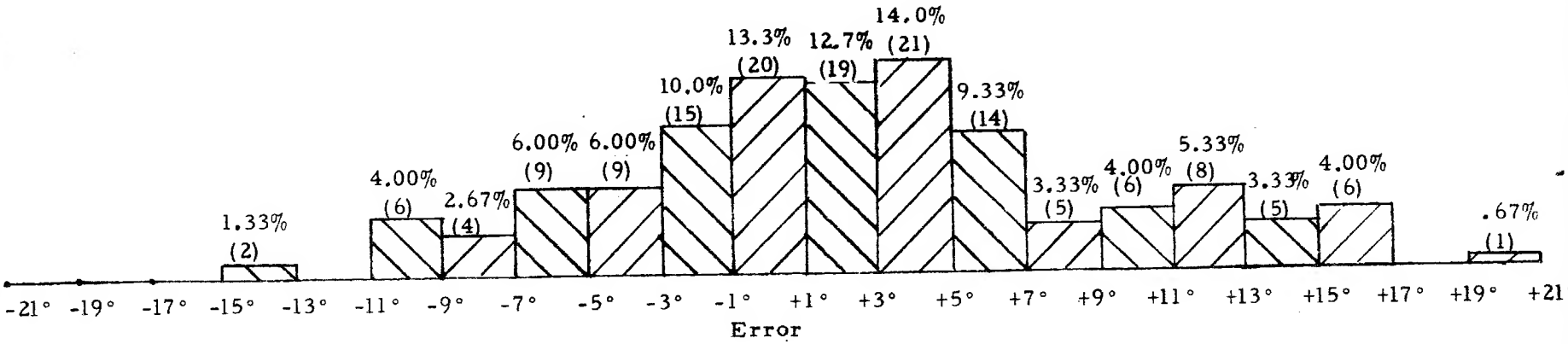

FIGURE 58
HISTOGRAM OF FINAL ANTENNA SKYWAVE BEARING DATA -
ALL 100 MILE DATA

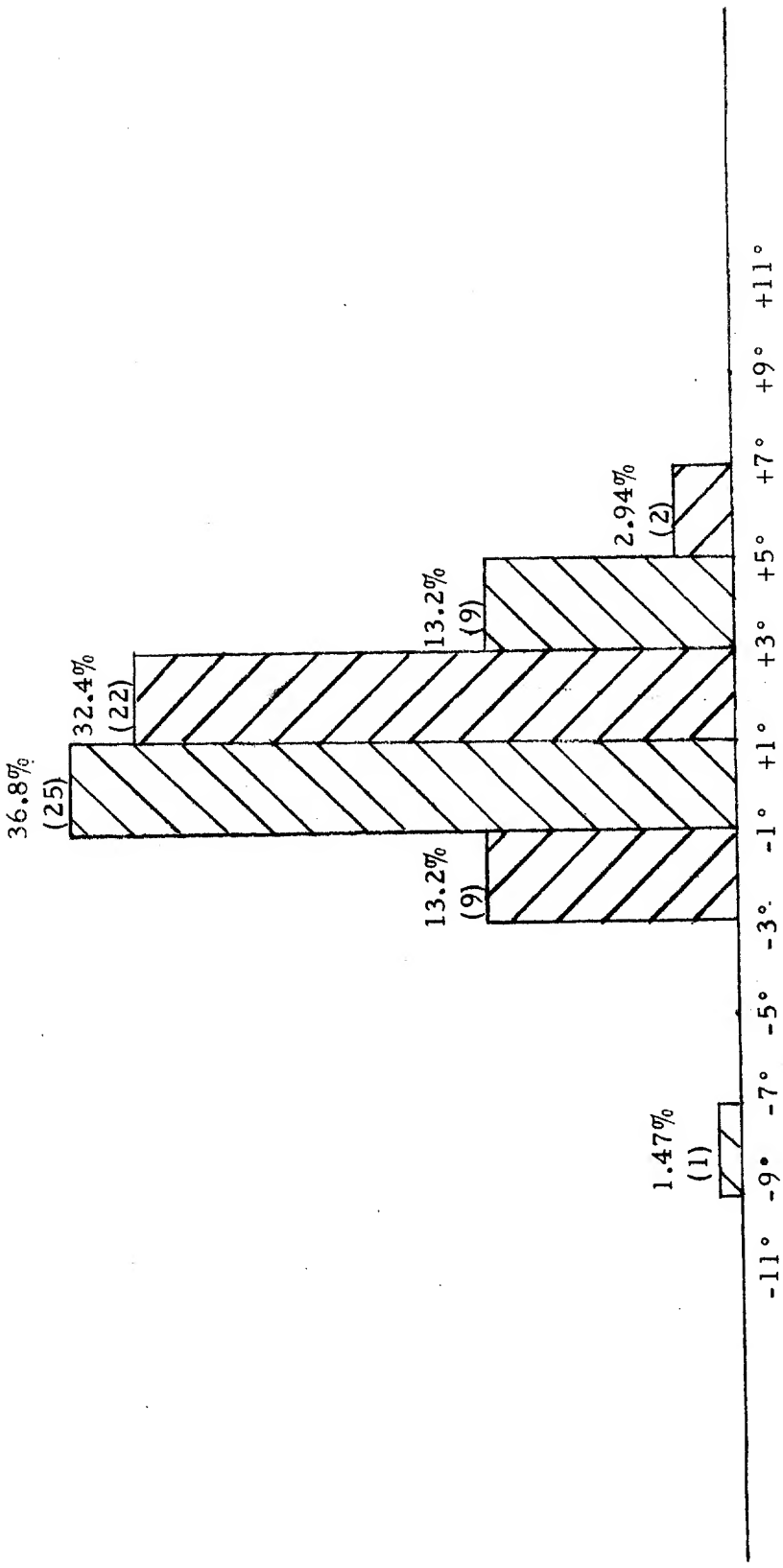

FIGURE 59
HISTOGRAM OF FINAL ANTENNA SKYWAVE BEARING DATA -
200 MILE KLC AT GALVESTON, TEXAS

the ionosphere. A comparison test using a half-wave horizontal dipole at the same distance and true bearing was planned but not completed.

Operator standard deviation is another interesting factor. The mean error for three operators is compared in Table 8 for both breadboard and final antenna data. Operator 12 is considered an extremely experienced operator. His standard deviation increased significantly between the breadboard and final antenna tests from 2.10° to 2.90°. However, on the final tests, Operator 12 delighted in finding a weak CW signal with a lot of interference. Using aural null techniques, he was adept at obtaining a bearing, but his standard deviation probably suffered.

Operator 23 is a retired Army Warrant Officer. He has many years of experience with Army DF equipments. Operator 23 is a cautious operator and probably did more unconscious signal selecting than the other operators.

Operator 38 was used in the tests of the final antenna because he had no previous DF experience or exposure to the spaced loop. (He is, however, a skilled technician with an above average technical knowledge.) The standard deviation of 2.81° for Operator 38 is consistent with the other two primary operators.

Response time with the spaced loop was a product of operator skill, mode of operation, and propagation conditions with the latter two factors the more significant. With continuous 30-rpm rotation, response time to bearing including the sense operation after signal identification varied from 5 seconds averaging 10 to 12 seconds to 32 seconds. The higher times were required for Class E and F signals which never produced a full spaced loop pattern.

Using aural null techniques, the sense was determined at 30 rpm. The pedestal was then switched to the low speed CW-CCW rotation mode and the null located. Response time in this mode was as low as 8 seconds to as high as 53 seconds, averaging approximately 20 seconds.

4.3.3.6 Power and Torque Requirements in Relation to Rotation Speed

The HF spaced loop direction finder set was designed for a portable application. As a consequence, power requirements were of primary concern. The amplifiers and antenna tuning use solid state components for minimum power. All remote control functions utilize momentary relays to further conserve power.

With the 70-rpm motor ordered with the modified AN/PRD-7 and 8 pedestal, power requirements for the system were excessive for a 26-volt

TABLE 8
Operator Standard Deviation and Mean Error

Operator No.	Antenna	Mean Error	Standard Deviation	Sample Size	Comments
12	Breadboard	-.54°	2.10°	51	
12	Final	.18°	2.90°	202	
23	Breadboard	-.20°	2.41°	144	
23	Final	.15°	2.31°	199	
38	Final	.28°	2.81°	107	Untrained with no previous exposure to spaced loop

battery pack using four BA-411A batteries. A summary of the current requirements with the 70-rpm motor and anticipated battery life is given in Table 9. The high power consumption, along with low torque and gear head problems, was a factor in changing to the original 30-rpm AN/PRD-7 and 8 drive motor.

With the 30-rpm motor, a more reasonable anticipated battery life of 23 hours for continuous operation with the antenna rotating at 30 rpm as shown in Table 10. The spaced loop antenna with a current requirement of 0.045 ampere at 24-volt DC requires the least power of the system components.

Increased rotation speed is desirable to reduce response time. Keyed CW and SSB signals do not produce a complete pattern in the 30-rpm mode. Other skywave signals never produce a complete pattern because the rate of polarization change is greater than the antenna rotation rate as previously discussed. For the portable system, the increased speed can be obtained only at the expense of larger battery packs or power sources. Operation of the system is possible now on all types of signals. Response time suffers for keyed signals. Operator training and practice have proven to be one method of reducing the response time with a given condition.

Torque requirements for a 60-rpm rotation speed with the HF spaced loop on the pedestal have been measured indirectly by using four Slo-Syn 60-rpm synchronous motors with torques of 75, 150, 300, and 400 oz-inch. Pedestal rotation shaft requirements with the HF spaced loop are estimated at 120 to 170 oz-in. at 60 rpm with no wind load based on measurements using the four motors. A rotation shaft torque of 300 oz-in. at 60 rpm should provide reliable operation under all reasonable wind conditions. Estimates of the pedestal rotation shaft torque with the original AN/PRD-7 and 8 30-rpm drive motor is 225 to 250 oz-in. at 30 rpm. The drive motor runs at 75 rpm, driving the shaft through a 2.5:1 gear train. Shaft torque at output of the motor is estimated at 100 oz-in. at 75 rpm.

4.3.4 Maintenance

The maintenance information on this first advanced development/feasibility model is limited. Normal trouble shooting techniques can be used for most problems. The only maintenance problems with the system during the tests at this laboratory were failures of the voltage regulator, an intermittent RF connection traced to a coaxial connector in a mast section, failure to tune the antenna because of a high impedance short on

TABLE 9
Current Drain and Predicted Battery Life
Using 70-RPM AN/TRQ-23 Pedestal Motor

Current drain AN/TRQ-23 at 70 RPM with no antenna	285 mA
Current drain of pedestal at 70 RPM with HF spaced loop antenna	490 mA
DF Indicator	70 mA
HF Spaced Loop Antenna	45 mA
Total drain with HF spaced loop	585 mA
Anticipated battery life at 70 RPM continuous rotation. Battery pack discharged to 18 volts (1.1 volts per cell). Four BA-411A batteries in series.	8 hrs.
Anticipated battery life - same conditions except 4 hrs/day	14 hrs.

TABLE 10
Current Drain and Predicted Battery Life Using
30-RPM AN/PRD-7 & 8 Pedestal Drive Motor

Current drain AN/ PRD-7 & 8 at 30 RPM with no antenna	115 mA
Current drain of pedestal at 30 RPM with HF spaced loop antenna	165 mA
DF Indicator	70 mA
HF Spaced Loop Antenna	45 mA
Total drain with HF spaced loop	315 mA
Anticipated battery life with continuous 30 RPM rotation. Battery pack discharged to 18 volts (1.1 volts per cell). Four BA-411 batteries in series.	23 hrs.
Anticipated battery life - same conditions except 4 hrs/ day	40 hrs.

the pedestal slip rings, and an intermittent RF connection in the pedestal rotary joint. The voltage regulator problem is discussed later in this section.

The RF connector problem was caused by improper assembly procedures. The high impedance short circuit on the slip ring is a basic problem in using high Q varactor diode tuning. For high antenna tuned circuit Q, the tuning bias is fed through a one (1) megohm resistor (see Figure 21). A dirty slip ring can have a resistance well below this value. The problem usually first appears as a signal level intermittent with antenna rotation. Removing a cover on the pedestal and cleaning the slip ring will solve the problem. Routine preventive maintenance probably should include cleaning of the slip ring at some regular interval. Signal level intermittents can be a clue to this problem as well as the rotary joint problem discussed below.

The pedestal rotary joint problem can also begin as an intermittent loss of signal. The problem also increases the VSWR on the RF cable from the pedestal to the receiver, increasing stray pickup. The problem was usually pinpointed at this laboratory by using a strong vertically polarized signal. If the shape of the pattern changes between various tuning conditions of the antenna control unit (all four nulls move), then the rotary joint is usually at fault. (Other faulty RF connections beyond the pedestal could produce the same effect.) Removal, dissassembly, and cleaning of the rotary joint corrected the problem. A lens-cleaning tissue is recommended. No lubricant should be used on the rotary joint.

The following check-out procedure is recommended:

(a) Turn the MAIN power switch (S-301 of Figure 30). A 24-VDC voltage should be obtained at TB-301-1 in the control unit (see Figure 30) and at TB-701-12 in the antenna (see Figure 20).

(b) Measure for 16 ± 0.5 VDC at TB-701-8 or -9 at the output of the voltage regulator.

(c) With the control unit tuning bias set to line, measure the tuning bias in the control unit at TB-301-4 in the antenna at TB-701-4 as the TUNING is varied from 000 to 999. The voltage should vary from 100 VDC to 0.5 VDC.

(d) Operate the BAND CHANGE on the control unit and observe the bandswitch solenoid M-701 in the antenna for proper

operation. A 24-VDC voltage should appear on each terminal on TB-301 in the control unit and on TB-701 in the antenna associated with the band set by the BAND CHANGE control.

(e) Operate INTERCEPT-DF-SIMPLE switch (S-303) on the control unit. A voltage of +24 VDC should be obtained at TB-301-3 and at TB-702-3. Operation of the crossover switching network can be physically checked with a multimeter by disconnecting the loop element leads with the antenna in Band 1 position (see Figure 26). Generally, an increase in sensitivity as the antenna is switched from the spaced loop function to simple loop function will indicate the switches are operating. Maintenance of this unit is not recommended unless it is removed from the antenna.

(f) Activate the RIGHT SENSE control (S-308) on the control unit. A voltage of +24 VDC should be measured at TB-301-10 and TB-702-2. At the test points of each sense network on the east loop, the resistance to ground should be 0 ohms when the RIGHT SENSE switch is depressed. The resistance between the two test points will be 180 ohms ± 5 ohms with switch normal.

(g) Activate the LEFT SENSE SWITCH (S-302). A voltage of +24 VDC should appear at TB-301-2 and TB-702-3. The test sequence described in the preceding section should be repeated on the west loop sense networks.

(h) The voltage regulator (Figure 22) should perform properly unless an excessive load, such as a short, appears on the output. Care should be taken not to short terminals during maintenance with the unit in operation. Transistor replacement has corrected all problems with similar circuits to date. The circuit was redesigned before antenna shipment. Additional tests after shipment indicated the 10-ohm resistors, R-704 and R-705 of Figure 23, would provide control reliability by increasing short circuit protections as discussed on page 42.

(i) Each side of the balanced field effect source follower circuits (Figure 21) should have a voltage gain of 0.4 to 0.7 over the frequency range of the antenna with a 50-ohm source and 50-ohm output load. Test levels should be limited to 30 millivolts. (Removal of the amplifier is recommended for this test.)

(j) The balanced broadband transistor amplifier (Figure 16) should have a gain of 25 dB at 4 MHz and 20 dB at 8 MHz into a 50-ohm load using either side using a 50-ohm signal generator with 50-ohm load resistors on each side of the balanced input.

Generally, proper operation of the antenna may be quickly checked by tuning across the frequency range according to the tuning chart. A definite noise peak will be observed on the receiver output as the antenna is tuned to resonance.

The sense networks are encapsulated subassemblies. The network is shown installed at the loop gap in the cross section at the top of Figure 60. A cross section of the encapsulated subassembly is given at the center of Figure 60. A schematic diagram is given at the bottom of Figure 60. Removal of this sense network is a critical operation. Reference should be made to the Instruction Book on the VHF spaced loop antenna when working in this area.[19]

4.3.5 Recommendations for an Improved Design

The recommendations for an improved design given in this section are divided into two categories. First, there are those improvements which would improve the performance of the first antenna. Second, there are changes in design philosophy which should be considered in future work.

The following initial mechanical tolerances were set in design drawings:

(a) Loop flatness ± 0.020 inch

(b) Loops to form a rectangular parallelpiped when assembled within ±1/32 inch

(c) Loop sides to be equal within ±0.015 inch

The first model did not meet the tolerance with respect to the loops forming a rectangular parallelpiped. The break-apart flanges did not provide the stability necessary. The brace system shown in Figure 18 was necessary. Tests with the corners distorted indicated the ±1/32-inch tolerance was necessary.

The problem could be overcome by an improved flange at the break-apart points. However, increased weight might be required. As an

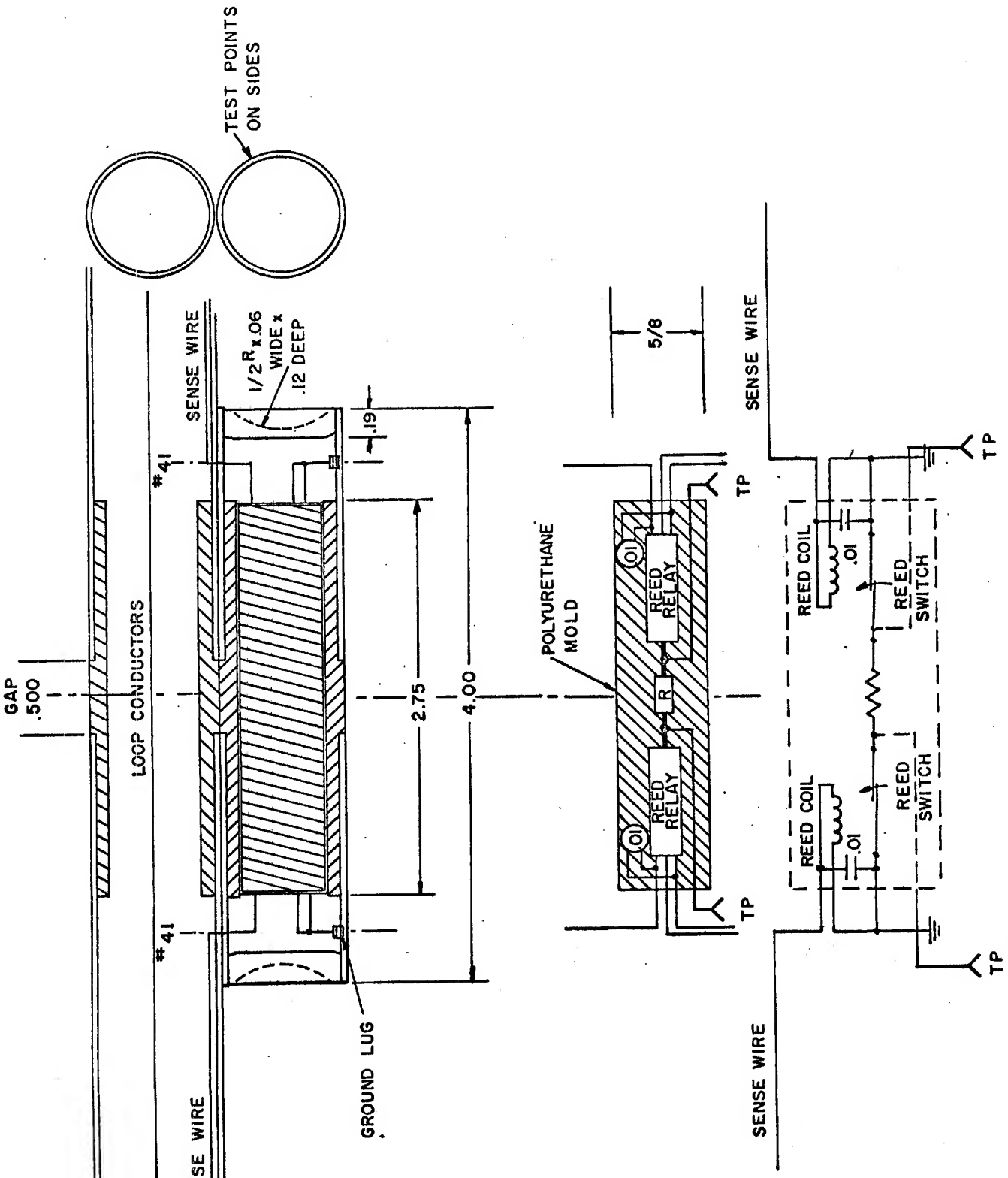

FIGURE 60.
SENSE NETWORK

alternate, bracing of loop corners to the center housing would allow weight reduction of materials used in fabricating the antenna. The corner of each loop could be positioned with respect to the center by a snap in brace (8 braces).

Loop flatness is slightly out of tolerance. This resulted from loop dimensions changing after fabrication. An improved assembly jig and more careful heat treatment for relief of stresses should help this point. Electronically, the system has been reliable in tests at this laboratory. Within the antenna, the reed switches in the sense network, and possibly the crossover switching network, should be eliminated and replaced with diode switching networks. Although the reed switch is reliable, a diode network would be more reliable.

A change in the voltage regulator of Figure 23 has already been discussed. The 10-ohm resistors, R-704 and R-705, of Figure 23 should be added to provide short circuit protection.

On the control unit, the major improvement recommended is the control system for low speed CW-CCW rotation for aural null. The Southwest Research Institute control unit uses one control for speed and one for rotation direction. After experience in the tests of this antenna, it is suggested that the original control system on the AN/PRD-7 and 8 control unit, which combined speed and rotation direction into one control, is superior.

There are a number of areas for improving the overall design philosophy. Now that a 10-μv/m sensitivity goal and pattern quality requirements have been met with three-turn loops, there is no basic reason for not increasing the number of turns to increase sensitivity. In this first known spaced loop with multiturn loops, the goal was to prove the principal and initial design. The series resonance of the antenna is above 22 MHz. This means operation to 20 MHz is possible. For the 4 to 8 MHz frequency range, additional turns to each loop can probably be added until the series resonance of the spaced loop is slightly above 9 MHz. If practical methods can be found to series and parallel loop turns, then additional turns are practical with all turns in series initially at the lower frequency limit. The series resonance would be raised above upper frequency limit by paralleling loop turns.

A major objection to the system (not the antenna) is the slow response time for CW and SSB signals. The left-right rotation with the DC motor in the pedestal has a time lag even with the control improvements previously suggested. Experience at this laboratory indicates that an

operator with headphones rotating the antenna with the pedestal hand wheel could significantly improve response on keyed signals. Physical control of the antenna eliminated the time lag of the DC motor.

Where power requirements are not a problem, increased rotation speed is the answer. For the portable requirement, increasing rotation speed to 60 rpm and using the unblanked trace for DF would help. Operator training in aural null techniques is believed the only answer for those signals which do not produce a readable DF pattern in a reasonable time at this speed. This probably applies to all portable DF equipments using a similar pedestal on skywave.

An alternate is the use of the two sense patterns. As discussed earlier, the CW and CCW sense patterns have an intersection which is the spaced loop null for all polarization conditions. The diode sense networks suggested earlier could be sampled at a fast rate. With the A-scope presentation of Figure 28 of Quarterly Report No. 1, [3] the operator would have an aid in finding the null. Caplin and Bagley[1] used a meter readout. With the appropriate circuitry, a left-right meter and more positive control of the antenna would reduce response time for portable requirements where power is limited.

Provisions were made for automatic left-right circuitry in the control unit for the HF spaced loop, but time did not permit the development of circuitry to adequately implement the system in a deliverable form. Breadboard circuitry was constructed which did demonstrate the feasibility of the technique on all types of signals, including keyed signals. This circuitry has been further developed by the U. S. Army and is being used with the airborne HF spaced loop constructed under Contract DA 28-043 AMC-02368(E).

5. LIST OF REFERENCES

1. Caplin, F., and Bagley, J. H., "A Mobile Spaced Loop Direction Finder," JIEE, Vol. 94, Part IIIA, pp. 676-682, (1947).

2. Bailey, A. D., "Studies and Investigations Leading to the Design of a Radio Direction Finder System for the MF-HF-VHF Range," First Quarterly Progress Report, Contract No. DA 36-039 SC-84525, University of Illinois, 11 March 1959.

3. Moore, J. D., et al., "HF Spaced Loop Antenna," Technical Report ECOM-01960-1, Quarterly Report No. 1, Contract DA 28-043 AMC-01960(E), Southwest Research Institute, May 1966.

4. Moore, J. D., et al., "HF Spaced Loop Antenna," Technical Report ECOM-01960-2, Quarterly Report No. 2, Contract DA 28-043 AMC-01960(E), Southwest Research Institute, May 1966.

5. Moore, J. D., et al., "HF Spaced Loop Antenna," Technical Report ECOM-01960-3, Quarterly Report No. 3, Contract DA 28-043 AMC-01960(E), Southwest Research Institute, November 1966.

6. Travers, D. N., and Hixon, S. M., "Abstracts of the Available Literature on Radio Direction Finding: 1899 - 1965," Task Report No. XXI, Contracts NObsr-64585, NObsr-85086, and NObsr-89167, Southwest Research Institute, 1 July 1966.

7. Moore, J. D., Castles, M. P., and Travers, D. N., "Improved Spaced Loop Direction Finder Antenna (20 - 150 mc)," Technical Report ECOM-01733-1, Quarterly Report No. 1, Contract DA 28-043 AMC-01633(E), Southwest Research Institute, October 1965.

8. Travers, D. N., "Performance Characteristics of a Spaced Loop Antenna Formed by Arbitrarily Oriented Parallel Loops," Task Summary Report XIII, Contract NObsr-89167, Southwest Research Institute, 1 April 1963.

9. Travers, D. N., "Characteristics of Electrically Small Spaced Loop Antennas," IEEE Transactions on Antennas and Propagation, Vol. AP-13, No. 4, pp. 639-641, July 1965.

10. Moore, J. D., Sherrill, W. M., and Travers, D. N., "Portable Spaced Loop Antenna," First Quarterly Report, Contract DA 36-039 AMC-03405(E), Southwest Research Institute, 31 December 1963.

5. LIST OF REFERENCES (Cont'd)

11. Moore, J. D., Travers, D. N., and Laenger, C. J., "Portable Spaced Loop Antenna," Second Quarterly Report, Contract DA 36-039 AMC-03405(E), Southwest Research Institute, 31 March 1964.

12. Moore, J. D., Laenger, C. J., and Travers, D. N., "Portable Spaced Loop Antenna," Third Quarterly Report, Contract DA 36-039 AMC-03405(E), Southwest Research Institute, 30 June 1964.

13. Moore, J. D., and Travers, D. N., "Portable Spaced Loop Antenna," Final Progress Report, Contract DA 36-039 AMC-03405(E), Southwest Research Institute, 31 January 1965.

14. Moore, J. D., Castles, M. P., and Lambertson, T. J., "Improved Spaced Loop Direction Finder Antenna (20 - 150 MHz)," Technical Report ECOM-01633-2, Quarterly Report No. 2, Contract DA 28-043 AMC-01633(E), Southwest Research Institute, January 1966.

15. Castles, M. P., Moore, J. D., and Lambertson, T. J., "Improved Spaced Loop Direction Finder Antenna (20 - 150 MHz)," Technical Report ECOM-01633-3, Quarterly Report No. 3, Contract DA 28-043 AMC-01633(E), Southwest Research Institute, April 1966.

16. Castles, M. P., Moore, J. D., and Lambertson, T. J., "Improved Spaced Loop Direction Finder Antenna (20 - 150 MHz)," Technical Report ECOM-01633-4, Quarterly Report No. 4, Contract DA 28-043 AMC-01633(E), Southwest Research Institute, July 1966.

17. Castles, M. P., Moore, J. D., and Lambertson, T. J., "Improved Spaced Loop Direction Finder Antenna (20 - 150 MHz)," Technical Report ECOM-01633-5, Quarterly Report No. 5, Contract DA 28-043 AMC-01633(E), Southwest Research Institute, October 1966.

18. Castles, M. P., Moore, J. D., and Lambertson, T. J., "Improved Spaced Loop Direction Finder Antenna (20 - 150 MHz)," Technical Report ECOM-01633-F, Final Report, Contract DA 28-043 AMC-01633(E), Southwest Research Institute, January 1967.

19. Moore, J. D., "Tuned VHF Spaced Loop," Technical Report ECOM-C0039-F, Final Report, Contract DAAB07-67-C0039, Southwest Research Institute, January 1967.

5. LIST OF REFERENCES (Cont'd)

20. Castles, M. P., and Moore, J. D., "Improved Spaced Loop Direction Finder Antenna (20 - 150 MHz)," Technical Report ECOM-01633-9, Instruction Manual, Contract DA 28-043 AMC-01633(E), Southwest Research Institute, December 1966.

21. Martin, Paul E., et al., "An Experimental Beverage Antenna Array for Land Based Direction Finding between 1.5 to 30 mc," Final Progress Report, Contract DA 36-039 AMC-02346(E), Southwest Research Institute, 30 September 1964.

22. Travers, D. N., et al., "Use of the Beverage Antenna in Wide Aperture High Frequency Direction Finding [Part III: Bearing Accuracy(U)]," Interim Report for Contract NObsr-89345, Southwest Research Institute, 23 March 1964. CONFIDENTIAL

6. DISTRIBUTION LIST

Copies	
1	OFFICE OF ASSISTANT SECRETARY OF DEFENSE (RESEARCH AND ENGINEERING) ATTN: TECHNICAL LIBRARY, RM 3E1065 WASHINGTON, D.C. 20301
1	BUREAU OF SHIPS TECHNICAL LIBRARY ATTN: CODE 312 MAIN NAVY BUILDING, ROOM 1528 WASHINGTON, D.C. 20325
1	CHIEF, BUREAU OF SHIPS ATTN: CODE 454 DEPARTMENT OF THE NAVY WASHINGTON, D.C. 20360
2	DIRECTOR U.S. NAVAL RESEARCH LABORATORY ATTN: CODE 2027 WASHINGTON, D.C. 20390
1	COMMANDING OFFICER AND DIRECTOR U.S. NAVY ELECTRONICS LABORATORY ATTN: LIBRARY SAN DIEGO, CALIFORNIA 92101
1	AFSC STLO (RTSND) NAVAL AIR DEVELOPMENT CENTER JOHNSVILLE, WARMINSTER, PA. 18974
1	ROME AIR DEVELOPMENT CENTER (EMTLD) ATTN: DOCUMENTS LIBRARY GRIFFISS AIR FORCE BASE NEW YORK 13440
1	SYSTEMS ENGINEERING GROUP (SEPIR) WRIGHT-PATTERSON AIR FORCE BASE OHIO 45433

Copies

2 ELECTRONIC SYSTEMS DIVISION (ESTI)
L. G. HANSCOM FIELD
BEDFORD, MASSACHUSETTS 01731

1 U.S. AIR FORCE SECURITY SERVICE
ATTN: ESD
SAN ANTONIO, TEXAS 78241

2 CHIEF OF RESEARCH AND DEVELOPMENT
DEPARTMENT OF THE ARMY
WASHINGTON, D.C. 20315

2 COMMANDING GENERAL
U.S. ARMY MATERIEL COMMAND
ATTN: R&D DIRECTORATE
WASHINGTON, D.C. 20315

1 COMMANDING OFFICER
52D USASASOC
FORT HUACHUCA, ARIZONA 85613

1 COMMANDING GENERAL
U.S. ARMY COMBAT DEVELOPMENTS COMMAND
ATTN: CDCMR-E
FORT BELVOIR, VIRGINIA 22060

3 COMMANDING OFFICER
U.S. ARMY COMBAT DEVELOPMENTS COMMAND
COMMUNICATIONS-ELECTRONICS AGENCY
FORT MONMOUTH, NEW JERSEY 07703

1 COMMANDING OFFICER
U.S. ARMY SEC AGCY COMBAT DEV ACTV
ARLINGTON HALL STATION
ARLINGTON, VIRGINIA 22212

2 U.S. ARMY SECURITY AGENCY
ATTN: OACofS, DEV (IARD)
ARLINGTON HALL STATION
ARLINGTON, VIRGINIA 22212

Copies

1 HARRY DIAMOND LABORATORIES
ATTN: LIBRARY
CONNECTICUT AVENUE AND VAN NESS STREET
WASHINGTON, D.C. 20438

1 COMMANDING GENERAL
U.S. ARMY ELECTRONIC PROVING GROUND
ATTN: TECHNICAL INFORMATION CENTER
FORT HUACHUCA, ARIZONA 85613

1 CHIEF, MOUNTAIN VIEW OFFICE
ELECTRONIC WARFARE LAB., USAECOM
P.O. BOX 205
MOUNTAIN VIEW, CALIFORNIA 94042

1 CHIEF, INTELLIGENCE MATERIEL DEV OFFICE
ELECTRONIC WARFARE LAB., USAECOM
FORT HOLABIRD, MARYLAND 21219

1 CHIEF, WILLOW RUN OFFICE
CSTA LAB., USAECOM
P.O. BOX 618
ANN ARBOR, MICHIGAN 48107

1 USAECOM LIAISON OFFICER
ROME AIR DEVELOPMENT CENTER
ATTN: EMPL
GRIFFISS AIR FORCE BASE, NEW YORK 13440

COMMANDING GENERAL
U.S. ARMY ELECTRONICS COMMAND
FORT MONMOUTH, NEW JERSEY 07703

1 ATTN: AMSEL-EW
1 AMSEL-PP
1 AMSEL-IO-T
1 AMSEL-RD-MAT
1 AMSEL-RD-MAF (Record Copy)
1 AMSEL-RD-LNA
1 AMSEL-RD-LNR
1 AMSEL-XL-D
1 AMSEL-NL-D
1 AMSEL-VL-D
1 AMSEL-KL-D
1 AMSEL-HL-CT-D
1 AMSEL-BL-D
8 AMSEL-WL-C

Copies

20 DIRECTOR
NATIONAL SECURITY AGENCY
ATTN: TDL
FORT GEORGE G. MEADE, MARYLAND 20755

1 UNIVERSITY OF ILLINOIS
COLLEGE OF ENGINEERING
ATTN: PROFESSOR A. D. BAILEY
URBANA, ILLINOIS

1 CHIEF, BUREAU OF SHIPS
ATTN: CODE 686B
DEPARTMENT OF THE NAVY
WASHINGTON, D.C. 20360

2 NASA SCIENTIFIC & TECHNICAL INFO FACILITY
ATTN: ACQUISITIONS BRANCH (S-AK/DL)
P.O. BOX 33
COLLEGE PARK, MARYLAND 20740